Title
HIGH RESOLUTION ELECTRONIC SPECTRA OF ORGANIC MOLECULES IN LOW TEMPERATURE MATRICES: THE SHEOLSKII EFFECT

Author
Macnab, Robert Marshall.

Publication Date
1969-07-01

UCRL-19269

cy. 2

HIGH RESOLUTION ELECTRONIC SPECTRA OF ORGANIC MOLECULES IN LOW TEMPERATURE MATRICES: THE SHPOLSKII EFFECT

Robert Marshall Macnab
(Ph.D. Thesis)

July 1969

AEC Contract No. W-7405-eng-48

LAWRENCE RADIATION LABORATORY
UNIVERSITY of CALIFORNIA BERKELEY

UCRL-19269

cy. 2

DISCLAIMER

UCRL-19269

HIGH RESOLUTION ELECTRONIC SPECTRA OF ORGANIC MOLECULES IN LOW TEMPERATURE MATRICES: THE SHPOLSKII EFFECT

Robert Marshall Macnab

Laboratory of Chemical Biodynamics
Lawrence Radiation Laboratory
University of California,
Berkeley

July, 1969

ABSTRACT

By the Shpolskii effect we mean the occurrence of an electronic transition of a guest molecule in a low temperature mixed crystal, without any accompanying change in the phonon energy of the host. In addition to the intrinsic interest of the phenomenon itself, its usefulness as a spectral technique has attracted many workers. Because the guest is uncoupled from the environment, its spectrum consists of narrow bands (quasi-lines), which enable precise determination of electronic and vibrational energies. The spectra usually have a multiplet structure; there are several electronic origins, each giving rise to a vibronic spectrum. This is believed to result from a multiplicity of substitutional sites in the host crystal. Typical systems for which the effect is observed are aromatic molecules in n-alkane matrices. Size of the n-alkane is critical.

Attempts to extend the technique to biologically interesting molecules (e.g. purine, pyrimidine) were largely unsuccessful, the spectra consisting only of broad bands; coupling to the matrix is

thought to be too strong. Acridine in n-heptane at 4°K gives some sharp lines and appears to be a borderline case for the usefulness of the technique.

The absorption and fluorescence spectra of anthracene and $[D_{10}]$-anthracene were taken in several n-alkane matrices, and vibrational analyses carried out. Several corrections are made to existing data for anthracene; the data for $[D_{10}]$-anthracene have not appeared previously. Deuteration leaves the multiplet structure of the spectra unaltered, except for a shift of 68 cm^{-1} to higher energy. A line exactly one vibrational quantum to the high energy side of the main origin in the fluorescence spectrum of anthracene in n-heptane had been observed by a previous author. A plausible explanation of this would be that vibrational relaxation is unusually slow, and therefore emission is occurring before it is complete. The existence of the line was confirmed, but studies with $[D_{10}]$-anthracene showed that it is a secondary origin and that the agreement with the value of a vibrational quantum is coincidental.

HIGH RESOLUTION ELECTRONIC SPECTRA OF ORGANIC MOLECULES IN LOW TEMPERATURE MATRICES: THE SHPOLSKII EFFECT

Contents

Contents (continued)

I. GENERAL INTRODUCTION TO THE SHPOLSKII TECHNIQUE

In 1952, E. V. Shpolskii and co-workers in the first[1] of a long line of papers (e.g. refs. 2-12) published in the USSR described how if certain molecules, usually polycyclic aromatics, are dissolved in appropriate n-alkane solvents, the low temperature electronic spectra, both in absorption and emission, of the guest molecule consist of large numbers of narrow lines, in contrast to the broad-band spectra which are usually observed in solution.

A certain amount of work in this field has been done by other groups of scientists, e.g. Bowen and Brocklehurst[13,14] in Britain, and Pesteil, Rabaud and others[15,16] in France; however, since the great majority of work has come from Shpolskii or his associates, the phenomenon has come to be named after him. The spectra have also been described, particularly in the Russian literature, as "quasi-line" or "quasi-linear" spectra, invoking comparison with the extremely narrow line spectra of, for example, metal arcs.

Early work suffered from the fact that frequently neither solute nor solvent was pure; impure solutes caused extraneous lines, while a failure to use pure single n-alkanes prevented optimal narrowing of lines, and in extreme cases prevented formation of the crystalline matrix which, as we shall see later, is an essential feature of the technique. Prior to about 1962, work was carried out only at 77°K (the temperature of liquid nitrogen); at this

temperature, the general features of the technique are evident but there is much less information than at 20°K (liquid hydrogen) or 4°K (liquid helium).

A summary of the main characteristics of Shpolskii spectra will be given, followed by a discussion of them.

(i) Vibronic bands are very narrow, typically 15 cm^{-1} or less.

(ii) The position of the pure electronic transition of the molecule is the same in absorption and in emission. The lines are said to be resonant.

(iii) The spectrum has a multiple character; there are a number (ca. 1-10) of identical spectra of different intensities and displaced from each other.

(iv) The size of the solvent molecule for optimum sharpness of the solute spectrum is critical and is related to the size of the solute molecule.

(v) The intensity of the sharp spectrum increases as the temperature is reduced. There is a redistribution of intensity between broad bands and sharp lines, rather than a narrowing of the bands.

A discussion of these features follows:*

For $^{1}_{A}$ transitions between electronic states of the same multiplicity, the lifetime of the upper state is typically 10^{-8} to 10^{-9} sec, which gives rise to an uncertainty broadening of the transition energy of 5×10^{-4} to 5×10^{-3} cm^{-1}. This radiative linewidth is

---

*See also the review written by Shpolskii.[17]

seldom observed as there are several other sources of line broadening, viz.

(a) Doppler broadening, generally about 10^{-2} to 10^{-1} cm^{-1} at room temperature.

(b) Non-resolved molecular or rotational levels.

(c) Non-uniformity of environment. This broadens the molecular energy levels and hence the transitions between them.

(d) Energy exchange with the environment. Changes in the quantum state of a molecule in a condensed phase are generally accompanied by changes in the quantum state of the environment surrounding the molecule. Since the environment has a continuum of low lying energy levels, the transitions of molecule + environment are not resolved but manifest themselves as a broadening of the molecular transition, with a shift to higher energy in absorption and to lower energy in emission because the average energy transferred from the molecule to the environment is positive at all accessible temperatures.

In the gas phase at low pressures there are no molecules close enough to the molecule of interest either to perturb its energy levels or to exchange energy with it. Under these circumstances, particularly if the molecule has high symmetry and therefore a relatively simple allowed vibronic structure, this structure is often fully resolved provided the degree of rotational excitation is not too high. For example, the spectrum of benzene vapor at room temperature has a highly resolved vibrational structure with bandwidths

of ca. 10 cm^{-1}, [18,19] presumably limited by non-resolved rotational levels.

This linewidth, though considerably greater than the Doppler width (ca. 0.05 cm^{-1}), is still much less than is encountered in the great majority of condensed phase spectra. For many molecules no vibrational analysis of their electronic spectrum in solution is possible, and even in the optimum case of molecules which have widely spaced vibrational levels and which interact weakly with the environment (e.g. benzene in hexane), a lower limit of ca. 200 cm^{-1} bandwidth is reached in liquid solution, and even in low temperature glasses the limit is ca. 100 cm^{-1}.

Crystallinity of the environment therefore is a prerequisite for obtaining highly resolved spectra in the condensed phase. A number of pure crystals at low temperature have such spectra, e.g. benzene,[20,21] naphthalene,[22,23] and phenanthrene.[24] However, if the aim is a study of the quantum states of the isolated molecule, pure crystal work is rather unsatisfactory on account of complications such as exciton interaction.

The insertion of the molecule of interest into a host crystal removes this complication. In the Shpolskii technique the guest molecule is in a uniform environment in the host crystal; it is not known with certainty whether it occupies a substitutional or an interstitial site, although the former seems more likely.

The molecular dimensions of the guest, or at least the long axis dimension, has to be close to that of the n-alkane comprising the host (point (iv) in the list of characteristics given above) before sharp

lines can be observed in the spectrum, and this is now seen as the necessity of obtaining a precise fit in the lattice site. Low temperature (point (v)) also plays a part in this by reducing the time-dependent fluctuations in the environment, although it will be seen that temperature also enters into the phenomenon in a more fundamental way.

As has been noted already, the appearance of sharp lines in a spectrum implies that either there is no energy exchange with the lattice, or the amount transferred is confined to a narrow range. The former is shown to be correct by the fact that the position of the pure electronic transition (0-0) is the same in absorption and emission (point (ii)). (Note that since lattice relaxation is a faster process than radiative emission, resonant emission of lattice energy is not possible.) The phonon energy of the lattice is unchanged by the molecular transition; it is a phononless transition.

The multiple character (multiplet structure) of the spectrum consists of components which are resonant in absorption and emission. As far as the guest molecule is concerned, therefore, they involve only electronic energy and can be described as multiple origins. They are believed to be the result of the superposition of the spectra of several classes of molecules, each class consisting of those molecules in a particular lattice site. That is, there is not simply one but several well-defined sites in the lattice, the natures of which are not well understood, although it has been suggested that frozen-in rotational isomers of the n-alkane molecules may be the cause.[17] The theory of multiplicity of sites is supported

by two observations. First, although the intensity distribution of the vibrational structure of the spectrum is the same for each component of the multiplet, the intensity distribution of the components of the multiplet is a function of the rate of freezing of the sample (see e.g. ref. 7). When longer freeze times are used, more of the spectral intensity goes into one component of the multiplet, presumably the one for the site of lowest free energy. The second observation is that when a particular component of the multiplet is excited selectively with a narrow band of light, only the spectrum derived from that component appears in emission.[25]

Two main questions remain to be answered. What is the reason for high phononless transition probability in Shpolskii systems, and what is the reason for the strong temperature dependence of the phenomenon?

The theory of phononless optical transitions and its temperature dependence has been developed by Trifonov,[26] and by Rebane and Khizhnyakov.[27,28] The phenomenon has much in common with the Mössbauer effect,[29,30] where gamma radiation is emitted or absorbed by a nucleus imbedded in a crystal, with the exact energy of the nuclear transition, i.e. without a change in the phonon energy of the crystal.* Gamma radiation has sufficient momentum to perturb the lattice vibrational states, and it is this momentum that couples the nuclear transition to the lattice, whereas the photons involved in optical transitions have negligible momentum in this context. However, during an optical transition large changes in the shape of the electronic cloud occur and the consequent change in the

*For illuminating discussions by Lipkin of the Mössbauer effect, see refs. 31 and 32.

adiabatic potential of the lattice can cause changes in the phonon energy; nuclear transitions of the type involved in Mössbauer spectroscopy do not substantially affect the lattice potential. Thus complementary factors perturb the lattice in the two effects. The invariability of the lattice energy under the transformation of position and momentum is the reason underlying the close similarity of the theories.

According to the theory of Trifonov,[26] the probability density function of the lattice having acquired an energy $\omega-\omega_o$ during an electronic transition ω_o is given by

$$w(\omega) = \frac{1}{2\pi} \int_{-\infty}^{\infty} \exp[-i(\omega-\omega_o)t+f(t)]dt \qquad (1)$$

where $f(t) = \sum_{\alpha} \frac{\Delta q_\alpha^2}{2} [\pm i \sin \omega_\alpha t-(2m_\alpha+1)(1-\cos \omega_\alpha t)]$

the Δq_α's are the displacements of the equilibrium values of the normal coordinates of the lattice as a result of the electronic transition, the ω_α's are the lattice oscillation frequencies, and the m_α's are the quantum numbers of the lattice modes, or rather the Boltzmann averages of the quantum numbers.

The integral in equation (1) is divergent because of a delta singularity at $\omega=\omega_o$. That is, the probability of zero energy transfer is discontinuously greater than the adjacent probability of small energy transfer.

This phononless transition probability is given by

$$P(\omega_o) = \exp[-\sum_{\alpha} \frac{\Delta q_{\alpha}^2}{2} (2\bar{m}_{\alpha}+1)] \qquad (2)$$

Since $\bar{m}_{\alpha}$ is the average quantum number of the lattice resulting from thermal population ($\bar{m}_{\alpha} = 1/[\exp \frac{\omega_{\alpha}}{kT} -1]$) the strong inverse temperature dependence of the phononless transition probability can be readily understood.

Taking the limit of zero temperature, equation (2) reduces to

$$P(\omega_o) = \exp [-\sum_{\alpha} \frac{\Delta q_{\alpha}^2}{2}] \qquad (3)$$

It can be shown that the first moment μ_1 of the spectral distribution of the transition (its displacement from the pure transition, commonly called the average Stokes loss) is equal to

$$\mu_1 = \pm \sum_{\alpha} \frac{\Delta q_{\alpha}^2}{2} \omega_{\alpha}$$

and hence equation (3) becomes

$$P(\omega_o)_{T=0} = \exp [-\mu_1/\omega_{ave}]$$

where ω_{ave} is an average of the frequencies of the participating lattice modes.

Thus the phononless transition probability has an inverse exponential dependence on the ratio of the average Stokes energy loss to the average lattice frequency.

This average lattice frequency is not easy to calculate. It requires a knowledge of the degree to which all the modes are perturbed by the optical transition of the guest, and this calculation has not been made, although it is assumed that only local modes will participate to a significant degree. Intermolecular bonding in an n-alkane matrix results from weak van der Waals forces and should not produce accoustical modes of particularly high frequency, nor are there any obvious reasons why the intramolecular modes which participate in energy transfer should be unusually high for an n-alkane matrix.

Stokes losses, on the other hand, are low in typical Shpolskii systems. Data published in spectral handbooks (e.g. ref. 33) are usually misleading since they refer to the distance between the center of gravity of the entire (vibronic) transition in absorption and emission, whereas only the pure electronic transition is relevant. On the basis of my observations of the displacement of the center of gravity of the electronic band in a liquid n-alkane from the position of the phononless transition in the corresponding n-alkane crystal, I would place the average Stokes losses of such systems at several hundred cm^{-1}.

Therefore, if the Shpolskii effect is not observed in the majority of low-temperature condensed-phase systems it seems likely that the reason is not that the participating lattice frequencies are too low (since n-alkane matrices do not have unusually high lattice frequencies), but rather that Stokes losses are high (strong coupling of the guest to the host lattice) or that the environment

II. AN ATTEMPT TO OBTAIN HIGH RESOLUTION SPECTRA OF SOME MOLECULES OF BIOLOGICAL INTEREST

1. Introduction

From the description of Shpolskii spectra given in part I of this thesis, it will be apparent that they are capable of giving a great deal of information about a molecule. Instead of the broad, featureless bands usually encountered in solution spectra, there are numerous well resolved lines, which enable electronic and vibrational levels to be determined with precision, and which because of their sharpness have high absorbance values, making the detection of weak transitions easier.

This detailed information would be of great value to the scientist faced with understanding the more diffuse optical properties of molecules in liquid solution, or of molecular aggregates, the two most common situations encountered in systems of biological interest. For such systems it is often uncertain how many electronic transitions are involved, what their relative intensities are, what symmetries are involved, which are pure electronic bands and which are vibronic bands, and so on.

In particular, it was felt that the extensive studies by Tinoco and co-workers (see e.g. ref. 37) on the optical properties of the nucleic acids and the interactions of their component nucleotides would benefit from precise knowledge of the energy

levels of the purine and pyrimidine bases. Research with the same purpose was being carried out by Tomlinson[38] using matrix isolation techniques, i.e. co-condensing the solute (e.g. adenine) and the solvent (usually a rare gas such as argon) onto a cold window in a dewar and then measuring the solute spectrum.

It was recognized that there was no certainty that highly resolved spectra of these molecules could be obtained; there were several grounds for doubt:

(i) In spite of the large number of Shpolskii spectra in the literature, no mention had been made of simple heterocycles; it seemed likely that attempts would have been made to obtain their spectra.

(ii) The heterocycles generally have lower symmetry than their homocyclic analogues. Because of this we may expect their spectra to be more complex and therefore the prospects for resolving structure to be reduced. On the other hand, it must be said that many aromatic molecules of fairly low symmetry, e.g. 1,2-benzanthracene (Figure II.1) nevertheless do have resolved Shpolskii spectra.[10] Also, as will be mentioned in the results section, the vapor spectrum of some heterocycles, e.g. pyrimidine, has detailed structure.

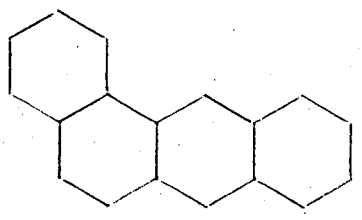

Figure II.1. 1,2-Benzanthracene

(iii) The heterocycles are generally less soluble in non-polar solvents such as the n-alkanes; this might give rise to difficulties in detection of spectra.

(iv) As was indicated in part I of the thesis, one of the criteria for a high phononless transition probability (and hence a highly resolved spectrum) is that the Stokes energy loss to the solvent should be low. This condition is met by aromatic molecules, but the introduction of hetero-atoms creates a permanent dipole, or at least substantial point monopoles, and these can greatly increase the coupling to the solvent. For example, the Stokes loss reported for anthracene is 1790 cm^{-1}, but introduction of one hetero-atom to form acridine (Figure II.5) increases this to 2720 cm^{-1} (ref. 33, pp. 122-123).*

So some difficulties were anticipated, but in view of the potential importance of the results the effort seemed worthwhile.

Most of the Shpolskii spectra reported in the literature are of condensed ring aromatics, and it was thought that these would make

*A realistic value for Stokes loss is difficult to calculate from experimental data. In ref. 33 it was calculated as the shift from absorption to emission of the center of gravity of the entire vibronic spectrum. Since the Stokes loss relates to the shift in the pure electronic transition, the values quoted above are unduly large. Note, however, that because of this the proportional change on going from anthracene to acridine is larger than these values indicate.

suitable model compounds for comparison with their heterocyclic analogues. Thus, benzene could be chosen as a model compound for pyrimidine (Figure II.2a) and naphthalene as a model compound for purine (Figure II.2b).

(a) 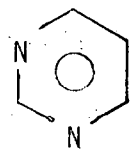

(b) 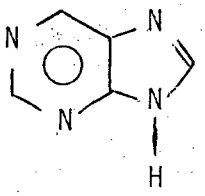

Figure II.2. (a) Pyrimidine, and (b) purine.

The Shpolskii spectrum of naphthalene was known,[15] and was not taken in the present work. Although low temperature spectra of the benzene crystal had been reported,[20,21] there were no high resolution spectra for the molecule isolated in a low temperature matrix (ref. 39 was published after this work was completed) and therefore this was the first task.

A description of the work with benzene will be followed by a brief description of the unsuccessful attempts to obtain high resolution spectra of pyrimidine and purine.

Because of the lack of success with these, other approaches were tried. Instead of using a n-alkane matrix, the mixed crystal technique of McClure[40] was used. McClure took advantage of the fact that durene (sym-tetramethyl benzene, see Figure II.3a) has very similar overall dimensions to naphthalene (Figure II.3b), but has a spectrum to sufficiently high energy that it does not

(a) 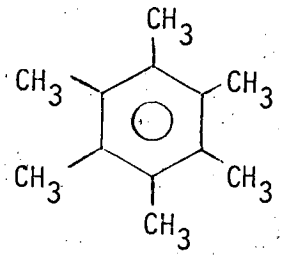 (b) 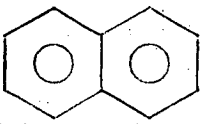

Figure II.3. (a) Durene, and (b) naphthalene

interfere with the spectrum of naphthalene. Thus naphthalene can occupy substitutional sites in a durene crystal, and this gives a very high resolution spectrum of the isolated naphthalene molecule.

The most interesting guest molecule in the present context would have been purine, but I decided to proceed more cautiously and selected quinoline, and isoquinoline (Figure II.4), since they are more closely related to naphthalene, the guest used by McClure.

(a) 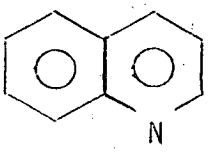 (b) 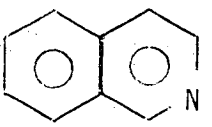

Figure II.4. (a) Quinoline, and (b) isoquinoline.

This approach was also unsuccessful, and so I decided to make the smallest step possible away from a well-established Shpolskii spectrum. For this purpose anthracene was chosen as the model compound, and acridine (Figure II.5) as the heterocyclic analogue.

The anthracene spectrum in n-heptane at 4°K had been reported,[11] and consisted of many sharp lines. Acridine, with only one

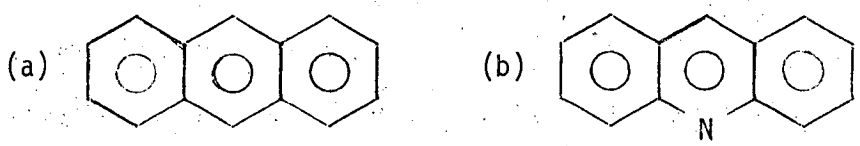

Figure II.5. (a) Anthracene, and (b) acridine.

hetero-atom, which was fairly well shielded by the adjacent rings from interaction with the matrix, seemed to be a hopeful candidate to also give a sharp spectrum. As will become evident when the results are presented, acridine is a borderline case for the usefulness of the Shpolskii technique.

Finally, a brief mention will be made of efforts to obtain a high resolution spectrum of β-carotene, a molecule of interest to those working in the field of visual pigments, and in photosynthesis.

All of the spectral measurements in this part of the thesis were made in absorption, using a Cary 14 Spectrophotometer.

2. Materials

The following materials were used without further purification:

Benzene: AR quality, ex Baker Chemical Co.

Cyclohexane: spectroquality, ex Matheson, Coleman and Bell.

n-Butane: Instrument grade, ex Matheson Co.

Pyrimidine: C grade, ex Calbiochem.

density filters into the reference beam because of the highly scattering nature of the polycrystalline sample. In theory there was no limit to the optical density that could be measured by this technique, but of course the instrument quickly became noise limited. Samples with an optical path of about 1 mm constituted a practical limit, although by the use of sealable cuvettes the scattering of samples could have been greatly reduced, as was found out in the work of part III of this thesis. This is presumably because more effective outgassing is possible.

The Cary 14 is not intended primarily as a high resolution spectrometer, and it was recognized that the measurement of spectra with bandwidths of perhaps <10 cm^{-1} would be at the limit of its capability. The specified resolution of the instrument is 0.5 to 1.0 Å (ca. 5 to 10 cm^{-1} in the near ultraviolet) and this was confirmed by measuring the spectrum of a holmium oxide disc.

In order to achieve the highest accuracy possible in measuring line position, a careful calibration of the instrument was carried out. First of all a survey over the visible and near ultraviolet using a mercury arc revealed that the instrument had a mean error of ca. 3 Å.

An adjustment was made to remove this mean error, and then a more detailed calibration was carried out in the region 3800 to 3200 Å. The mercury arc lamp does not have a sufficient density of lines for this purpose, and so four different lamps were used as line sources, viz. thallium, mercury, cadmium, and zinc. Considerable difficulty was encountered in reproducing the position of

emission lines even though great care was taken to use the same scanning technique each time. However, if the instrument power was left on for a long time (say, 8 hr) the reproducibility was improved, so that readings differed by less than 0.5 A. It appears that heat dissipation from the instrument power prevents equilibration of the wavelength drive for several hours (the specified wavelength/temperature coefficient of the instrument is 0.3 A/°C). Table II.1 and Figure II.6 show the calibration obtained.

Table II.1. Calibration of wavelength readout of Cary 14MR, Serial No. 467.

Source	λ_{true}	$\lambda_{indicated}$	Difference
Tl	3775.7	3774.2	1.5
Hg	3663.1	3662.1	1.0
Hg	3654.8	3654.2	0.6
Hg	3650.1	3649.5	0.6
Cd	3610.5	3610.4	0.1
Tl	3519.2	3517.5	1.7
Cd	3466.2	3465.1	1.1
Cd	3403.7	3403.7	0.0
Zn	3345.0	3344.4	0.6
Hg	3341.5	3341.2	0.3
Zn	3302.6	3302.2	0.4
Zn	3282.3	3281.6	0.7
Cd	3261.1	3261.2	-0.1
Tl	3229.8	3230.4	-0.6

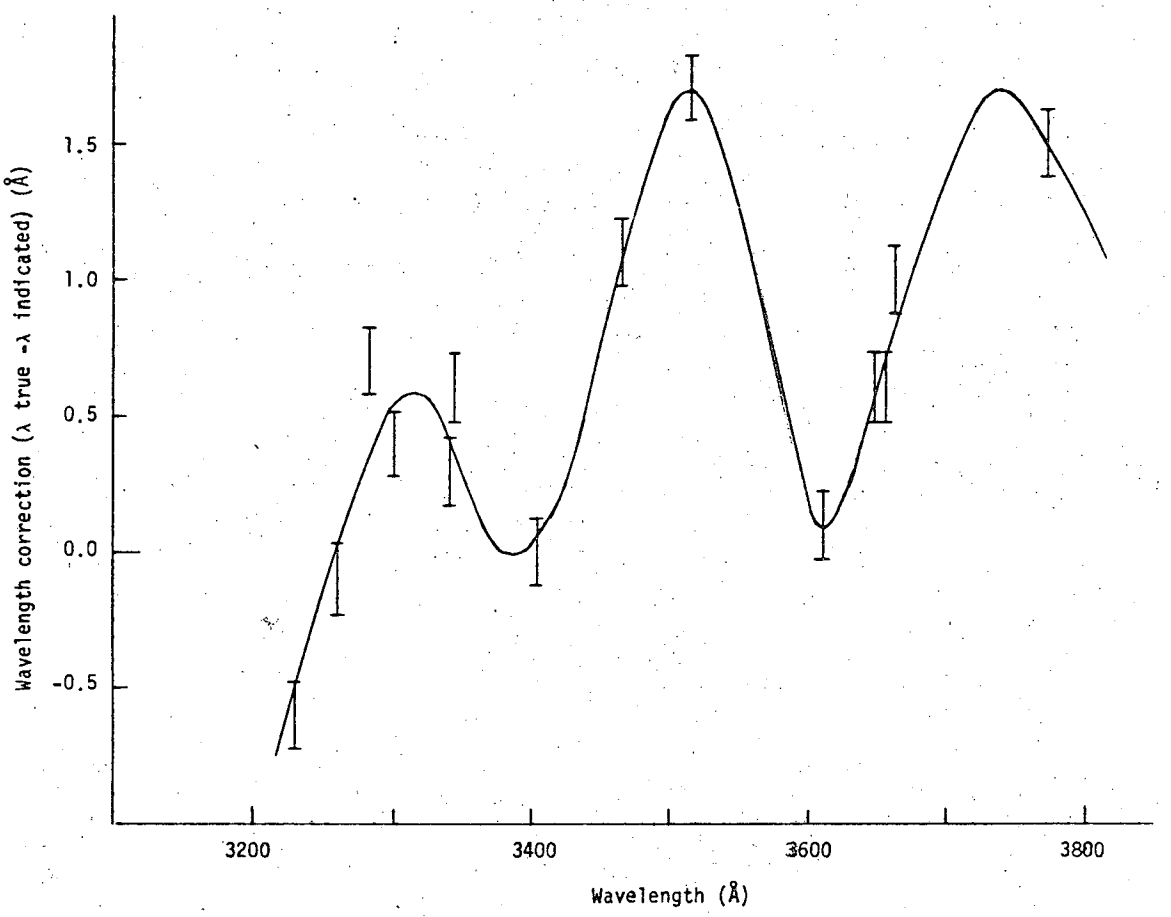

Figure II.6. Calibration of wavelength readout of Cary 14MR, Serial No. 467.

As can be seen from Figure II.6, the error function is periodic with an amplitude of ca. 1.5 A and a period of 200 A (corresponding to one turn of the lead screw in the scan mechanism).

With the use of this calibration it is estimated that line positions can be measured to within ca. 0.5 A.

A set of "typical" operating conditions for the measurement of spectra is given as Appendix B, although it must be realized that there was considerable variation in these conditions, depending on solubility, oscillator strength, etc.

4. Results and discussion

a) Benzene

The long axis dimension of benzene, measured from CPK* models, is 6.95 A; this is midway between the long axis dimensions of propane (6.4 A) and n-butane (7.5 A). n-Butane was selected as the matrix for the present work.

The solution (ca. 0.2 M) was prepared by condensing butane gas into a cuvette which was cooled by dry ice, and then adding benzene to the solvent by means of a syringe.

The absorption spectrum of benzene in n-butane at 77°K had relatively broad peaks (ca. 100 cm^{-1} halfwidth). The positions of the more intense peaks are given in Table II.2.

---

*Corey-Pauling-Koltun (supplied by the Ealing Corporation).

Table II.2. Principal peaks in the absorption spectrum of benzene in n-butane at 4°K. Wavelengths in A.

2642	2388
2606	2375
2578	2356
2544	2334
2518	2321
2485	2307
2430	2253

It does not seem likely that the coupling of benzene to an n-alkane matrix would be substantially greater than that of other aromatic molecules such as naphthalene, for which Shpolskii spectra are well known. There may well be a high phononless transition probability for benzene in n-butane, which does not manifest itself in a sharp spectrum because of non-uniformity of environment. The degree of mismatch in the dimensions of the two molecules is probably sufficient to prevent the benzene molecule from occupying a well-defined site in the matrix. Also the closeness of the long and short axis dimensions of benzene (6.95 and 6.4 A, respectively) may permit substantial librational or even rotational movement. Leach and Lopez-Delgado[60] have obtained similarly broad spectra in a number of longer chain n-alkane matrices.

Because of its chemical similarity to the n-alkanes and the fact that its size and shape are comparable to those of benzene, cyclohexane suggested itself as a likely matrix.

The low intensity of the first transition of benzene (ε = ca. 200), together with the fact that long pathlengths could not be used because of scattering, necessitated the use of high concentrations. The spectrum of a 0.4 M solution of benzene in cyclohexane at 77°K consisted of around 60 lines, with halfwidths of 25 - 50 cm^{-1}. However, at a later time, when a sample was prepared under the same conditions and its absorption spectrum measured at 4°K it was found that the bands were, if anything, broader than had been obtained previously at 77°K. In addition, the later sample was more highly scattering and the consequently higher noise level made identification of low intensity peaks difficult. Numerous attempts to repeat the original 77°K spectrum failed in spite of considerable variation in the technique of freezing. The original spectrum had most of its intensity in one sharp component of a multiplet structure, whereas the later spectra were characterized by an intense broad component 86 cm^{-1} to higher energy of the sharp component, which was present with a much reduced intensity.

Similar observations have been made by Leach and Lopez-Delgado[60,61] and by Spangler and Kilmer,[39] who have explained them in terms of two different polymorphic forms of the cyclohexane crystal. The monoclinic form, stable below 186°K, gives rise to a sharp benzene spectrum; the cubic form, stable above this temperature, gives rise to a broad spectrum 84 cm^{-1} to higher energy. However, unless

samples are cooled slowly through the transition point, the high-temperature cubic form persists in a metastable state. The workers mentioned above used photographic detection; they were therefore able to work with very low benzene concentrations and long optical pathlengths, and could freeze slowly without risking the formation of benzene aggregates. With the higher concentrations necessary to achieve a measurable signal in the Cary 14 spectrometer, samples had to be frozen quickly, and so the metastable cubic form of the cyclohexane crystal predominated. Perhaps even at these higher benzene concentrations a careful annealing at the transition temperature might have allowed the formation of the monoclinic form without benzene aggregation; this may have happened fortuitously in the first sample, where the sharp spectrum was encountered.

b) Pyrimidine

The spectrum of pyrimidine in the near ultra-violet consists of two regions of absorption. The more intense, at around 240 nm in

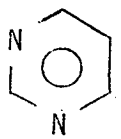

Figure II.7. Pyrimidine.

non-polar solvents, corresponds to the 256 nm π-π^* transition of benzene; the other region of absorption, in the region of 280-320 nm, is caused by an n-π^* transition of the lone pair electrons on the nitrogen atoms (ref. 18, pp. 361-367).

The spectrum of pyrimidine vapor was measured at room temperature, and confirmed the findings of Halverson and Hirt[41] that the $n-\pi^*$ transition is resolved into a large number of lines with a halfwidth of ca. 25 cm^{-1}, originating at 321.7 nm, while the $\pi-\pi^*$ transition consists of poorly resolved bands several hundred wavenumbers wide.

In cyclohexane solution (5×10^{-2} M) at room temperature the sharp lines of the $n-\pi^*$ transition in the vapor spectrum are replaced by broad bands (ca. 250 cm^{-1} halfwidth). Even in the frozen cyclohexane crystal at 77°K these bands are not significantly narrowed.

c) Purine

Because of the polar amine group on the five-membered ring purine (Figure II.8) is very insoluble in non-polar solvents. For

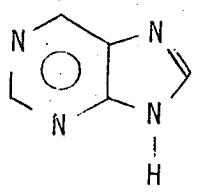

Figure II.8. Purine

example, a saturated solution at room temperature in n-pentane had a concentration of only 3×10^{-6} M, estimated from the absorbance of the solution. The spectrum (Figure II.9a) showed some structure including absorption at ca. 300 nm as well as two more intense peaks at 268 and 263 nm, whereas in polar solvents such as water or

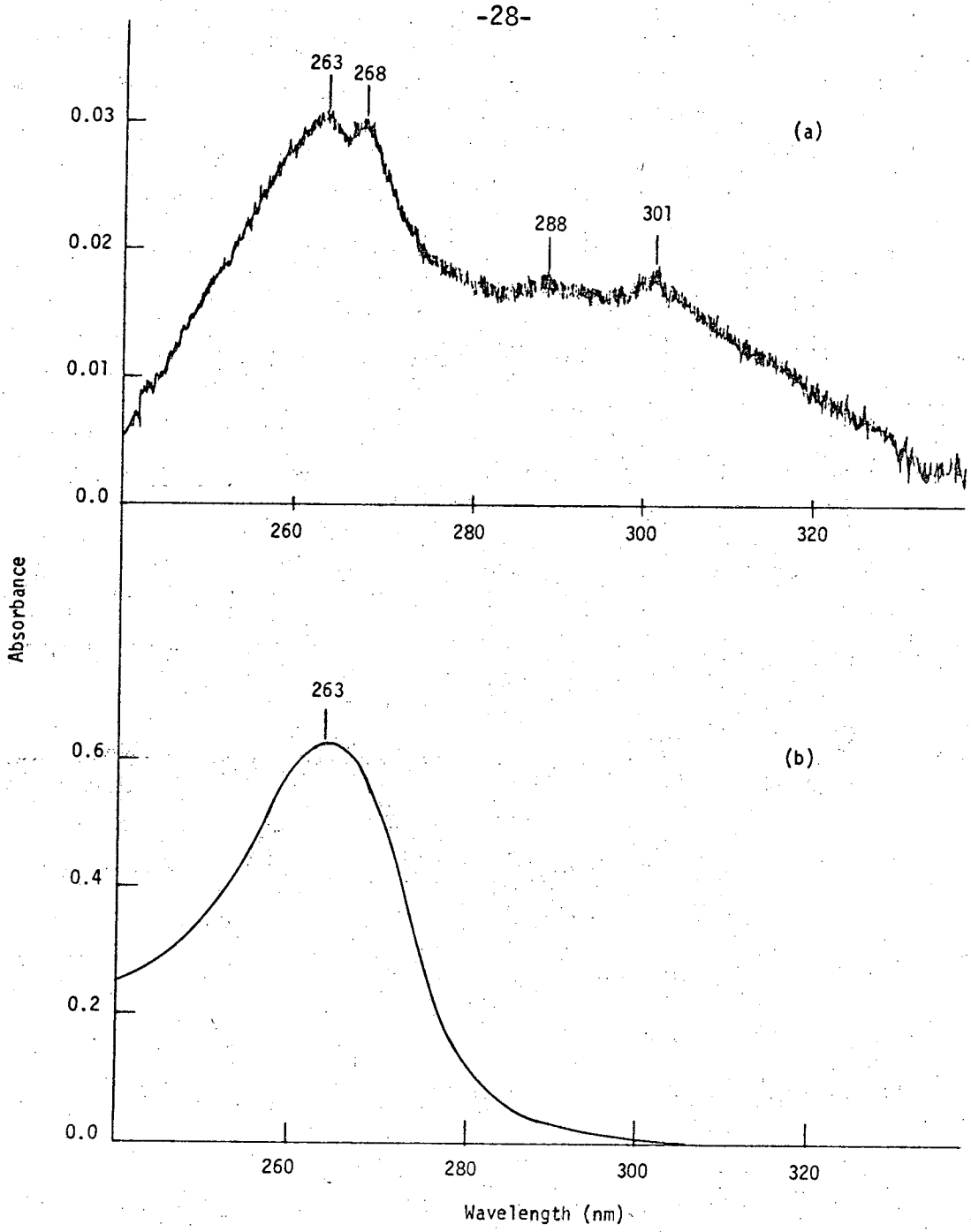

XBL 696-4328

Figure II.9. Absorption spectrum of purine at room temperature.

(a) 3×10^{-6} M in n-pentane, 1 cm cell;

(b) 5.6×10^{-3} M in 1-pentanol, 0.1 mm cell.

alcohols the spectrum (Figure II.9b) consists simply of one broad band at 263 nm with very little evidence of structure.

Drobnik and Augenstein[42] were able to prepare super-saturated solutions of purine in methylcyclohexane by the sudden dilution of a saturated solution in isopropanol or dioxane with large quantities (1500:1) of methylcyclohexane. A 10^{-4} M solution prepared by them in this way had a room temperature spectrum similar to that reported here for purine in pure n-pentane (Figure II.9a), consisting of about 6 poorly resolved bands.

Because of pathlength limitations imposed on my samples by scattering of the low temperature matrices, I was forced to attempt higher concentrations, and this was only possible by using a higher polar/non-polar solvent ratio.

n-Pentane was selected as the non-polar component since it was the matrix which had produced the sharpest lines in the Shpolskii spectrum of naphthalene,[15] a molecule of very similar dimensions to purine. As the polar component, 1-pentanol was chosen, since it was felt that this would cause minimum disruption of an n-pentane matrix.

Starting with a near-saturated solution of purine in 1-pentanol, I diluted with pentane to the maximum extent (100-fold dilution) which would still allow measurement of the spectrum in a 1 mm pathlength cuvette (the practical limit set by scattering). The room temperature spectrum of this solution was almost identical with that of a solution in pure 1-pentanol (Figure II.10), except for a slight amount of absorption at ca. 300 nm.

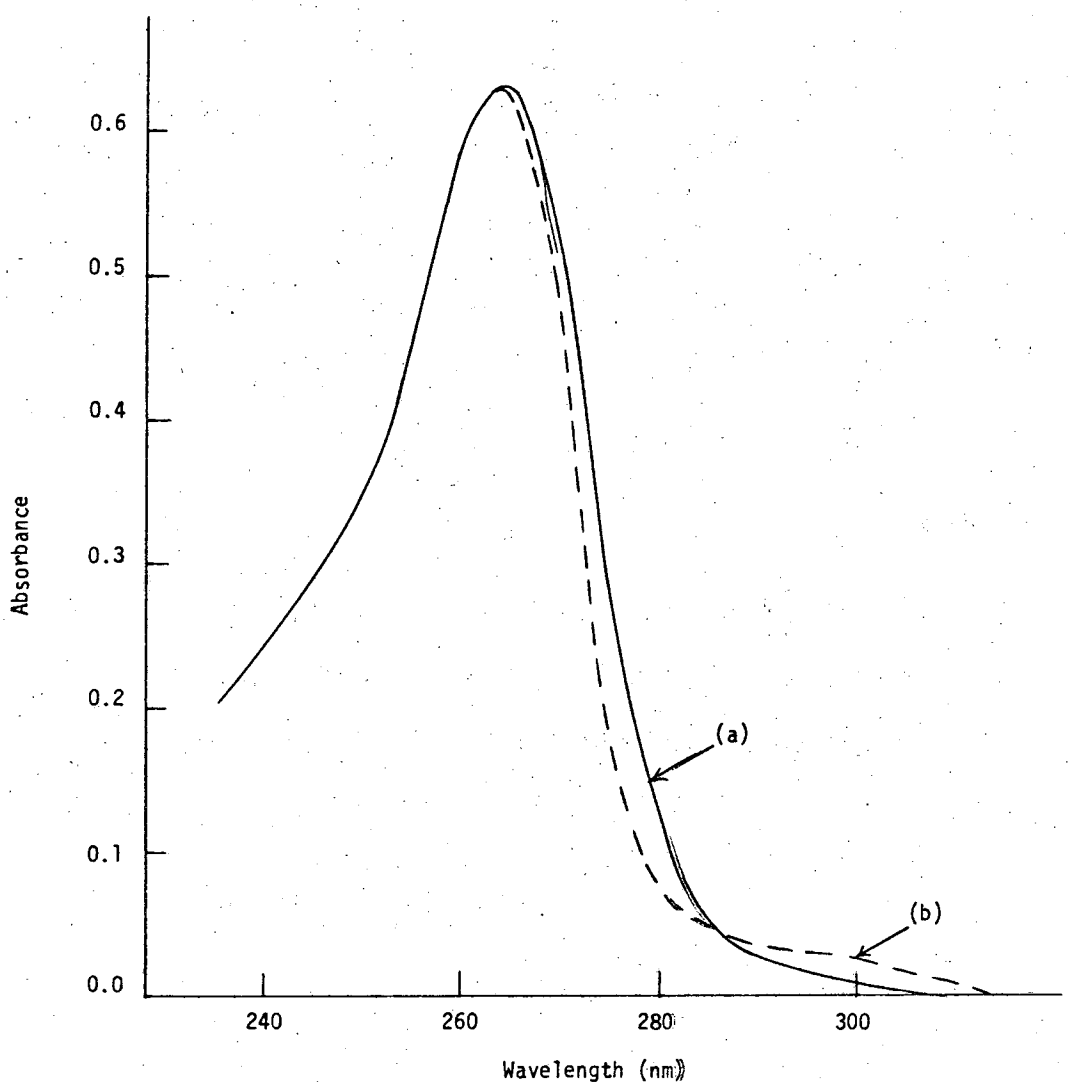

Figure II.10. Absorption spectrum of purine at room temperature. (a) 5.6×10^{-3} M in 1-pentanol, 0.1 mm cell (solid); (b) 5.6×10^{-5} M in a 1:100 mixture of 1-pentanol and n-pentane, 1 cm cell (dashed).

The lack of spectral structure indicates that most of the purine was interacting with the 1-pentanol rather than with the n-pentane, and the attempt to obtain a Shpolskii spectrum of this system was abandoned. A later publication,[12] by Sevchenko et al., has shown that sharp spectra can sometimes be obtained in cases where a polar component in the solvent forms a solvate with the molecule of interest. In this way they were able to obtain sharp spectra of the very insoluble metalloporphins in n-octane at 77°K by the addition of small quantities (amount unspecified) of a polar molecule such as ethanol or pyridine. Presumably the spectrum is that of a well-defined solvated complex which is surrounded by, and very weakly coupled to, the non-polar crystalline host.

d) Quinoline and isoquinoline

Figure II.11. (a) Quinoline, and (b) isoquinoline.

The absorption spectra of these two molecules are fairly similar. In n-pentane at room temperature the spectra (Figure II.12) consist of a number of bands about 200 - 300 cm^{-1} wide, starting at 313 nm in the case of quinoline and 317 nm in the case of isoquinoline, and extending to about 290 nm; a very broad band of comparable intensity extends from 290 to 240 nm. Only the narrow band region was examined in the present work.

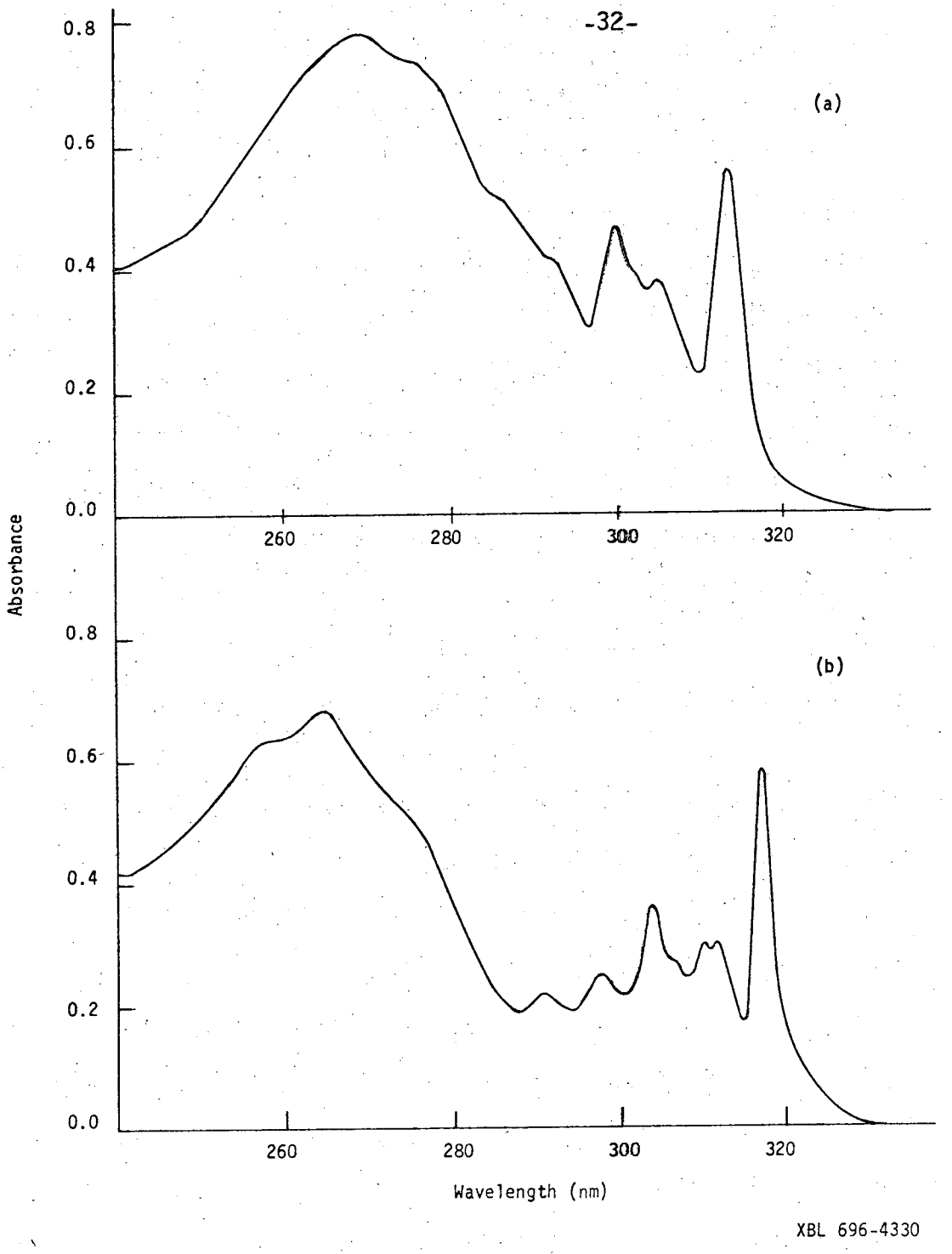

Figure II.12. Absorption spectra in n-pentane at room temperature.

(a) Quinoline, 2.3×10^{-3} M, 1 mm cell:

(b) Isoquinoline, 1.7×10^{-3} M, 1 mm cell.

The spectrum of isoquinoline is somewhat sharper and better resolved than that of quinoline, and this effect becomes more pronounced in an n-pentane matrix at 77°K (Figure II.13). Quinoline shows no improvement in resolution, whereas the spectrum of isoquinoline narrows significantly, to about 70 cm^{-1} halfwidth for the sharpest bands. Spectra were taken of both molecules in the vapor phase at room temperature. The spectrum of isoquinoline showed much more resolution. For example, the first band (λ_{max} = 313 nm) was resolved into sub-bands about 25 cm^{-1} wide; the corresponding band in the quinoline spectrum (λ_{max} = 310.5 nm) was 250 cm^{-1} wide and showed only a hint of structure. The higher resolution of isoquinoline in the low temperature matrix therefore does not seem to be a result of lower interaction with the matrix but rather to be an intrinsic property of the molecule. The absorption region under consideration has, on the basis of substitutional effects, been assigned[43] to a longitudinal (long axis) transition. If a perturbation is introduced on the axis of the transition dipole of a molecule, then the symmetry species of the perturbation operator will be the same as that of the dipole operator, and the perturbation cannot mix in any states not present in the unperturbed system. In the present example, the azo group lies closer to the transition dipole axis in isoquinoline than in quinoline; this, by reducing the number of vibronic transitions which the perturbation allows, may be the reason for the simpler and more highly resolved isoquinoline spectrum.

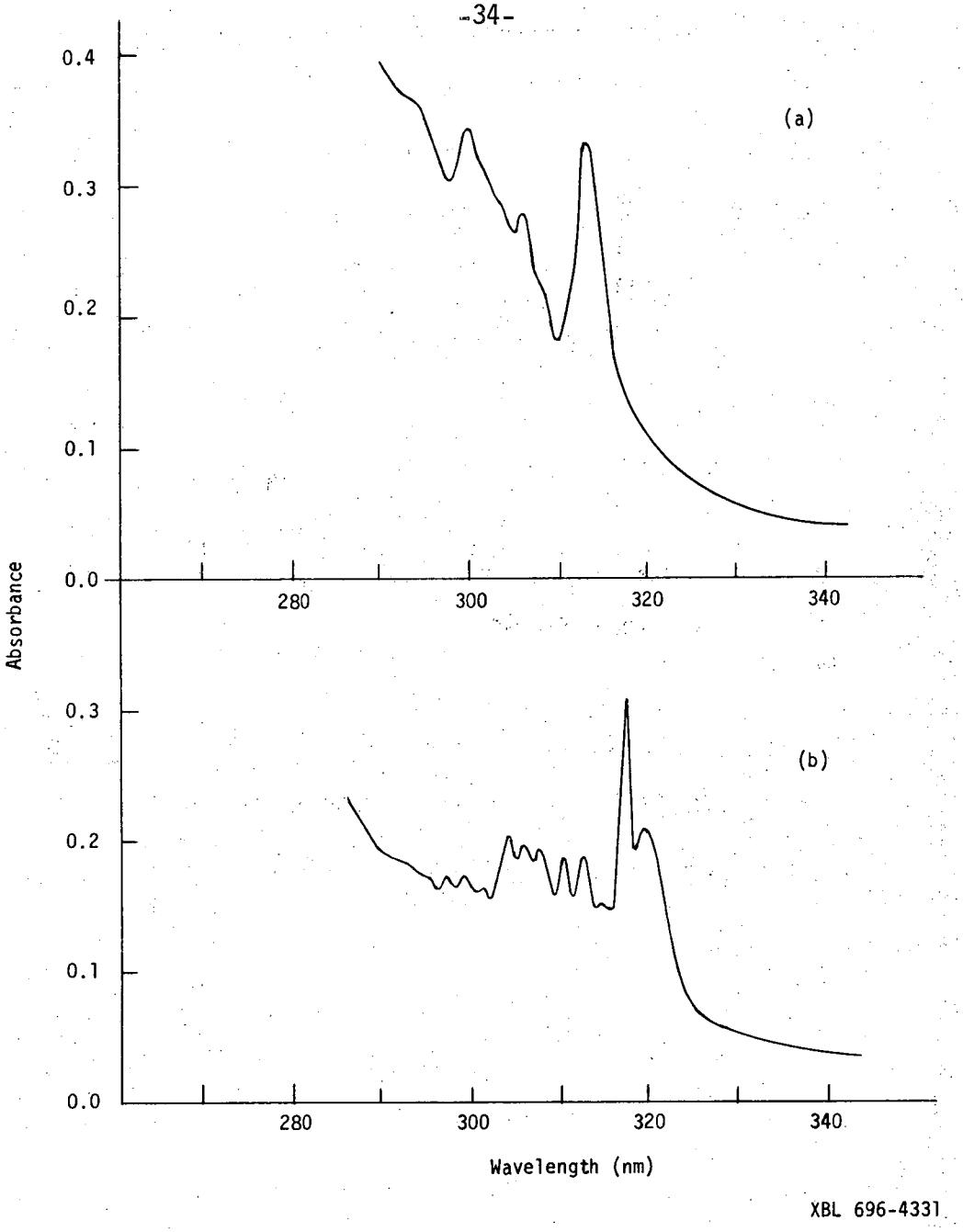

Figure II.13. Absorption spectra in an n-pentane matrix at 77°K.

(a) Quinoline, 2.3×10^{-3} M, 0.5 mm cell;

(b) Isoquinoline, 1.7×10^{-3} M, 0.2 mm cell.

There is a new band present at 77°K in the isoquinoline spectrum in n-pentane, 210 cm^{-1} to the red of the intense 318 nm band, and much broader than the rest of the spectrum in this region. It cannot be background absorption* of the 318 nm band since in that case it would have a center of gravity to higher energy of the sharp peak.[31,32] Possibly it represents absorption from dimers or other aggregates of isoquinoline.

Attempts to simulate McClure's experiments[40] with a durene (1,2,4,5-tetramethylbenzene) matrix, but using quinoline or isoquinoline instead of naphthalene as the guest, were unsuccessful. The spectra, shifted about 200 cm^{-1} to the red of the corresponding spectra in n-pentane at room temperature, were poorly resolved even at 77°K.

A summary of the spectra of quinoline and isoquinoline is given in Table II.3.

---

*By this term we mean absorption caused by transitions between the same energy levels of the guest molecule as are involved in Shpolskii transitions, but with energy exchange (Stokes losses) occurring with the solvent. The phononless transitions characteristic of Shpolskii spectra give rise to sharp lines, while transitions with energy exchange give a broad background band.

Table II.3. Summary of results of spectra of quinoline and isoquinoline.

Solute	Solvent	T (°K)	max (nm)	Appearance of spectrum (halfwidth of bands, etc.)
Quinoline	vapor	298	310.5	250 cm^{-1}, slight evidence of structure in first band
Quinoline	n-pentane	298	313	300 cm^{-1}
Quinoline	n-pentane	77	313	250 cm^{-1}
Quinoline	durene	298	315	400 cm^{-1}
Quinoline	durene	77	316	400 cm^{-1}
Isoquinoline	vapor	298	313	200 cm^{-1}; first band well resolved into sub-bands 25 cm^{-1} wide, at 313.9, 313.4, 313.1 and 312.5 nm. Other bands show some resolution.
Isoquinoline	n-pentane	298	317	200 cm^{-1}
Isoquinoline	n-Pentane	77	318	70 cm^{-1}; broad band at 320.1 nm, 210 cm^{-1} below first sharp band at 318 nm.
Isoquinoline	durene	298	320	400 cm^{-1}
Isoquinoline	durene	77	321	300 cm^{-1}

e) Acridine

Acridine (Figure II.14) has an absorption spectrum in non-polar solvents which is very similar to that of anthracene, its homocyclic analogue.

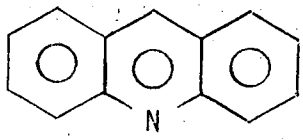

Figure II.14. Acridine

For example, in n-heptane at room temperature the first four intense bands are at 373, 356, 339 and 323 nm for acridine, and at 375, 356, 338 and 323 nm for anthracene. The bands are approximately 400 cm^{-1} wide in both cases. The acridine spectrum is somewhat less well resolved, probably as a result of lower molecular symmetry.

At 77°K in n-heptane, the two molecules started to exhibit different spectral behavior. Although the bands of both molecules were still fairly broad (ca. 200 - 300 cm^{-1} halfwidth), the band shape of the anthracene spectrum was decidedly asymmetrical and came to a pointed maximum, whereas the band shape for acridine was symmetrical and round-topped. This is shown for the first band of the two spectra, in Figure II.15.

At concentrations above about 10^{-3} M the acridine spectrum showed a broad band at 295 nm, absent in the room temperature spectrum, which by analogy with the corresponding band found at

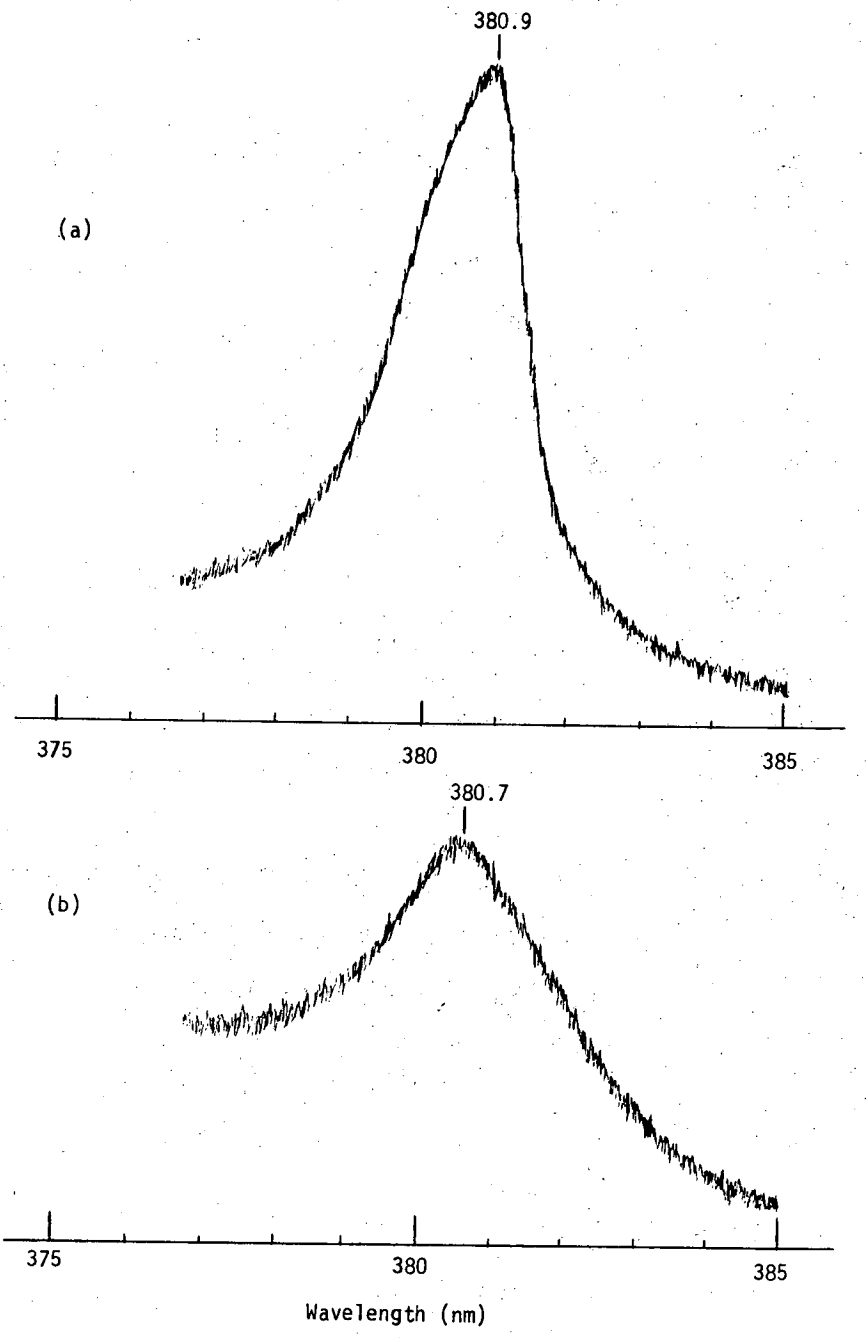

Figure II.15. Difference in the shape of the first band of the absorption spectrum in n-heptane at 77°K of (a) anthracene, and (b) acridine.

402 nm in concentrated anthracene solutions[44] is believed to be a dimer band.

At 4°K, the spectrum of anthracene in n-heptane displays an abundance of sharp lines, as is described fully in part II of the thesis.

Acridine, on the other hand, has a predominantly broad spectrum. At a concentration of 7.3×10^{-3} M a single sharp line was observed, at 381.9 nm. The presence of the dimer band mentioned above suggested that interaction between acridine molecules might be responsible for the overall width of the spectrum, and when the concentration was lowered to 4.9×10^{-5} M the dimer band disappeared and the sharp components of the spectrum increased to the point where 15 lines with a halfwidth of 25 - 50 cm^{-1} could be detected, superposed on a spectrum of bands whose width ranged from 100 to 300 cm^{-1}.

The lines and bands observed are listed, with their assignments, in Table II.4. A portion of the spectrum in the region of the origin is shown in Figure II.16.

As can be seen from the table, a large number (ten) of origins have been assigned. Some of these are probably lattice bands (see section 4d of part III of the thesis) but it was not possible to decide which, as the shape of the sharp spectrum is very difficult to determine bacause of the broad band background. Knowledge of the fluorescence spectrum would help, since pure electronic origins should be resonant.

Presumably more solute/solvent relationships are possible than in the case of anthracene since unless a site has D_{2h} symmetry in

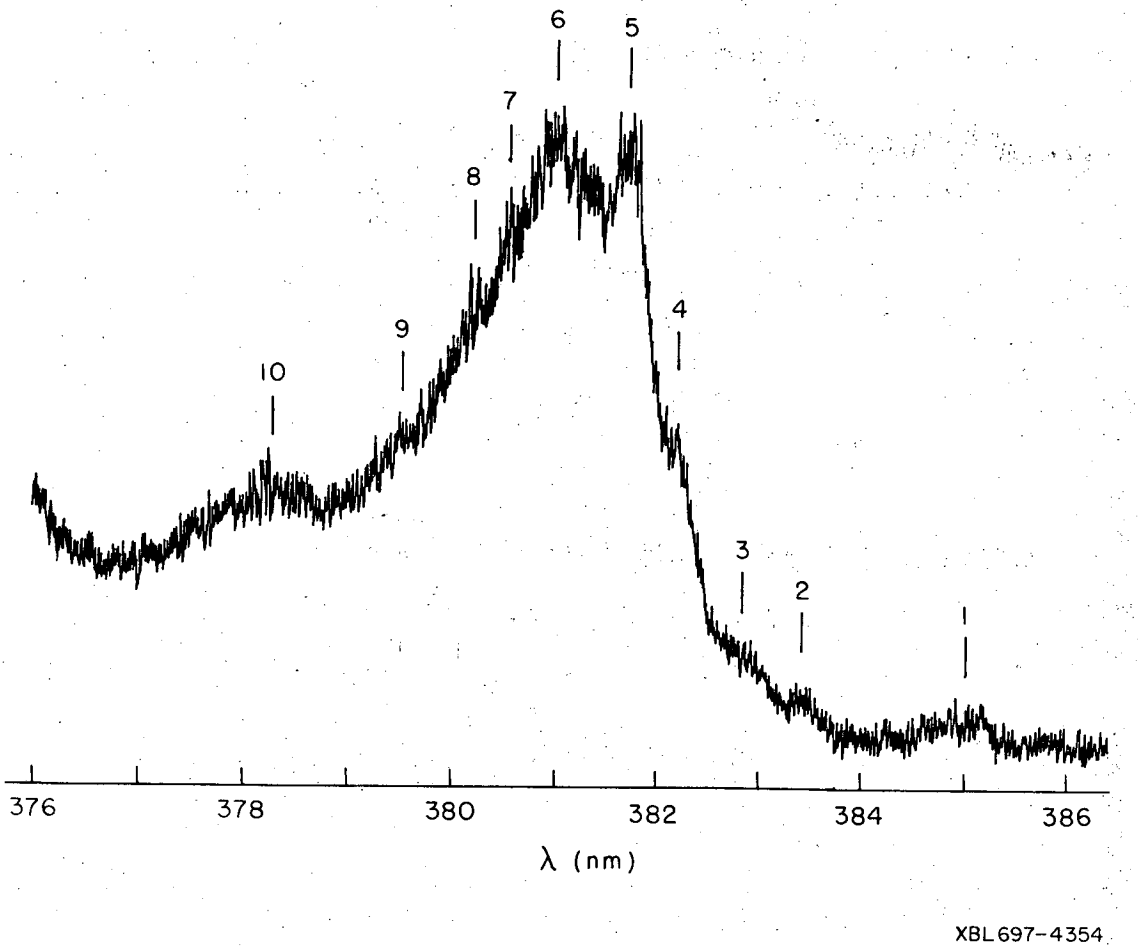

Figure II.16. Portion of the absorption spectrum of acridine (4.9×10^{-5} M) in n-heptane at 4°K.

Table II.4. Absorption spectrum of acridine in n-heptane at 4°K, 4.9×10^{-5} M.

Line or Band No.	Intensity	Sharpness	λ (A)	ν (cm^{-1})	$\Delta\nu(cm^{-1})$			Assignment
					0_4	0_5	0_6	
1	1	ms	3852	25960		-220		0_1
2	1	s	3836	26070		-110		0_2
3	1	ms	3830	26110		-70		0_3
4	1	s	3824	26150	0	-30		0_4
5	3	s	3819	26180		0		0_5
6	8	ms	3813	26230		50		0_6
7	1	s	3808	26260		80		0_7
8	1	s	3804	26290		110		0_8
9	1	s	3798	26330		150		0_9
10	3	mb	3785	26420		240	190	0_{10}
11	5	mb	3755	26630			400	0_6 + 400
12	4	mb	3723	26860			630	0_6 + 630
13	3	mb	3699	27030			800	0_6 + 2x400
14	4	mb	3671	27240			1010	0_6 + 400 + 630 - 20
15	1	s	3658	27340		1160		0_5 + 1160
16	3	ms	3648	27410			1180	0_6 + 1160 + 20
17	1	s	3633	27530	1380			0_4 + 1400 - 20
18	2	s	3626	27580		1400		0_5 + 1400
19	9	mb	3619	27630			1400	0_6 + 1400
20	1	ms	3606	27730		1550		0_5 + 400 + 1160 - 10
21	1	ms	3596	27810			1580	0_6 + 400 + 1160 + 20
22	10	b	3566	28040			1810	0_6 + 400 + 1400 + 10
23	7	b	3473	28790			2560	0_6 + 1160 + 1400
24	7	b	3451	28980			2750	0_6 + 2x1400 - 50

the crystal field, rotation of the molecule through π about the Z axis (Figure II.17) will alter the interaction with the site, and produce another origin in the spectrum.

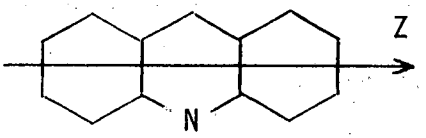

Figure II.17.

The broad band (#10) is believed to be an electronic origin rather than a vibronic band, because its position corresponds to that of the intense origin 184 cm^{-1} from the main origin in the spectrum of anthracene (see part III of the thesis).

Four vibrational frequencies have been extracted from the acridine spectrum. They are given in Table II.5.

Table II.5. Vibrational frequencies of acridine, with the corresponding frequencies for anthracene.

Frequency (cm^{-1})	
Acridine	Anthracene
400	390
630	or 587, 662 ?
1160	1159
1400	1397

The modes at 1160 and 1400 cm^{-1} were derived from 0_5 (Table II.4), an intense, sharp origin, and are believed to have an error of $\pm$ 5 cm^{-1}. The other two modes were only observed as bands derived from the broader origin 0_6 and have an estimated error of $\pm$ 25 cm^{-1}. Because of this low accuracy, it is not possible to say whether the differences between the acridine and anthracene frequencies are significant.

The reason for the dual nature of the acridine spectrum (sharp lines on a broad background) is of interest. Broad spectra frequently stem from molecular aggregates, and it could be that Shpolskii transitions are occurring only from that fraction of the molecules present in monomeric form. However, since the dimer band present at 7.3×10^{-3} M disappears when the concentration is lowered to 2.2×10^{-4} M, it seems certain that in the sample for which the spectrum is reported, with a concentration of 4.9×10^{-5} M, only monomer is present. The preponderance of broad bands would then simply indicate a low phononless transition probability, as a result of fairly high average Stokes losses (see part I of the thesis).

The distribution of probability between phononless transitions (giving sharp lines) and transitions with energy transfer to the solvent matrix (giving broad bands) is predicted by theory.[26,27] Acridine provides a clear demonstration of the validity of this prediction which has been somewhat lacking in the Shpolskii spectra described in the literature. I believe the reason for this is the following. The width of phononless lines is temperature dependent, probably because the environment which a molecule in a given site

experiences is dependent on the relative positions of the solute and solvent atoms, and these positions fluctuate with an amplitude which is dependent on the degree of librational and vibrational excitation. The probability of phononless transitions is also temperature dependent,[26-28] increasing rapidly with decreasing temperature. For a molecule with low average Stokes losses the bands representing transitions with energy transfer to the solvent will be relatively narrow (say 100 cm^{-1}) in a low temperature matrix. There will also be an appreciable phononless transition probability at relatively high temperatures, giving rise to rather broad Shpolskii lines (say 50 cm^{-1}). Superposition of these two (with the Shpolskii line at higher energy) will give a band shape similar to that in Figure II.18a, which is the sum of two Gaussians of equal amplitude, one with half the width of the other. The spectra of aromatic molecules in n-alkane matrices at 77°K frequently have band shapes like this. Lowering the temperature to narrow the Shpolskii lines reduces the non-Shpolskii intensity effectively to zero, and only the sharp lines are seen.

With a molecule like acridine, on the other hand, which has higher average Stokes losses, the spectrum is characterized by bands which are broad (say 200 cm^{-1}) even at 4°K; Shpolskii lines only appear at this low temperature, and with a low intensity, but they are narrow. This gives rise to a band shape like that in Figure II.18b, which is the sum of two Gaussians, the narrow one having 25% of the amplitude and 10% of the width of the broad one. Comparison with an actual band of the acridine spectrum (Figure II.16)

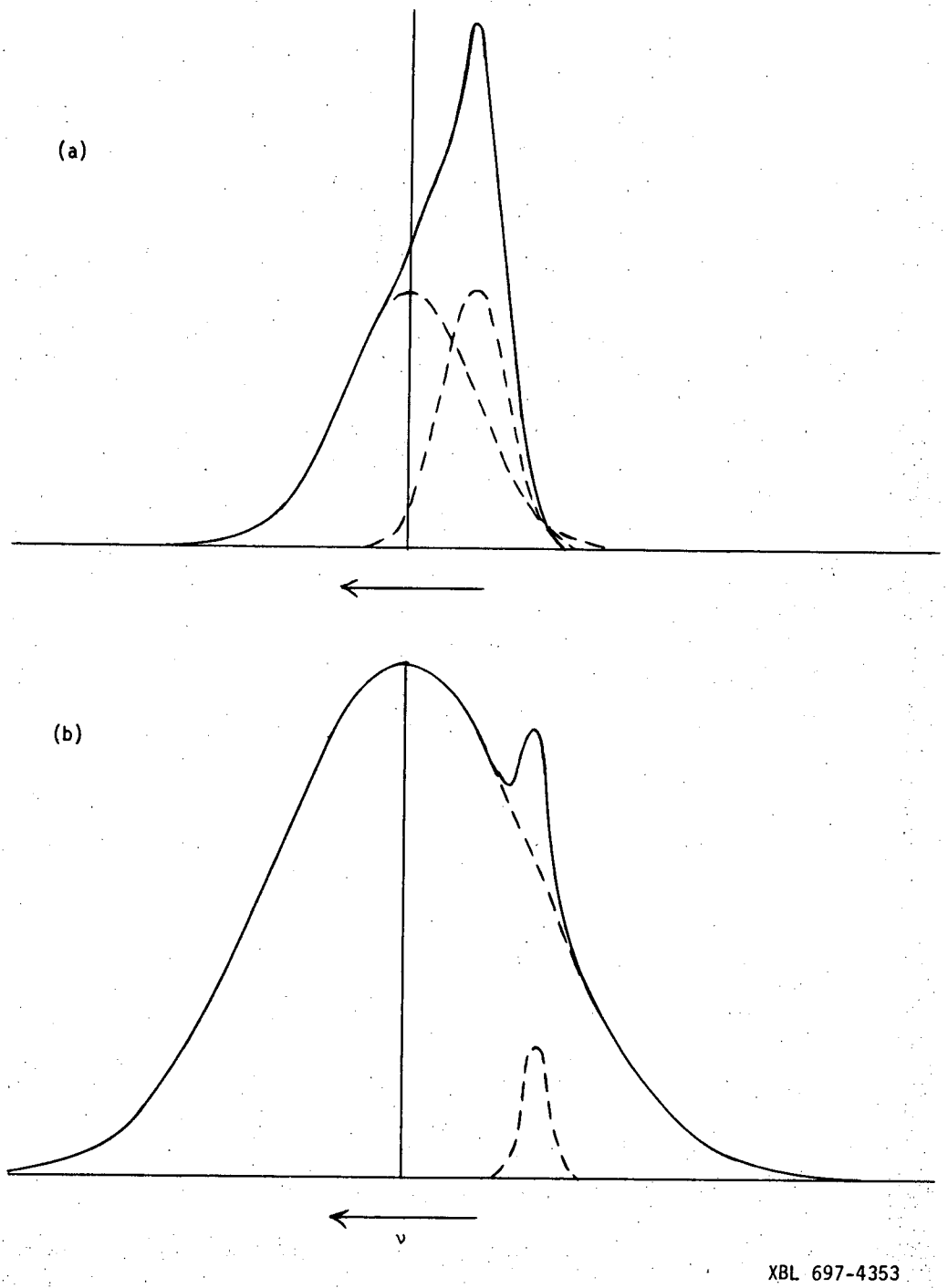

Figure II.18. Superposition of gaussians to simulate the appearance of Shpolskii spectra.

(a) Narrow band 50% of width, 100% of height of broad band;
(b) Narrow band 10% of width, 25% of height of broad band.

shows this, although the presence of multiple origins makes the band shape more complex.

f) β-Carotene

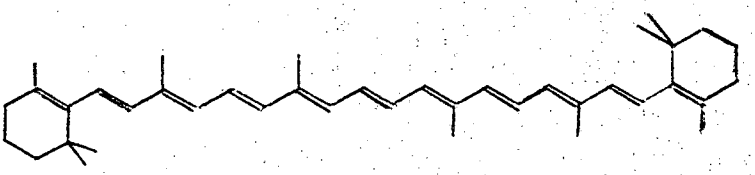

Figure II.19. β-Carotene.

In its all-trans form, β-carotene has a spectrum consisting of three poorly resolved bands in the region 390 - 500 nm. Cis-isomerization of the double bonds removes the center of symmetry of the molecule and allows another transition to take place, at ca. 340 nm. No cis-band was evident in the spectra taken in this work.

The long axis dimension of all-trans β-carotene is 32 A (measured from a CPK model). n-Octacosane ($n\text{-}C_{28}$), with a length of 37 A, was available commercially in 97% purity and was considered to be a reasonable candidate as a matrix.

The spectrum, however, turned out to be broad, even at 77°K, and showed little improvement in resolution over the room temperature spectrum in n-hexane. The only additional feature was a fourth band in the 1400 cm^{-1} vibrational progression of the spectrum.

Changes in the positions of the bands are of interest. Table II.6 shows the positions in hexane and n-octacosane.

Table II.6. Spectrum of all-trans β-carotene in n-hexane and in n-octacosane. Position of vibronic bands given in nm.

n-hexane	n-octacosane	
298°K	298°K	77°K
478	490	502
449	458	469
423	432	440
---	407	416

The unusually large shift of β-carotene on going to low temperatures has been recorded previously by Wald,[45] who explained it as follows. At high temperatures the molecule has a large amount of vibrational energy and therefore spends much of its time away from a true trans configuration. This has the effect of shortening the "resonance length" of the electron cloud (cf. theory of a particle in a one-dimensional box) and hence increasing the transition energy. As the temperature is lowered the molecule spends more of its time in the trans configuration, and so the spectrum is red-shifted.

The spectrum in n-octacosane provides interesting confirmation of this theory. The matrix is a solid at room temperature and provides the constraint on the β-carotene molecule normally produced by low temperature.

5. General discussion

It will have become apparent from reading the foregoing chapter that high resolution spectra of biologically interesting molecules are not easy to obtain. The difficulties encountered can be summarized as (i) spectral complexity resulting from low symmetry, (ii) insolubility, and (iii) low phononless transition probability.

The greatest degree of success achieved was with acridine in n-heptane at 4°K, when some 15 relatively sharp lines were measured. I believe there are several reasons for this. The molecule has fairly high symmetry; this simplifies the spectrum and reduces the number of multiplet components. The cuvettes used to study acridine were sealable, unlike those used in the earlier studies; this enabled freeze-pump-thawing, and the resultant improvement in transparency allowed lower solute concentrations to be used, and the sample to be frozen more slowly. Perhaps the most important factor was temperature. The rest of the molecules were studied at 77°K, before I was equipped to study spectra at the temperature of liquid helium (4°K).

It was thought then that the broad bands observed at 77°K implied that further temperature reduction would not produce significant spectral changes. However, the results with acridine together with the discussion of band-shape in chapter 4, section (e) show that this is not necessarily the case. Where bandwidth is limited by non-uniformity of the environment, as I believe is the case in the low temperature spectrum of benzene in n-butane, further

temperature reduction will not be effective, but where the limitation is placed by energy exchange with the matrix, then temperature reduction may increase the phononless transition probability to the point where it can be observed as low intensity sharp lines on a broad background, as in the acridine spectrum.

Acridine appears to be near the limit of the usefulness of the Shpolskii technique; because of scattering and the high background absorption the signal level was low, and the sharp lines were almost buried in noise. It seems likely that a molecule like purine, even if it could be dissolved directly in an n-alkane solvent, would couple too strongly to have a measurable Shpolskii spectrum. The Shpolskii lines in the acridine spectrum, ca. 25 - 50 cm^{-1} wide, are broader than those generally encountered in the spectra of aromatic molecules. I can think of two possible explanations of this. (i) The second "site", or rather solute/solvent interaction, which will result when the molecule is rotated through π about its z-axis (see chapter 4, section (e)) may be too close in energy to the original to be resolved and may simply result in line broadening. (ii) The linewidth of phononless transitions is several orders of magnitude greater than the radiation width. This is generally thought[17] to be a result of the fluctuations in solute/solvent interaction which accompany molecular libration and vibration and lattice vibration. These fluctuations cause alterations in the energy levels of the guest molecule and hence line broadening. (Note that this is quite distinct from the variable energy transfer accompanying usual transitions in a condensed environment.) The

linewidth will be determined both by the extent of the environmental variation, and the sensitivity of the energy levels of the guest to the variation. Temperature will affect the former of these, as will the precision of the fit of the guest molecule in the host lattice. Acridine and anthracene should not differ greatly in this respect, but by virtue of the lone pair electrons on the nitrogen atom, acridine will be more sensitive to environmental variation, and will have a broader Shpolskii spectrum. In the non-Shpolskii portion of the spectrum this effect is obscured by the much greater broadening caused by variable energy transfer.

6. Conclusions

(i) Cyclohexane as a monoclinic crystal can be used as a matrix for Shpolskii spectra, as is shown by my early spectra of benzene in cyclohexane at 77°K and by the work of Leach and Lopez-Delgado,and Spangler and Kilmer. To avoid the cubic form of the crystal, which gives rise to a broad solute spectrum, solutions must be frozen slowly and this places a limit on the solute concentration which can be used.

(ii) The spectrum of benzene in n-butane at 77°K is broad. Phononless transitions are probably occurring but are obscured by environmental broadening caused by the loose fit of the benzene molecule in the n-butane crystal.

(iii) Pyrimidine in cyclohexane at 77°K has a broad spectrum. The spectrum might be narrowed by slow cooling to avoid freezing in the cubic form of the cyclohexane crystal.

(iv) Purine is very insoluble in n-alkanes. In n-pentane, with 1% of 1-pentanol to increase solubility, the spectrum was poorly resolved at 77°K.

(v) Quinoline in n-pentane at 77°K has a poorly resolved spectrum. Isoquinoline has a much sharper spectrum with several bands ca. 70 cm^{-1} wide. The greater sharpness of the spectrum of isoquinoline was found to apply in the vapor phase also, and is thought therefore to be an intrinsic property of the molecule. A hypothesis put forward to explain this relates the symmetry species of the transition dipole operator to that of the perturbation introduced by the azo group.

(vi) The spectra of quinoline and isoquinoline in durene at 77°K are poorly resolved.

(vii) Acridine in n-heptane has a broad spectrum at 77°K, but at 4°K a moderately sharp spectrum appeared with low intensity over an intense broad background. About 15 lines were measured and 4 vibrational frequencies extracted.

(viii) All-trans β-carotene in n-octacosane at 77°K has a broad spectrum. This could be because of a low phononless transition probability, or simply because of environmental broadening. The large red shift of the spectrum in n-octacosane, even at room temperature, compared to the spectrum in a liquid solvent such as n-hexane confirms Wald's theory of increased trans character in the constrained β-carotene molecule.

7. Suggestions for future work

In the light of the acridine results, it is apparent that more work at 4°K is desirable. Isoquinoline in n-pentane, and pyrimidine in a slowly cooled cyclohexane matrix would make an interesting start.

Another approach would be to block azo or other polar groups in an attempt to reduce the coupling to the matrix. This could be done either by covalently bound blocking groups, e.g.,

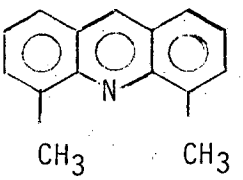

or by forming a solvated complex as has been done with some porphyrins. An additional advantage gained by blocking polar groups is the increased solubility in a non-polar solvent such as an n-alkane.

Wherever possible, fluorescence spectra should also be taken. They are often sharper than absorption spectra, and are less obscured by lattice bands. Comparison of absorption and fluorescence helps in differentiating between multiple origins and vibrational modes.

Sealable cuvettes should be used and samples thoroughly freeze-pump-thawed to remove dissolved gases, which are a major cause of scattering in the frozen matrix. As low a solute concentration as possible should be used so that the matrix can be frozen more slowly. This results in a more transparent crystal, and also a greater concentration of spectral intensity in one component of the multiplet structure, making detection of the sharp spectrum easier. In this context it would be profitable to study the effect of annealing on the sharpness and intensity of the Shpolskii spectrum.

The Cary 14 was not really suitable as a spectrometer for this type of work. The wavelength scan was insufficiently accurate, the resolution inadequate, and the signal/noise ratio for highly scattering samples was low. In addition, only absorption spectra could be taken.

Future work should be carried out on a high resolution single-beam spectrometer, with either a very high gain photo-tube or photographic detection. Such an apparatus was used successfully in studying the Shpolskii spectrum of anthracene, to be described in the next part of the thesis.

III. THE ABSORPTION AND FLUORESCENCE SPECTRA OF ANTHRACENE AND [D_{10}]-ANTHRACENE IN A VARIETY OF MATRICES AT 4°K

1. Introduction

In part II of this thesis, studies of the low temperature electronic absorption spectra of a number of molecules were described. The purpose was to move from relatively well studied molecules such as aromatics to other molecules which were of interest in biological systems. One of these studies was a comparison of the spectrum of anthracene with that of acridine, a heterocyclic analogue.

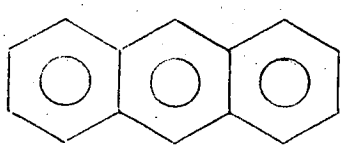

Figure III.1. Anthracene

The absorption and fluorescence spectra of anthracene in n-heptane at 4°K had been reported previously by Bolotnikova,[11] and of course a comparison of her data with those of the present work was made.

One feature reported in ref. 11 was of great interest, and I quote here at length:

"The main interest lies in the behaviour of anthracene in n-heptane.* In this case the linear dimensions of anthracene correspond to the linear dimensions of the solvent molecule. The splitting of the 0-0 band in the fluorescence and absorption spectra is 390 cm^{-1}, which is equal to a very intense vibrational frequency of anthracene.

Cases in which a splitting of the 0-0 band was found in quasi-line spectra, with the frequency difference equal to a vibrational frequency, had been observed previously. Thus in the spectrum of naphthacene in n-nonane the splitting of the 0-0 band is 310 cm^{-1} (this is the lowest vibrational frequency of naphthacene appearing in fluorescence and absorption spectra). The 0-0 band of rubicene in n-nonane at 20°K displays a splitting of 195 cm^{-1}. The 0-0 band of stilbene in tolane shows a splitting of 206 cm^{-1} at 20°K. This problem requires further investigation."

In other words, two lines attributed to a splitting of the origin existed with a separation equal to one vibrational quantum. It is not strictly correct for Bolotnikova to say that it was observed in absorption since the weaker of the two lines lies to higher energy and is coincident with the intense first vibrational band of the 390 cm^{-1} mode.

Assuming that Bolotnikova's observation in fluorescence could be substantiated, the following questions had to be answered:

(i) Do both lines represent pure electronic transitions?

(ii) If they do, what is the cause of the splitting?

(iii) In what way is the splitting related to a vibrational quantum?

(iv) If the line to higher energy does not represent an electronic

---

*The spectra in n-hexane at 77°K were also reported.

transition, what does it represent, and why is it related by a vibrational quantum to the main origin?

(v) If the fact that the spacing between the two lines is equal to a vibrational quantum is simply a coincidence, are the lines just a part of the multiplet structure encountered in Shpolskii spectra?

Bolotnikova assumes that the answer to (i) is "yes" when she speaks of the splitting of the 0-0 band. However, she does not describe it as a splitting of the usual multiplet type. What other causes of a splitting there might be is not clear. Presumably any splitting resulting from exciton interaction would be concentration dependent (see, e.g., ref. 46), and no theoretical basis for an intramolecular degeneracy has been given. What, of course, is most obscure of all is how vibrational energy could enter into the splitting of two purely electronic energy levels.

At this point I concluded that either (a) the two lines are purely electronic and the relationship to vibrational energy is coincidental, or (b) the higher energy line is not purely electronic, but includes a quantum of vibrational energy.

If the coincidence theory is correct the lines could be explained in the usual way as components of a multiplet. In Shpolskii spectra there is nothing unusual in having secondary origins to higher energy than the main origin, although the energy difference here (390 cm^{-1}) is unusually large. Most of the spectra which have been reported in the literature have multiplet splittings of less than 100 cm^{-1}.

But the biggest difficulty in accepting the coincidence theory is simply the degree of coincidence, namely that, according to ref. 11, in at least four molecules a splitting exists which, within experimental error (ca. 1 or 2 cm^{-1}) is exactly equal to a vibrational quantum.

Initially I made the hypothesis that the high energy fluorescence line represents a vibronic transition from the first excited vibrational level of the upper electronic state to the zero-point vibrational level of the ground electronic state (Figure III.2).

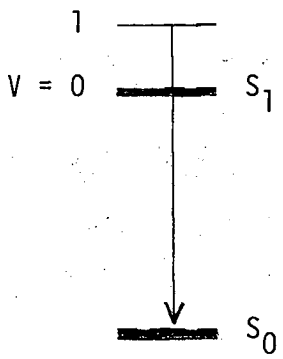

Figure III.2. Scheme to explain the line observed to high energy of the main origin in the fluorescence spectrum of anthracene in n-heptane at 4°K.

Since the temperature at which the spectra were taken (4°K) was too low to maintain thermally any substantial population of a level 390 cm^{-1} above the pure electronic level, the hypothesis was in fact that the radiative lifetime for the $(1' \rightarrow 0)$ vibronic transition was comparable to the lifetime for the $(1' \rightarrow 0')$ radiationless vibrational relaxation.

Vibrational relaxation is generally so much faster than radiative emission that the latter occurs from a Boltzmann distribution of vibronic levels of the upper state. As far as I am aware there are no recorded exceptions to this rule for a molecule in a condensed environment, and hence the present case is of great interest. The fluorescence lifetime of anthracene in cyclohexane solution is 4.9 nsec,[33] a typical value for singlet-singlet emission; we would expect a similar value in n-heptane.

The hypothesis is therefore that for anthracene in a low temperature n-heptane matrix, vibrational relaxation is unusually slow. Is there anything else in the nature of Shpolskii spectra to suggest this?

First, we may note that since we are considering a molecule with only one quantum of the least energetic vibrational mode, no intramolecular relaxation is possible, and so we are concerned only with relaxation to the lattice.

Then, recall that one of the outstanding features of Shpolskii spectra is that the molecule undergoes phononless transitions, because coupling to the lattice is weak; this is just the condition necessary to inhibit relaxation.*

---

*The nature of the coupling is not exactly the same in both cases. In one case the adiabatic potential between the molecule and its environment changes as a result of the optical transition. Only the electronic configuration of the molecule changes (the Born-Oppenheimer approximation) and we may expect it to produce a change in the Coulombic potential. In the other case the molecule and the lattice act as coupled oscillators; the change in the nuclear and electronic configurations of the one produces a change in the potential with respect to the other.

For theories of radiationless transitions, see e.g. refs. 47-50. Unfortunately, existing theories are concerned principally with relaxation from higher excited electronic states to the lowest excited electronic state, with the assumption that vibrational relaxation has already taken place.

The hypothesis of slow relaxation therefore appeared at least to be reasonable. In order to test it, the following experiments were planned.

(1) Repetition of Bolotnikova's experiments on anthracene in n-heptane to confirm that the observation was correct, and that the agreement with the vibrational frequency was exact.

(2) Search for lines to still higher energy. In particular, search for a line at ca. 1400 cm^{-1} from the origin to correspond to the other most intense vibrational mode of anthracene. If present, its intensity would give information on relative rates of relaxation from two vibrational levels of considerably different energy.

(3) Use of n-hexane and n-octane as matrices to see whether the phenomenon was sensitive to these variations.

(4) Study of the spectra of $[D_{10}]$-anthracene in all three matrices. Assuming that the phenomenon could still be observed, the high energy line should now be displaced from the origin by exactly the amount of a vibrational quantum of the deuterated molecule, which should be about 5%, or about 20 cm^{-1}, smaller than in the undeuterated molecule. If exact agreement with the deuterated mode was not observed, the phenomenon would require another explanation. If the line could not be observed or was of greatly different intensity this would demonstrate an interesting difference in the relative relaxation rates of the two molecules.

In addition to testing the main hypothesis, it was felt that the series of experiments would also give the following information:

(1) Vibrational analysis of anthracene; it was hoped that the use of several matrices would enable a more rigorous identification of frequencies than was made by Bolotnikova.

(2) Vibrational analysis of $[D_{10}]$-anthracene, which has not been reported hitherto.

(3) Correspondence of the modes in the undeuterated and deuterated molecules.

(4) Information on the nature of the multiplet structure by studying its appearance in the various matrices, in absorption and fluorescence, and the changes, if any, on using the deuterated guest. If the structure was similar to that with the undeuterated guest, this would make identification easier since the vibrational structure would be different.

The work to be described in this part of the thesis consisted then of the taking and examination of a series of 12 low temperature spectra:

2 (anthracene and $[D_{10}]$-anthracene) x 2 (absorption and fluorescence) x 3 (n-hexane, n-heptane, and n-octane matrices).

In order to carry this work out, it was no longer possible to use the Cary 14 spectrometer described in part II, and a completely new high resolution spectroscopic system, capable of taking fluorescence as well as absorption spectra, had to be built. The optical dewar of part II could be used, after modification to include a three window tail.

Chapter 4 presents the results and discussion of these experiments. The main data tables, with identification of the spectral lines, must inevitably come at the beginning, and in order to make the identification a vibrational analysis must be done. Consideration of the question of fluorescence from vibrationally excited levels therefore comes after a great deal of other detailed description.

In view of this, I will make the following brief comment to avoid misleading the reader:

The present work has confirmed the observation of Bolotnikova, but has demonstrated unambiguously that the hypothesis of fluorescence from vibrationally excited molecules is incorrect. Study of the spectra of deuterated anthracene showed that the agreement with a vibrational quantum in the case of undeuterated anthracene was in fact quite accidental.

2. Materials

The n-alkanes were 99% mol. minimum purity, ex Phillips Petroleum Company. In order to reduce the level of olefinic and aromatic impurity they were passed over an 8 ft long column of silica gel (gas chromatograph grade, 30/60 screen size, ex Coast Engineering Laboratory, Redondo Beach, Calif.) which had been activated at 400°C for 3 to 4 hours. Successive fractions were collected and their UV absorption spectra measured on a Cary 14. When the absorption rose

appreciably, collection was terminated and the previous fractions combined. The absorbance of this material in the range 200 - 250 nm was typically 10 to 20% of the untreated level.

The anthracene used in a number of preliminary investigations was specified by the manufacturer, Eastman Organic Chemicals, as "Anthracene (Blue-Violet Fluorescence)" and was vacuum sublimed before use. In later experiments a very high purity material, Prinz Quality (99.999% purity, i.e. impurities below the limits of detection by gas chromatography and mass spectroscopy), ex Princeton Organics, was used without further purification. The data reported in this section of the thesis were obtained with the Prinz material, although a visual comparison of the spectra of the two materials showed no evidence of impurity peaks in the Eastman material.

The $[D_{10}]$-anthracene, of >98% isotopic purity, was obtained from Schwarz Bio-Research and was used without further purification.

3. Experimental

a) Sample preparation

Solutions were prepared at room temperature. The concentration was calculated from the absorbance of the solution at the main (356 nm) peak of the ^1L_a transition and adjusted if necessary. As soon as possible after making up a solution (a maximum delay of two hours) it was transferred to a cuvette, subjected to about five freeze-pump-thaw cycles (to a final pressure of 10^{-3} mm Hg), and the cuvette was drawn off and sealed. Outgassing of the sample was done primarily because non-outgassed samples were much more highly

scattering, making absorption measurements difficult, and also to prevent sample oxidation. Risk of photo-decomposition was minimized by storing samples in the dark.

After experimenting with various cuvette designs, I settled for one with the following dimensions:

Optical faces: 50 mm high x 25 mm wide

Optical path: 4 mm (internal)

The cuvettes were made of Pyrex, in this laboratory, and were fused to 7 mm. Pyrex tubing which after sealing could be inserted into the sample mount of the dewar system. Because the cuvettes were fabricated without the use of low-temperature fluxes there was a certain amount of distortion of the optical faces, but this was considered unimportant in view of the high level of light scattering from the polycrystalline samples. With this design of cuvette and using angled front-face illumination and detection (see section b), a good signal/noise level was obtained.

Prior to the measurement of its low temperature spectrum, the sample was cooled in one of the following ways:

(i) Plunge freeze into liquid nitrogen (77°K),

(ii) Lowering by hand into liquid nitrogen sufficiently slowly (1-2 min) that freezing took place above rather than in the liquid nitrogen and proceeded smoothly from bottom to top of the sample.

(iii) Lowering by low-speed motor into liquid nitrogen. Using a 2 rev/hr motor with different size rubber wheels on the output axle, a range of freeze times of 1/2 to 2 hours was possible.

Results in Chapter 4 are for samples cooled by method (ii). After cooling to liquid nitrogen temperature the cuvette was quickly transferred to the pre-cooled optical dewar.

b) Apparatus for measuring spectra

The layout of the apparatus used for measuring low temperature absorption and fluorescence spectra is shown schematically in Figure III.3; photographs of various aspects of the apparatus are given as Figures III.4 through III.8.

For absorption measurements, white light from a xenon lamp was collimated, chopped, and then passed through the sample which was mounted inside an optical dewar. The transmitted light (divergent because of scattering) was condensed on the entrance slit of an analyzing monochromator. The diffracted exit beam from the monochromator was either photographed, or scanned and detected by a photomultiplier tube whose output was amplified and rectified by a lock-in voltmeter coupled to a strip-chart recorder.

For fluorescence measurements, the white light was diffracted by a low resolution monochromator and a selected band used as the excitation source for the sample. This light was chopped and condensed onto the sample at an angle of approximately 45° to the normal of the optical face. Emission at approximately 90° to the incident beam was collimated and condensed onto the entrance slit of the analyzing monochromator and detected as in the absorption measurements.

A more detailed description of individual components of the apparatus follows; for reference purposes, model numbers and manufacturers are given as appendix A.

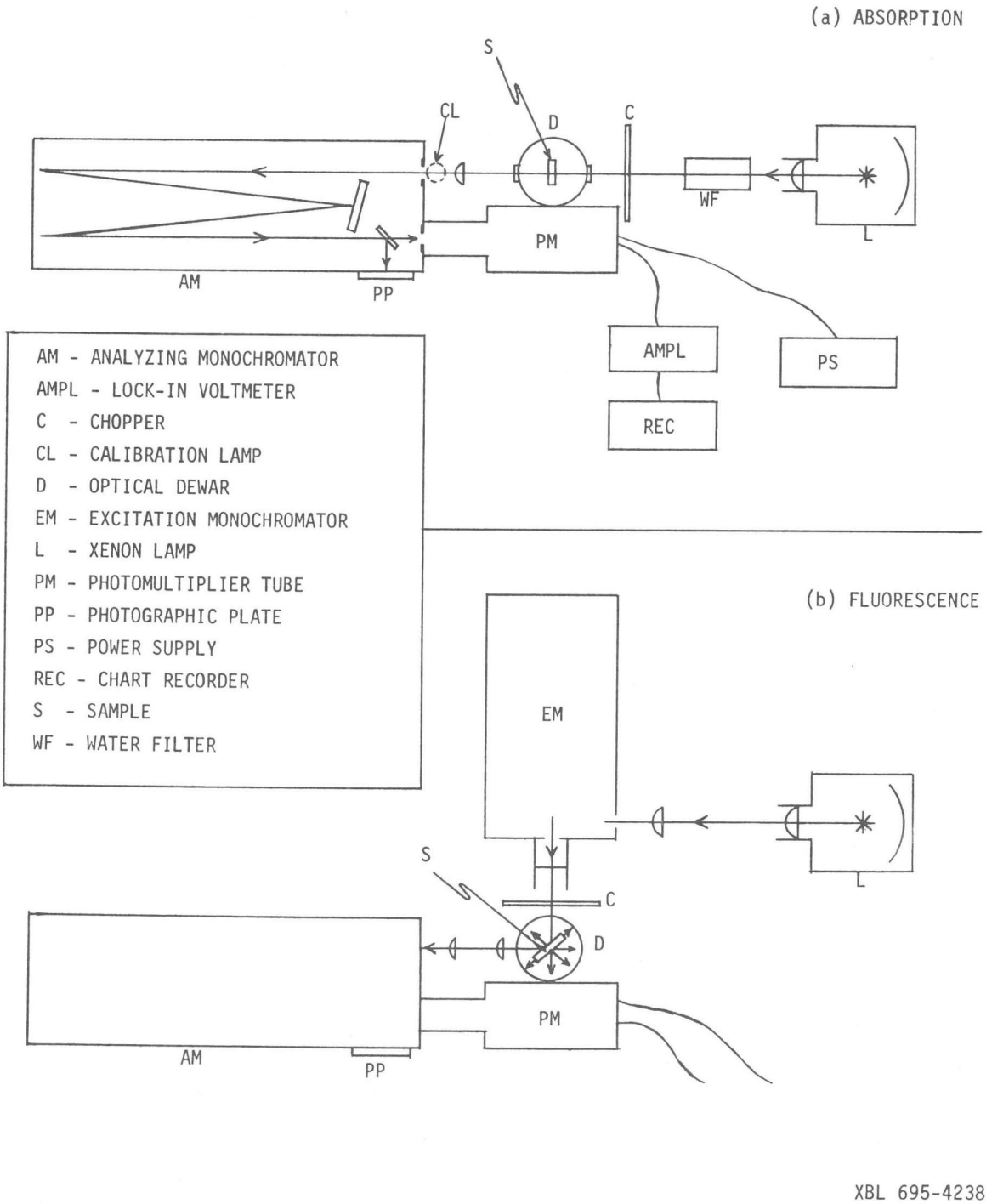

Figure III.3. Layout of apparatus for measuring spectra.

Approximate scale, 1 in : 1 ft.

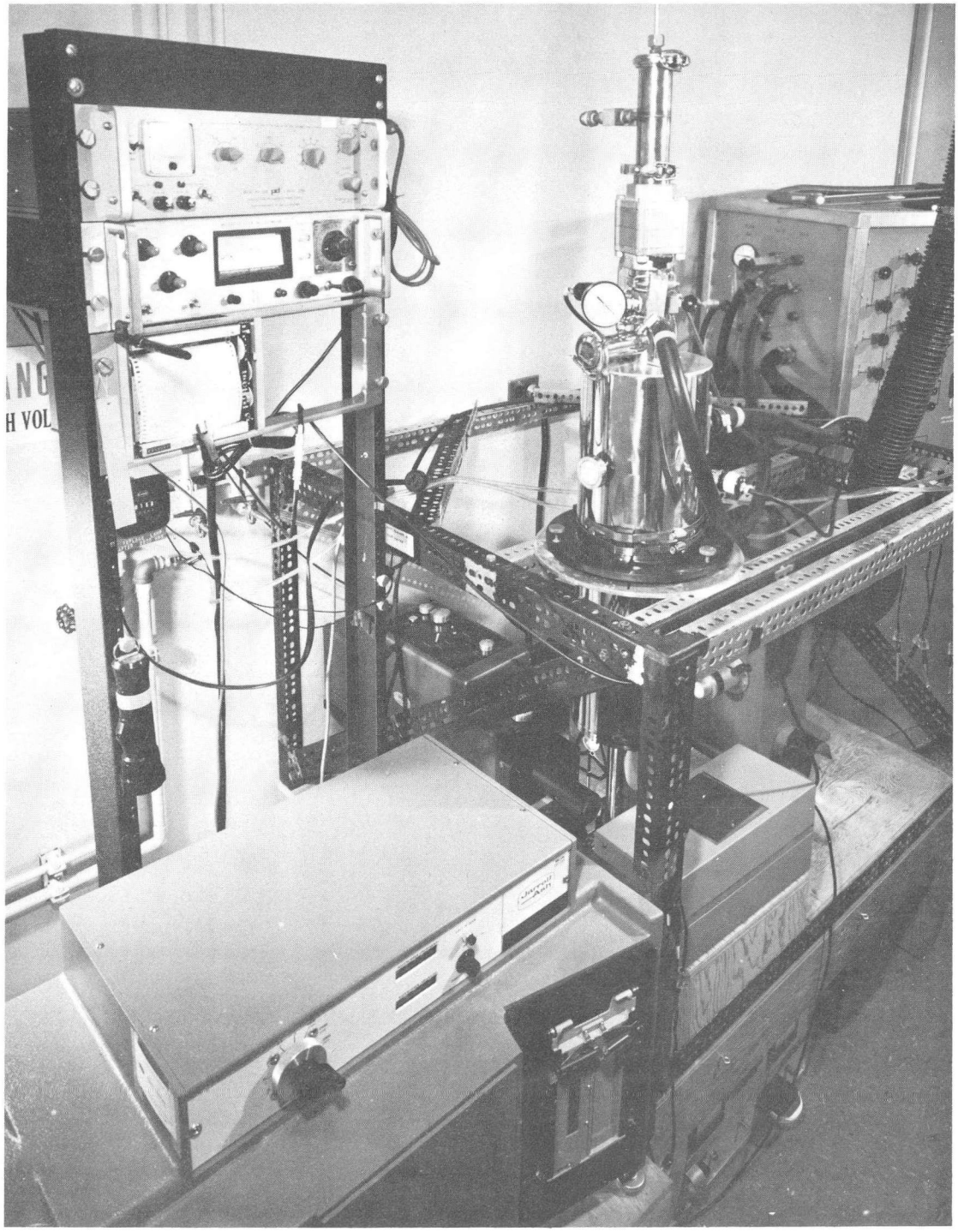

XBB 694-2674

Figure III. 4. General view of apparatus for measuring spectra.

XBB 694-2673

Figure III. 5. Arrangement of apparatus for fluorescence measurements.

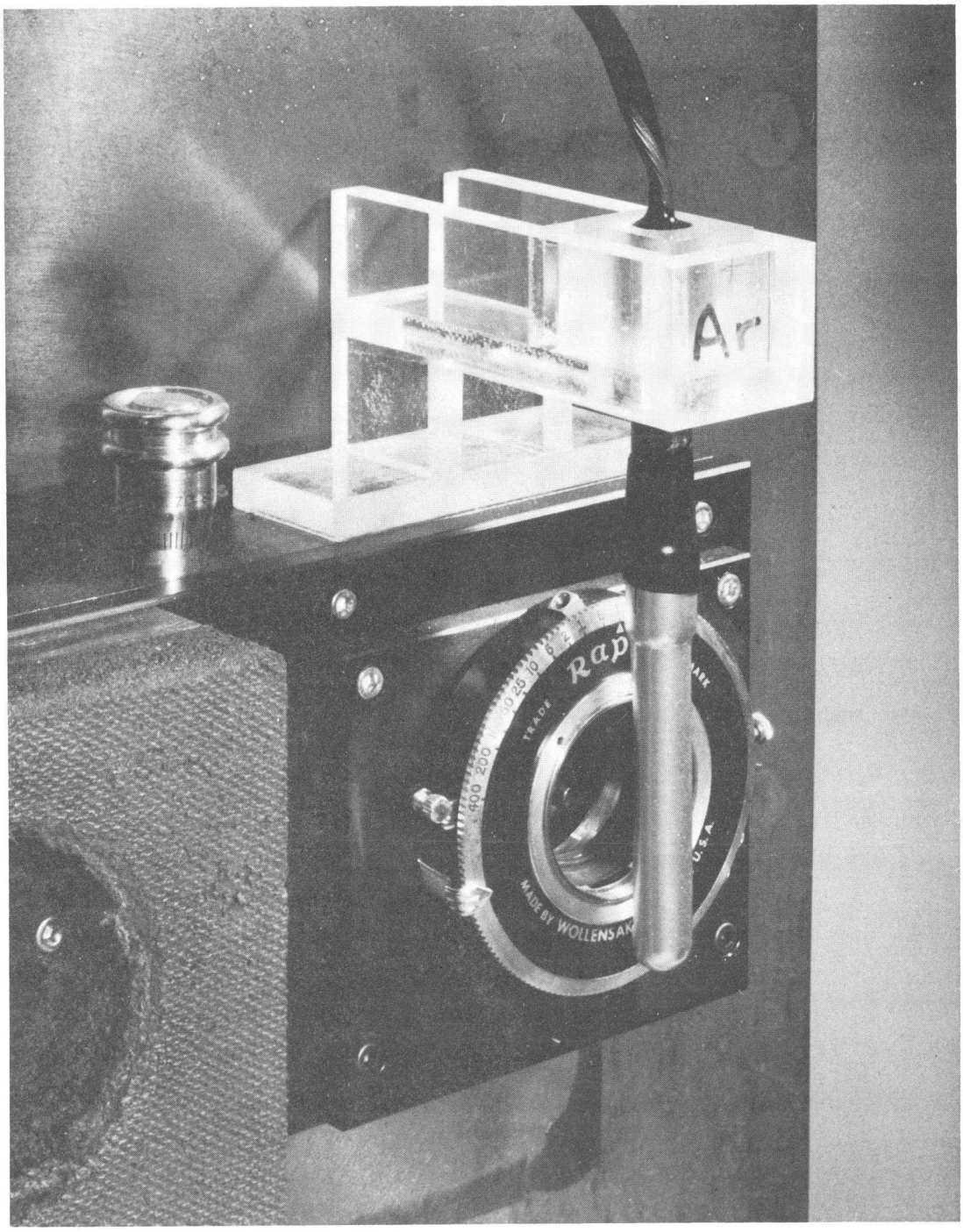

XBB 694-2677

Figure III. 6. Method of locating calibration lamps in front of monochromator entrance slit.

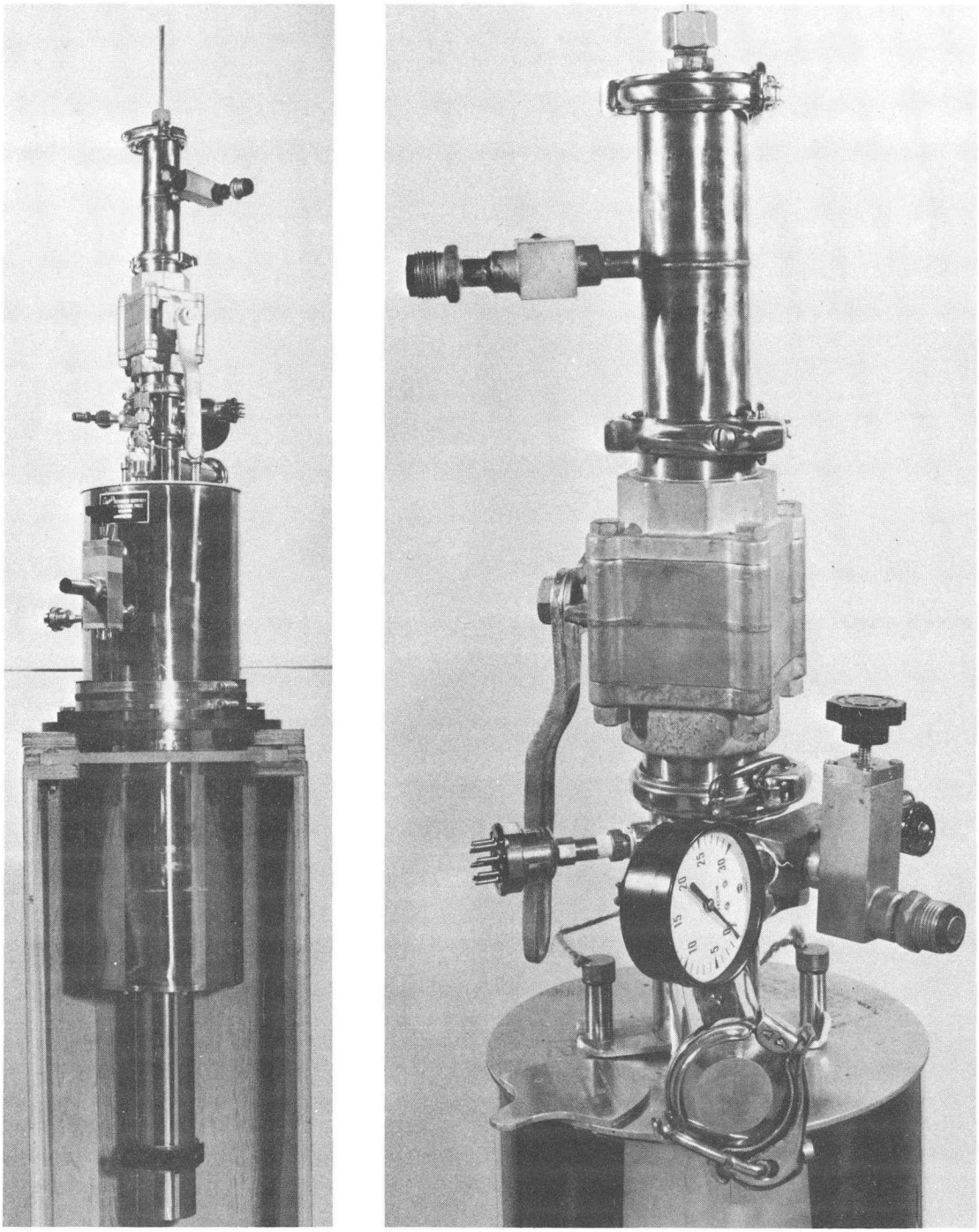

XBB 694-2675

Figure III. 7. Optical dewar.

(a) General view.

(b) Top works showing ball valve arrangement for changing samples.

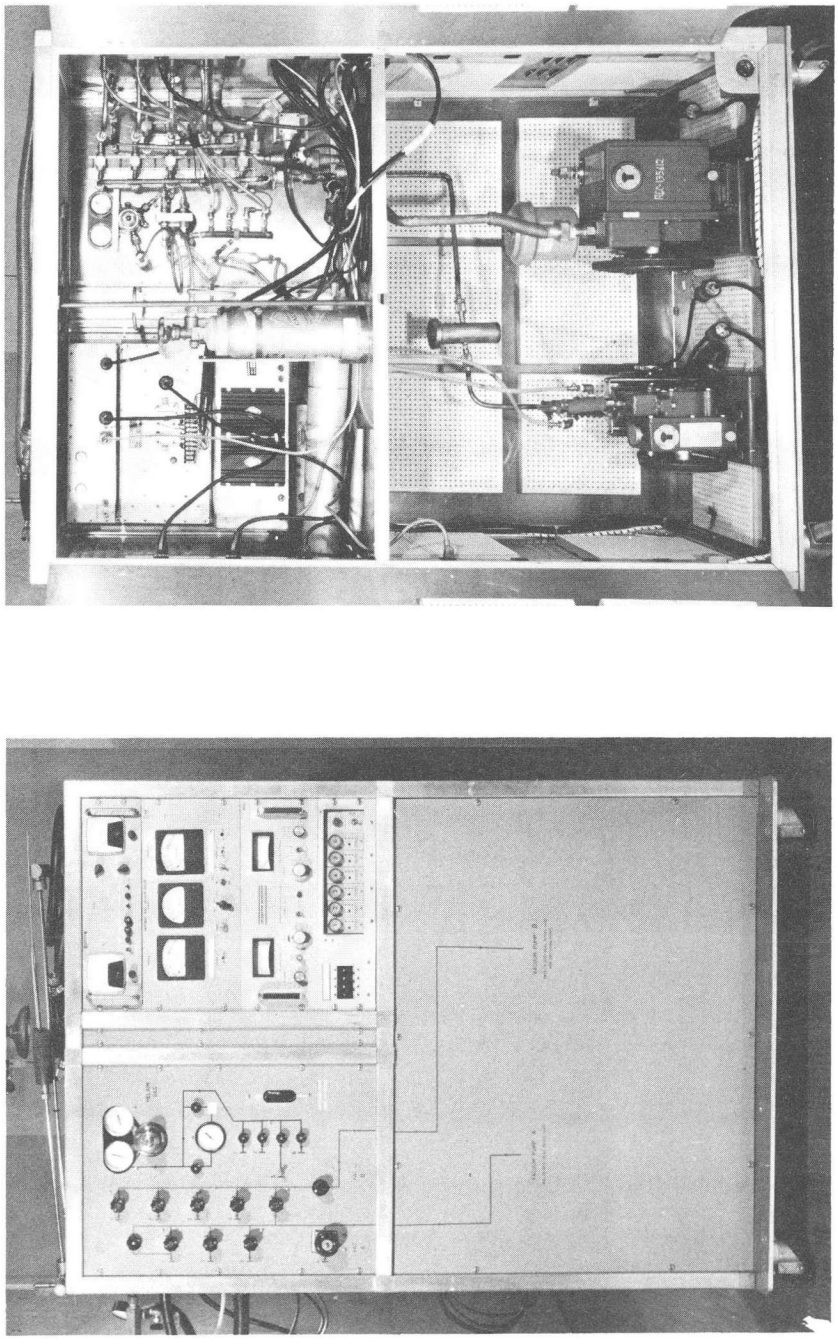

XBB 694-2676

Figure III. 8. Mobile cabinet for use with optical dewar. Contains vacuum pumps, helium gas supply, and electronic instrumentation.

The light source was a 450 watt high-pressure xenon arc lamp mounted in an air-cooled housing which was equipped with an arc re-imaging mirror and a variable focus condensing lens. Power was provided by a regulated, low ripple (1%, r.m.s.) d.c. supply with an output of 23 amps at 18 volts. The lamp was struck by means of a remote r.f. igniter. Current regulation was better than ± 1% for a 10% change in line voltage, and in practice neither ripple nor random current fluctuation contributed appreciably to system noise.

In order to reduce the heat input to the sample during absorption measurements, a Suprasil-quartz windowed water filter, 4 in long x 1-1/2 in diameter was inserted into the light beam.

The optical dewar was made of stainless steel, with Suprasil quartz windows in the optical tail. It consisted (see Figures III.7 and III.9) of three concentric chambers, the outer containing liquid nitrogen (77°K), the middle containing liquid helium (4°K), and the inner containing helium gas. The outer and middle chambers were separated by vacuum spaces, while the middle and inner chambers were in direct thermal contact. Both the liquid and gaseous helium chambers extended down into the optical tail, whereas the liquid nitrogen chamber was extended by means of a polished aluminum radiation shield thermally anchored to it. The sample cuvette, mounted on the end of a stainless steel tube by a grip fitting, was located in the tail of the helium gas chamber. It could be inserted or withdrawn without introducing air by the use of a large-bore (1-1/2 in) ball valve which, when closed, isolated the helium gas chamber from an upper chamber. To insert a pre-cooled sample, it

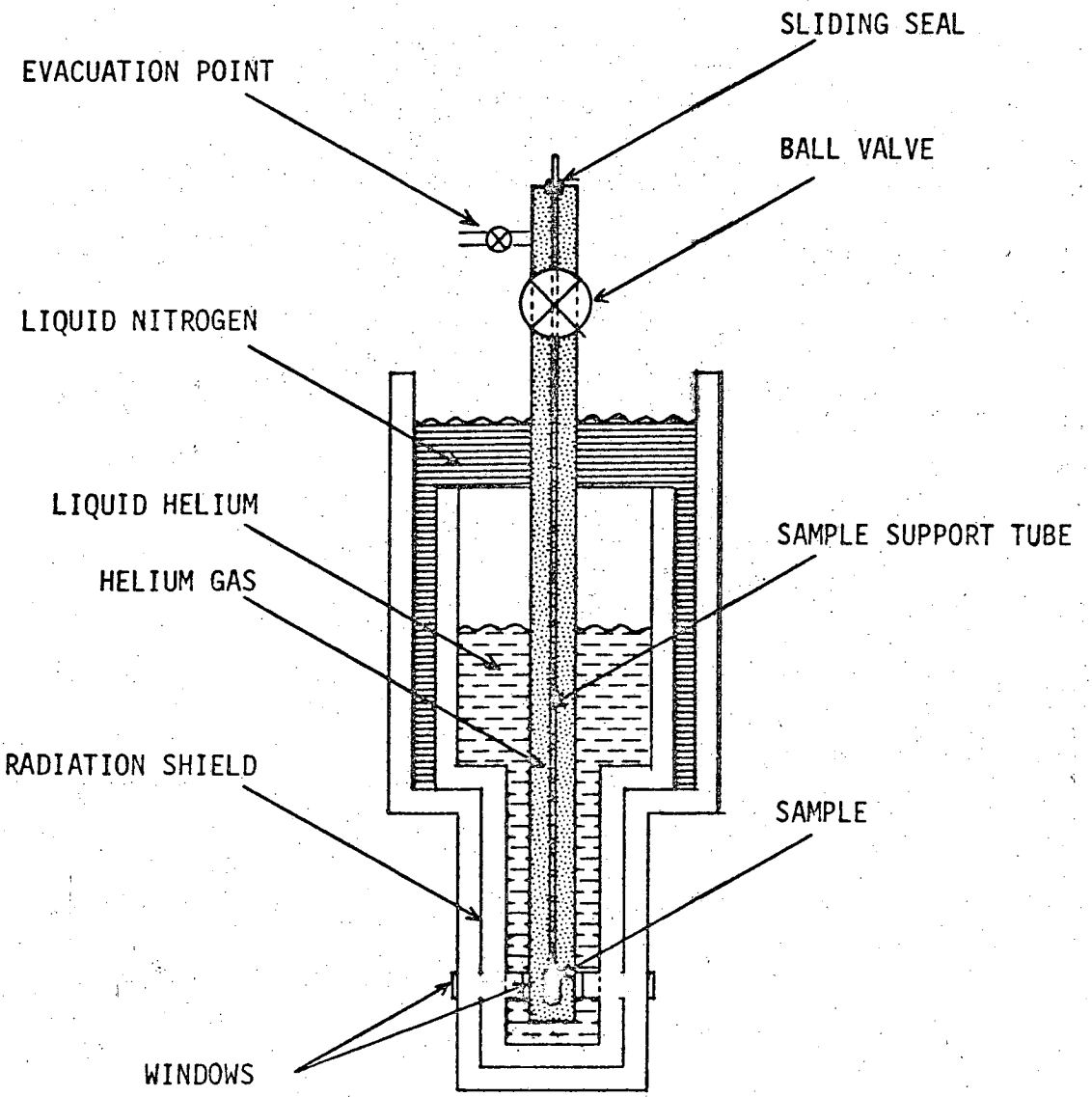

XBL 695-4239

Figure III.9. Simplified diagram of optical dewar.

was mounted on the support tube and sealed in the upper chamber, which was then rapidly evacuated. The ball valve was then opened and the sample moved down, through the valve port, to its location in the optical tail, the support tube sliding through a Wilson-type o-ring seal. Removal of the sample was effected by sliding the tube upwards, closing the ball valve, and breaking the upper chamber to atmosphere. The various components of the dewar top works were detachable, the couplings consisting of formed rubber gaskets with snap action clamps.

For operation with the sample at 4°K the helium gas surrounding it was held at a relatively high pressure (about 200 mm Hg) to ensure good heat transfer to the walls, which were anchored to liquid helium temperature (4°K). Higher sample temperatures could be achieved by using low helium gas pressure and mounting the sample in an open-windowed brass cylinder to which a controlled heat input was supplied by an electrical winding. The current to the winding was determined by a bridge circuit which compared the resistance of a precision platinum or germanium resistor mounted near the sample with a set valve. Deviation and rate of deviation signals combined to operate a servo motor on the heater circuit. For temperature-controlled operation a thin-walled (0.006 in) support tube was used to minimize heat losses by metallic conduction; for regular (4°K) operation a sturdier (0.02 in) tube was more convenient.

Two optical tail assemblies were available. The first had a rectangular two-window geometry with 1/2 in open diameter windows and was used for the work in section II of this thesis. The second,

used in the present work, was a three-window, 1/2 in open diameter design suitable for measuring emission as well as absorption spectra. Changing tail assemblies was a relatively simple matter; the outer tail had a rubber o-ring seal, the radiation shield was held in firm metal-to-metal contact by screws, while the inner assembly was sealed to the base of the liquid helium pot with an indium metal o-ring, which had to be cut and formed from indium wire each time the tail was replaced.

Windows were held in position by epoxy. In general this was satisfactory although on the one occasion when a leak developed, attempts to replace the windows (following manufacturers' instructions) resulted in shattering on the first cryogenic cycle and return to the manufacturer was necessary. It should also be mentioned that the recommended heat softening of the epoxy in order to remove windows was not effective, but overnight soaking in toluene was.

Sliding masks of aluminum were made for the windows. In this way each window could be blanked off or the open diameter reduced as required for a particular experiment.

The dewar was supported by a mounting flange, with levelling screws which rested on locating depressions in an aluminum annulus; the annulus, resting on a Dexion (slotted angle) aluminum framework, could be translated or rotated and this, together with the use of the levelling screws, enabled the tail of the dewar to be positioned precisely.

A liquid helium level indicator was used consisting of a number of carbon resistors as sensors positioned at 2 in vertical intervals

in the liquid helium chamber; each resistor operated a relay to give a visual signal indicating whether it was immersed in liquid or in gas. Simplicity of reading this instrument was a great help since it meant that more attention could be directed toward making the spectroscopic measurements.

Pressure measurements at various points in the system were taken with thermocouple gages and with conventional bellows gages.

As a guide to progress during dewar cool-down a micro-thermocouple was attached to the outer wall of the liquid helium chamber near the base of the tail, with the reference junction held at liquid nitrogen temperature.

Equipment auxiliary to the dewar (vacuum pumps, helium gas cylinder, gages, temperature controller, and liquid level indicator) were all contained within one mobile cabinet (Figure III.8). Hoses with standard LRL fittings connected the dewar to vacuum and gas manifolds in the cabinet.

The analyzing monochromator, a Jarrell-Ash 1 meter Czerny-Turner scanning spectrometer-spectrograph, combined moderate speed (f 8.7) with high resolution (0.1 A, which is about 1 cm^{-1} in the near UV). Curved slits were used so that with photo-electric detection maximum signal could be used without loss of resolution. The grating had 1180 grooves/mm and was blazed for 3000 A.

The scan drive mechanism on the instrument was somewhat unusual since instead of the conventional sine motion rotating the diffraction grating, a cosecant motion was employed, and in consequence the scan was linear in wavenumber instead of in wavelength. This type of

drive was chosen to enable direct assessment of energy differences between peaks on a spectral recording and in general it can be said that the choice was justified (see section 3d). The mechanism, however, was a prototype and unfortunately proved to be both difficult to adjust to linearity, and subject to long-term drift. The spectral plots obtained, while insufficiently accurate for measuring energy differences were invaluable as a visual guide in interpreting data from photographs.

Preliminary photographs of any particular spectrum were always taken on 4 in x 5 in Polaroid film. The photographs from which data were extracted were taken on conventional 4 in x 5 in plates. These were measured on a digitized comparator as described in section 3d.

Calibration sources consisting of a series of rare gas arcs provided lines in the region of the sample spectrum. These lamps (of the pen-lamp type) were reproducibly positioned in front of the entrance slit of the monochromator by means of a Lucite block on the lamp base which located in a matching recess on a Lucite stand mounted on the monochromator (Figure III.6).

The entrance slit mask used when taking photographs was of the Hartmann diaphragm type, and was modified as shown in Figure III.10 to give overlapping spectra.

The photomultiplier tube was mounted directly to the exit slit of the monochromator, with 1/2 in black sponge rubber providing a simple light-tight fit. It was characterized by a high gain (ca. 10^8) and a very low dark current (0.3 na at 2000 A/L). A further reduction of 10:1 in dark current was attained by surrounding the

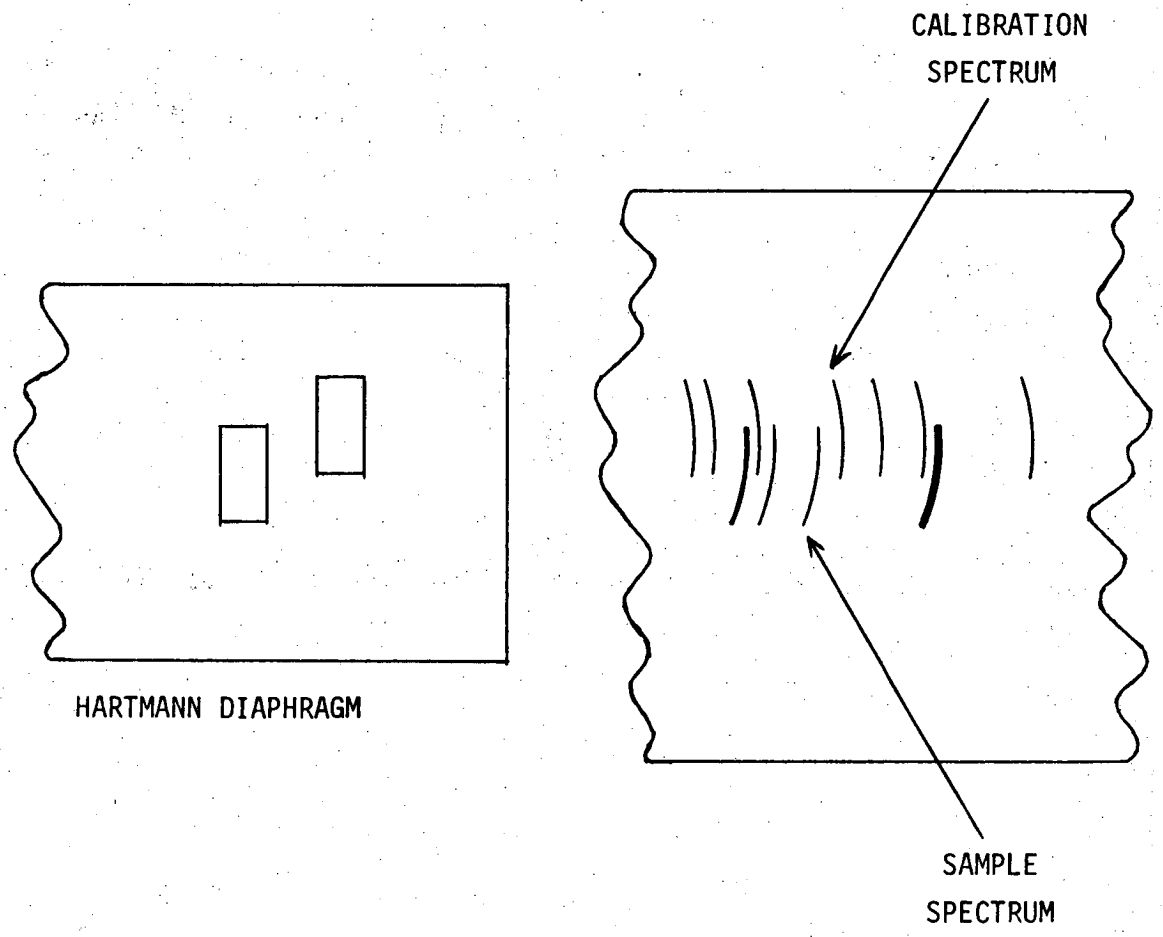

XBL 695-4235

Figure III.10. Modified Hartmann diaphragm and portion of resulting spectra.

tube with a dry-ice cooled housing, which was important with the low light levels encountered in emission measurements (but see below regarding amplifier performance).

Amplification system: Light incident on the sample was modulated by a mechanical chopper driven at a frequency determined by a plug-in circuit in the signal amplifier. The signal generated by the photo-tube across a 1 M 1% precision load resistor was led via a matching connector to a differential input preamplifier remote from the main amplifier. The latter, a lock-in instrument, consisted of (i) a filter amplifier with a relatively narrow but flat-topped response centered around the frequency of the chopper modulation, (ii) a synchronous rectifier triggered by a pulse from a magnetic pickup on the chopper, thus ensuring accurate lock-in, and (iii) a smoothing output stage.

Since plug-in frequency boards were used, the choice of modulation frequency was restricted. The exact value of frequency is unimportant provided that it is not a multiple or sub-multiple of any strongly interfering frequency such as 60 Hz; however, order of magnitude variations of frequency can affect the sensitivity of measurement (an obvious example is that in emission measurements the reciprocal frequency should be long compared with the lifetime of the excited state). In the present case three frequencies were tested, 11.3, 33.9, and 95 Hz, and since signal/noise was found to be the same in each case, 95 Hz was arbitrarily selected (or not quite arbitrarily - the flickering at 11.3 Hz bore a disturbing resemblance to the early days of cinema!).

There was one unfortunate feature of the system which did not greatly affect the present investigations, but which could have caused problems had the signal in emission experiments been much lower. When subjected to spike voltages, the filter amplifier resonated, representing a considerable loss in noise rejection capability. Where the phase relationship between spikes was random (as in photo-tube dark current) no d.c. output was recorded, but the noise level was much higher than would have been the case had the photo-tube (an EMI 6256 S) produced an equivalent dark current at a more continuous low-level. Attempts to smooth the incoming pulses by modifying the filter circuit reduced the gain proportionately, and so perhaps a better approach might be to investigate other tubes with different dark current characteristics.

A Beckmann DK was used as the excitation monochromator to select the desired exciting energy band for emission studies. With the slits wide open (2 mm) the bandwidth was ca. 1500 cm^{-1} in the UV and this is the way the instrument was usually operated. Cut-off was sufficiently sharp that interference of exciting light with emission measurements was negligible and so there was no advantage in using a cut-off filter in front of the analyzing monochromator.

UV grade quartz lenses were inserted at various points in the system as shown on the following page.

Although originally provision was made to enclose the light path, it was found that this was unnecessary since spectra could be taken with the room lights on without adverse effect. The only precaution taken was to shield the dewar from direct white light from the xenon lamp during emission measurements.

Open diameter (in)	Focal length (mm)	Type of measurement	Position
(i) 1-3/8	50	Both	In lamp housing
(ii) 1-1/2	150	Absorption	Between dewar and analyzing monochromator
(iii) "	100	Fluorescence	Before excitation monochromator
(iv) "	75	"	Between excitation monochromator and dewar.
(v) "	50	"	Between dewar and analyzing monochromator
(vi) "	150	"	Between dewar and analyzing monochromator

To reduce the effects of vibration (particularly from the cooling fan on the lamp housing) the analyzing monochromator was mounted on a sturdy separate table and all the other direct elements of the system (lamp, dewar, photo-tube, chopper, excitation monochromator, and lenses) on an adjacent table. Both monochromators, lenses (iii) and (iv), and the photo-tube were kept in a fixed position. The xenon lamp, calibration lamps, chopper, and various lenses were moved into position as appropriate. Final "tuning" of the system was done by adjusting the position of the dewar, sample, and (in emission studies) lens (v).

c) Procedure for measuring spectra

A general description of the procedure is given here; details of typical operating conditions are tabulated as Appendix C, as follows:

Table 1. Absorption spectrum, photoelectric detection

Table 2. " " , photographic "

Table 3. Fluorescence spectrum, photoelectric detection

Table 4. " " , photographic "

Table 5. Processing of photographic plates.

i) Cooling of dewar. The dewar vacuum jacket was pumped out using a mechanical vacuum pump, flushed with a small amount of air (to remove any residual helium gas), and repumped to a pressure of ca. 2 microns. Virtually all of the gas remaining is frozen out at the temperature of liquid helium.

Cooling of the dewar to 77°K was done simply by filling the outer chamber (see Figure III.9) with liquid nitrogen, and keeping the middle and inner chambers at about 1 atmosphere of helium gas. Convection cooling from the top of the middle (liquid helium) chamber reduced the dewar temperature to close to 77°K in about 4 hours. Completion of this stage was indicated both by the temperature of the micro-thermocouple at the base of the tail (see description of apparatus, section b) and by a levelling off of the helium gas pressure in the middle chamber.

At this point the sample, pre-cooled to 77°K (see section a), was introduced to the dewar; any subsequent sample changes were made with the dewar at 4°K.

After raising the pressure in both middle and inner chambers to 1 atmosphere with helium gas, liquid helium was transferred from a 25 l storage dewar, via a copper bellows transfer tube, to the

middle* chamber of the optical dewar, at a pressure of ca. 0.75 psig. Transfer of about 2 liters (up to sensor #4 on the liquid level indicator) took about 15 minutes, and this amount was usually enough for the measurement of the absorption and fluorescence spectra of one sample. Under these conditions of relatively high helium gas pressure in the sample chamber, the temperature of the sample (as indicated by the temperature-control sample mount) very quickly dropped to ca. 4°K.

With liquid helium in the dewar the vacuum jacket pressure was <<1 micron, measured by thermocouple gage. This, and also the disappearance of condensation (present at 77°K) from the outer tail, indicated satisfactory functioning of the dewar.

ii) Measurement of the spectra. About 4 hours before taking spectra, photographic plates were removed from refrigerated storage and allowed to warm up before loading into plate-holders; about 1 hour before using the photo-tube, the housing was filled with crushed dry ice and topped up later as necessary.

Absorption measurements: With the sample in place, the white light beam was passed through the water filter and dewar tail and condensed onto the analyzing monochromator. Signal optimization was not critical in absorption measurements, and could usually be attained satisfactorily by visual observation of the transmitted light image on the slit.

---

*N.B. Not the inner (sample) chamber.

A chart recording of the spectrum was then made, using photo-electric detection. Because of the wavelength-dependent scattering from the matrix, it was not possible to maintain a constant base-line and, scanning from higher to lower energy, it was sometimes necessary to switch to lower sensitivity to keep the signal on scale.

The spectrum was then photographed, together with suitable calibration spectra (in this case neon and helium arcs). Polaroid pictures were used as a guide to the selection of wavelength region and exposure time; a Polaroid (type 57)/plate (Kodak 103-0) exposure ratio of close to 1 was found suitable. Several photographs at different exposures were taken on the 4 in x 5 in plates, which were then processed under the conditions given in Table 5, Appendix C.

Fluorescence measurements: After altering the apparatus to the correct geometry (Figure III.3) a suitable exciting band was selected and, with the sample at approximately 45° to the exciting beam, the analyzing monochromator wavelength was set to receive scattered light, which was of much higher intensity than the emission. Using photo-electric detection, the signal was roughly maximized by adjusting the sample angle and the position of the dewar and lenses. This degree of "tuning" was adequate to allow the experimenter to locate the stronger peaks of the fluorescence spectrum. Then, with the analyzing monochromator sitting on one of these peaks, the final tuning to give maximum emission signal could be accomplished. The slit-width was selected to give as

much signal as possible without compromising the resolution of the spectrum.

Polarity of the recorder was reversed with respect to absorption measurements so that, with the energy axis going in the same sense, recordings of both types of spectra would show peaks (rather than troughs).

Photo-electric and photographic measurements of the spectrum were then made in the same way as for the absorption spectra, using argon, helium, and krypton arcs as calibration sources.

d) Extraction and analysis of data

Details of the computer programs which were used to treat data will be found in Appendix D. Data deck set-up, source listing and sample output are given for each.

i) Extraction of data from photographic plates. The instrument used to measure the plates was an AMP Comparator, housed in the Department of Astronomy, and kindly made available by Professor J. G. Phillips. It is shown in schematic form in Figure III.11.

The plate to be measured was attached to the transparent top of a table which was driven in the X direction by a precision screw whose rotational movement was digitized. A collimated light beam shone vertically up through the plate and acted as the source both of an enlarged visual image of the plate and as the signal to a photomultiplier tube. By means of a rotating glass block the beam could be displaced laterally, so that a given spectral line was

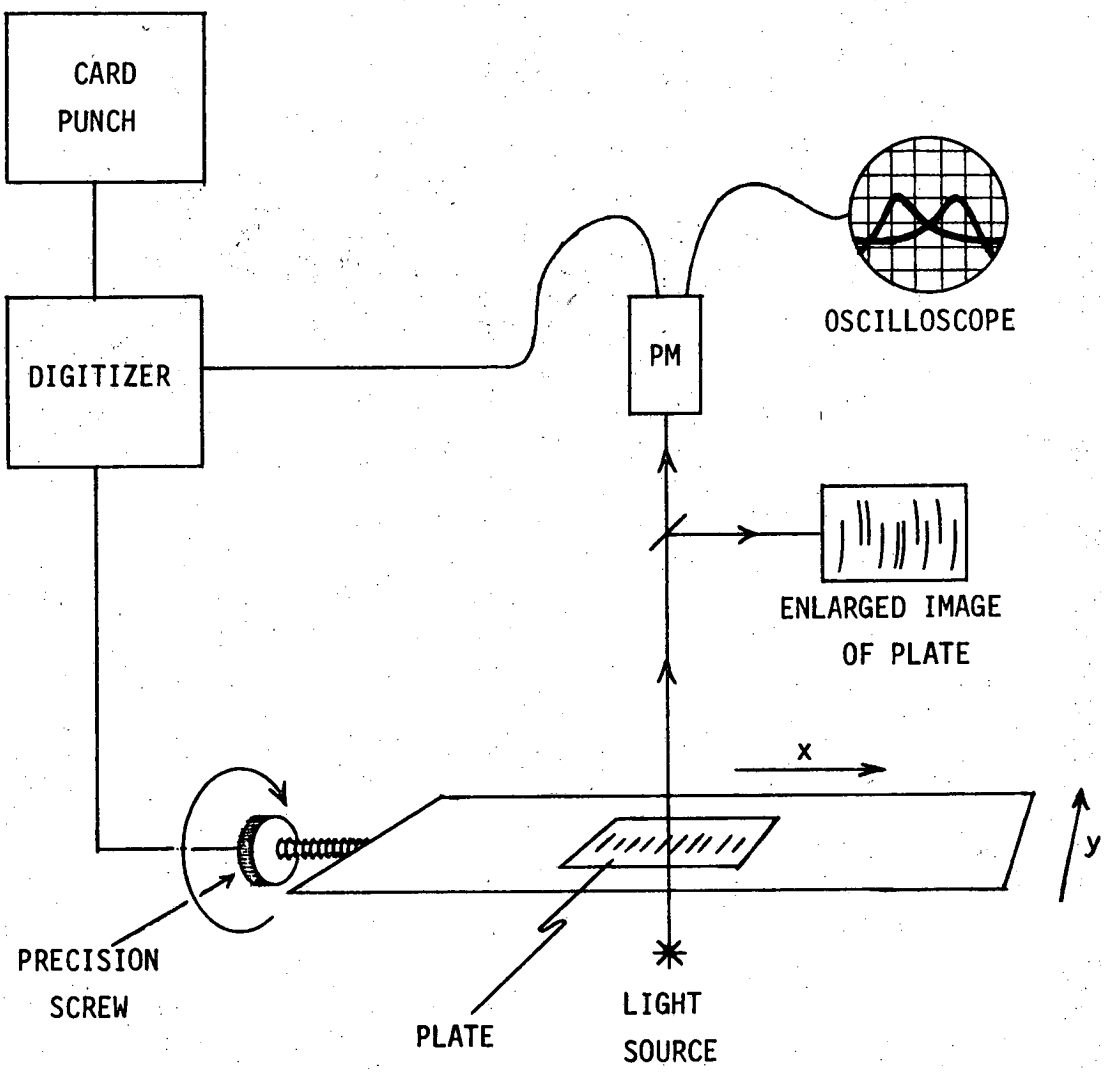

XBL 695-4233

Figure III.11. AMP Comparator for measuring spectral plates.

swept across a slit in front of the photo-tube. The output of the tube, connected to a synchronized oscilloscope, gave a visual display of the density profile of the spectral line. In fact, two images moving in opposition were used and by moving the table until they were brought into coincidence the line was positioned ready for measurement.

Where a molecular and calibration line were superposed, it was necessary to move the table along the Y-axis to reach a non-overlapping portion of the lines (see Figure III.10); this required a correction to be made to the X-axis position because of the curved shape of the spectral lines.

Lines were assigned a code which indicated whether they were molecular or calibration, and whether or not their position required correction.

With the line zeroed into position, the appropriate code button on a panel was pushed, causing the transfer of code, line position, and line intensity via the digitizer to a card punch.

ii) Processing of data. The cards comprised the data input for the program RREDUK, which is a modified version by me of REDUKT, obtained from Professor Phillips.

The first mode in which RREDUK is used is to identify the standards or calibration lines. Since the dispersion of a spectrograph is, to zero order, linear with wavelength, a linear interpolation between two known lines at the extremes of the spectrum is sufficiently accurate to enable identification of the remaining lines

by comparison with spectral tables. The booklet "Typical Spectra of Spectral Lamps", published by Oriel Optics Corporation, gave a useful visual guide to identification; actual wavelength values were taken from the American Institute of Physics Handbook, 2nd Edition, Tables 7g.

After insertion of true wavelength values of the standards into the data deck, RREDUK operates to express, by the method of least squares, wavelength as an eighth (or less if desired) degree polynomial function of position along the X-axis of the plate. The least squares fit is made twice, the second time excluding those standards whose deviation from the first fit exceeds a specified amount (the discriminant).

Finally the wavelengths of the molecular lines are obtained by substitution into this polynomial, and the values converted into wavenumbers in vacuo.

In the spectra presented in the next chapter, most of the lines were measured in this way. However, some weak lines which were not detected on the plate were evident on the chart recording of the spectrum. In such cases local linearity of the recording with wavenumber was assumed (see description of the analyzing monochromator, section (b) of this chapter) and the line position was measured by referring it to the nearest line which had been measured photographically. The estimated error in measuring these lines is $\pm$ 10 cm^{-1}, whereas in the most favorable case (a discrete narrow line measured photographically) it is $\pm$ 2 cm^{-1}.

To assist in analysis of the spectra two further computer programs were written by me.

The first of these, VIBRAN, uses the punched output of RREDUK as its data deck. It obtains and orders energy differences between lines, while keeping the information about the component lines in step. Starting with the most obvious energy differences from the main origin (e.g. ca. 390 and 1400 cm^{-1} in the case of anthracene), which could be clearly spotted on the chart recording of the spectrum, all pairs of lines with these differences were immediately available from VIBRAN. The strongest lines not explained on this basis were then assumed to be fundamentals, VIBRAN was again consulted, and so on.

Reference was also made to published data[11,51-55] on the vibrational frequencies of anthracene, obtained in a variety of ways (ultra-violet, infra-red, and Raman spectroscopy, liquid and vapor phase, pure and mixed crystal).

Comparison of spectra of the same molecule in different solvents was useful in that lines common to all (referred in each case to the main origin) could be assumed to be vibrational bands of the main origin; lines peculiar to one solvent were probably "multiplet" components (see Introduction, Part I, and Results and discussion, chapter 4 of this part of the thesis) or vibrational bands of these components.

A complementary means of differentiating was to compare either the absorption and fluorescence spectra of the same system, or the

(e.g. fluorescence) spectra of the deuterated and undeuterated molecule in the same solvent. In these cases the multiplet components proved to be in coincidence (see Chapter 4) whereas the vibrational frequencies were not.

The other program, WISHFUL, was devised to synthesize spectra from assumed multiplet origins and vibrational frequencies. Empirical rules were set up to determine the intensity of combination lines. A maximum of three vibrational quanta per line was used in forming the combinations, and lines with an intensity less than zero were excluded from the spectrum. The final output of the program was a listing of spectral lines in order of increasing energy, together with their composition and a visual indication of their intensity (see Appendix D). The program could of course only be used after quite a lot was known about the real spectrum; its usefulness lay in the identification of the more difficult lines, and also in detecting accidental degeneracies.

Reference was made throughout analyses to the chart recordings of spectra. In particular, they gave the best indication of line intensities; the values obtained from plates and used in RREDUK and VIBRAN could be very misleading, especially for absorption spectra, since no correction was made to the baseline, or for overlapping lines. Intensities in the main data tables (chapter 4) are based on visual estimates from the chart recordings.

4. Results and discussion

a) Data tables

Absorption and fluorescence spectra were taken, at 4°K, of anthracene and of $[D_{10}]$-anthracene in each of the following matrices: n-hexane, n-heptane, and n-octane. Typical examples of these spectra are shown in Figure III.12 (photoelectric recording) and Figure III.13 (photographic recording).

Tables III.1 through III.12 list the data obtained from the spectra, as follows:

Table III.1	Absorption	spectrum of	anthracene in	n-hexane at 4°K
Table III.2	Fluorescence	"	"	" "
Table III.3	Absorption	"	"	n-heptane "
Table III.4	Fluorescence	"	"	" "
Table III.5	Absorption	"	"	n-octane "
Table III.6	Fluorescence	"	"	" "
Table III.7	Absorption	"	$[D_{10}]$-anthracene in	n-hexane "
Table III.8	Fluorescence	"	"	" "
Table III.9	Absorption	"	"	n-heptane "
Table III.10	Fluorescence	"	"	" "
Table III.11	Absorption	"	"	n-octane "
Table III.12	Fluorescence	"	"	" "

Each table consists of a listing of the lines observed in a given spectrum. The energy (in cm^{-1}) of each line is given, its intensity, its displacement ($\Delta\nu$) from the origin(s) to which it has been assigned, and its assignment.

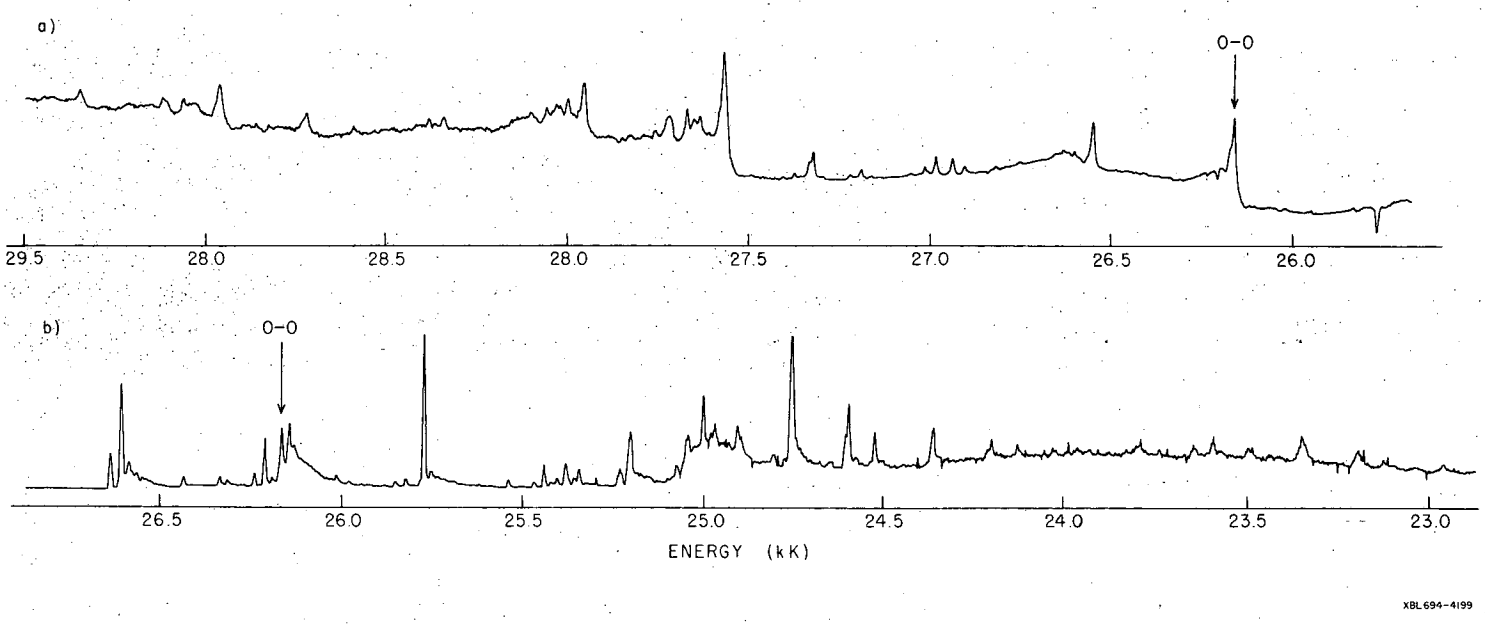

Figure III.12. Spectra of anthracene in n-octane at 4°K (photo-electric recording). (a) Absorption; (b) Fluorescence.

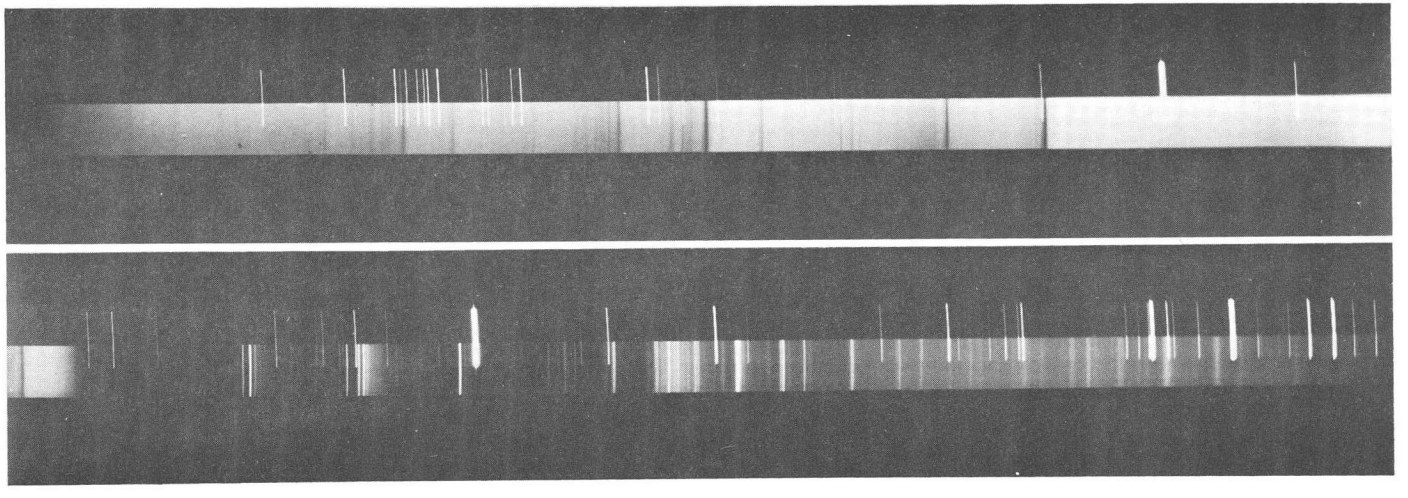

XBB 694-2680

Figure III. 13. Spectra of anthracene in n-octane at 4°K (photographic recording). (a) Absorption, and (b) fluorescence.

Notes: (i) For the significance of the term "origin" used here, see Part I of the thesis and also section (d) of this chapter.

(ii) The symbols used for origins (0_1, 0_2, etc.) are arbitrary. In particular the symbols used for the same sample in absorption and fluorescence do not correspond.

(iii) A double asterisk has been placed in front of one origin in each spectrum (e.g. $**0_5$); this is the origin which gives rise to the most intense vibronic spectrum, and is referred to in the discussion as the "main origin". In no case was there any ambiguity about its selection.

(iv) "latt" signifies lattice vibrational energy; see section (d) of this chapter.

(v) The majority of lines, designated by a simple numeral, e.g. 15, were measured photographically. Lines designated by a numeral and a letter, e.g. 15a, were measured, with a somewhat lower accuracy, from the chart recording of the spectrum (see chapter 3, section d). In a very few cases the existence of a line was inferred from other data, although it was too weak to be observed; the energy value of these lines is given in parentheses and no intensity value is given.

(vi) Abbreviations used for intensities are as follows:

vs	= very strong	w	= weak
s	= strong	vw	= very weak
m	= medium	vvw	= very very weak

Table III.1 Absorption spectrum of anthracene in n-hexane at 4°K.

No.	Intensity	Energy $\nu(cm^{-1})$	$\Delta\nu(cm^{-1})$			Assignment
			0_1	0_2	$**0_3$	
1	--	(26323)	0		-164	0_1
1a	vw	26447		0	-40	0_2
2	s	26487			0	$**0_3$
3	s	26509			22	$**0_3$ + latt.
4	w	26723	400		236	0_1 + 389 + 11
4a	vw	26836		389	349	0_2 + 389
5	vs	26876			389	$**0_3$ + 389
5a	vw	26900			413	$**0_3$ + 389 + latt
5b	vw	27096			609	$**0_3$ + 609
5c	w	27218			731	$**0_3$ + 731
6	m	27265			778	$**0_3$ + 2x389
6a	vw	27350	1027		863	0_1 + 1018 + 9
6b	w	27375			888	$**0_3$ + 888
6c	vw	27480	1157		993	0_1 + 1155 + 2
6d	w	27505			1018	$**0_3$ + 1018
7	s	27642			1155	$**0_3$ + 1155
8	m	27722	1399		1235	0_1 + 1393 + 6
8a	vw	27784			1297	$**0_3$ + 1297
8b	vw	27825	1502		1338	0_1 + 1497 + 5
9	vs	27880	1557		1393	$**0_3$ + 1393; 0_1 + 389 + 1155 + 13
9a	vw	27952			1454	$**0_3$ + 1465
10	m	27984			1497	$**0_3$ + 1497

Table III.1 (continued).

No.	Intensity	Energy $\nu(cm^{-1})$	$\Delta\nu(cm^{-1})$			Assignment
			0_1	0_2	$**0_3$	
11	w	28050			1563	$**0_3$ + 1563
12	s	28273			1786	$**0_3$ + 389 + 1393 + 4
13	m	28377			1890	$**0_3$ + 389 + 1497 + 4; $**0_3$ + 731 + 1155 + 4
14	w	29037			2550	$**0_3$ + 1155 + 1393 + 2
15	m	29277			2790	$**0_3$ + 2x1393 + 4
16	w	29379			2892	$**0_3$ + 1393 + 1497 + 2

Table III.2 Absorption spectrum of anthracene in n-heptane at 4°K.

No.	Intensity	Energy $\nu(cm^{-1})$	$\Delta\nu(cm^{-1})$			Assignment
			$^{**}0_1$	0_2	0_3	
1	vs	26218	0			$^{**}0_1$
2	vs	26243	25			$^{**}0_1$ + Latt
3	s	26264	46	0		0_2
4	s	26402	184		0	0_3
5	s	26414	196		12	0_3 + latt
6	w	26431	213		29	
7	vs	26608	390			$^{**}0_1$ + 390
8	s	26626	408			$^{**}0_1$ + 390 + latt
9	m	26634	416			$^{**}0_1$ + 390 + latt
10	vw	26785	567		383	0_3 + 390 - 7
11	w	26805	587		403	$^{**}0_1$ + 586; 0_3 + 390 + latt
11a	vw	26880	662			$^{**}0_1$ + 662
12	w	26961	743			$^{**}0_1$ + 743
13	s	26997	779			$^{**}0_1$ + 2x390 - 1
14	vw	27110	892			$^{**}0_1$ + 892
15	m	27246	1028			$^{**}0_1$ + 1028
16	w	27278	1060			?
17	s	27377	1159			$^{**}0_1$ + 1159
18	vw	27382	1164			$^{**}0_1$ + 3x390 - 6
18a	vw	27521	1303			?
19	vw	27551	1333		1149	$^{**}0_1$ + 743 + 587 + 3; 0_3 + 1159 - 10
20	vvw	27597	1379			$^{**}0_1$ + 2x390 + 587 + 12
21	vs	27615	1397			$^{**}0_1$ + 1397

Table III.2 (continued).

No.	Intensity	Energy $\nu(cm^{-1})$	$\Delta\nu(cm^{-1})$			Assignment
			$^{**}0_1$	0_2	0_3	
22	m	27640	1422			$^{**}0_1$ + 1397 + latt; $^{**}0_1$ + 390 + 1028 + 4
23	m	27682	1464			$^{**}0_1$ + 1464
24	m	27721	1503			$^{**}0_1$ + 1503
25	m	27768	1550	1504		$^{**}0_1$ + 1550; $^{**}0_1$ + 390 + 1159 + 1; 0_2 + 1503 + 1
25a	vvw	27796	1618		1394	0_3 + 1397 - 3
26	vw	27911	1693		1509	0_3 + 1503 + 6
27	s	28008	1790			$^{**}0_1$ + 390 + 1397 + 3
27a	vw	28075	1857			$^{**}0_1$ + 390 + 1464 + 3
28	w	28110	1892			$^{**}0_1$ + 390 + 1503 - 1
29	w	28397	2179			$^{**}0_1$ + 2x390 + 1397 + 2
30	vvw	28642	2424			$^{**}0_1$ + 1028 + 1397 - 1
31	vw	28781	2563			$^{**}0_1$ + 1159 + 1397 + 7
32	vw	28878	2660			$^{**}0_1$ + 1159 + 1503 - 2
33	m	29019	2801			$^{**}0_1$ + 2x1397 + 7
34	vw	29083	2865			$^{**}0_1$ + 1397 + 1464 + 4
35	w	29120	2902			$^{**}0_1$ + 1397 + 1503 + 2
36	w	29170	2952			$^{**}0_1$ + 1397 + 1550 + 5; $^{**}0_1$ + 390 + 1159 + 1397 + 6
37	vw	29408	3190			$^{**}0_1$ + 390 + 2x1397 + 6
38	vw	29478	3260			$^{**}0_1$ + 390 + 1397 + 1464 + 9
39	vw	29508	3290			$^{**}0_1$ + 390 + 1397 + 1503
40	vvw	30178	3960			$^{**}0_1$ + 1159 + 2x1397 + 7
41	vw	30414	4196			$^{**}0_1$ + 3x1397 + 5
42	vw	30571	4353			$^{**}0_1$ + 2x1397 + 1550 + 9

Table III.3 Absorption spectrum of anthracene in n-octane at 4°K.

No.	Intensity	Energy $\nu(cm^{-1})$	$\Delta\nu(cm^{-1})$				Assignment
			$**0_1$	0_2	0_3	0_4	
1	vs	26161	0				$**0_1$
2	m	26172	11				$**0_1$ + latt
2a	--	(26432)	271	0			0_2
3	vs	26551	390				$**0_1$ + 390
4	w	26600	439		0		0_3
4a	vw	26628	467			0	0_4
4b	vw	26751	590				$**0_1$ + 590
4c	vw	26822	661	390			0_2 + 390; $**0_1$ + 661
5	w	26905	744				$**0_1$ + 744
6	m	26941	780				$**0_1$ + 2x390
7	m	26987	826		387		0_3 + 390 - 3
7a	w	27017	856			389	0_4 + 390 - 1
7b	vw	27052	891				$**0_1$ + 891
8	w	27190	1029				$**0_1$ + 1029
8a	vw	27220	1059	788			0_2 + 2x390 + 8; $**0_1$ + 390 + 661+8
9	s	27321	1160				$**0_1$ + 1160
10	w	27333	1172				$**0_1$ + 3x390 + 2
10a	vw	27374	1213		774		0_3 + 2x390 - 6
10b	vvw	27401	1240			773	0_4 + 2x390 - 7
10c	vvw	27459	1298				$**0_1$ + 1298
11	vs	27563	1402				$**0_1$ + 1402
12	w	27631	1470				$**0_1$ + 1470
12a	vw	27648	1487				$**0_1$ + 2x744 - 1

Table III.3 (continued)

No.	Intensity	Energy $\nu(cm^{-1})$	$\Delta\nu(cm^{-1})$				Assignment
			$^{**}0_1$	0_2	0_3	0_4	
13	w	27666	1505				$^{**}0_1$ + 1505
14	w	17716	1555				$^{**}0_1$ + 1555
15	vvw	17755	1594		1155		0_3 + 1160 - 5
16	s	27952	1791				$^{**}0_1$ + 390 + 1402 - 1
17	w	27996	1835		1396		0_3 + 1402 - 6
17a	vw	28027	1866				$^{**}0_1$ + 390 + 1470 + 6
18	vw	28052	1891				$^{**}0_1$ + 390 + 1505 - 4
19	vw	28341	2180				$^{**}0_1$ + 2x390 + 1402 - 2
19a	vvw	28381	2220		1781		0_3 + 390 + 1402 - 11
19b	vvw	28595	2434				$^{**}0_1$ + 1029 + 1402 + 3
20	w	28725	2564				$^{**}0_1$ + 1160 + 1402 + 2
21	m	28963	2802				$^{**}0_1$ + 2x1402 - 2
22	vw	29039	2878				$^{**}0_1$ + 1402 + 1470 + 6
23	vw	29063	2902				$^{**}0_1$ + 1402 + 1505 - 5
24	vw	29118	2957				$^{**}0_1$ + 1402 + 1555
25	vw	29351	3190				$^{**}0_1$ + 390 + 2x1402 - 4

Table III.4 Fluorescence spectrum of anthracene in n-hexane at 4°K.

No.	Intensity	Energy $\nu(cm^{-1})$	$\Delta\nu(cm^{-1})$		Assignment
			$**0_1$	0_2	
1	vvw	23285	3201		$**0_1$ - 1563 - 1638
2	vvw	23365	3121		$**0_1$ - 2x1563 + 5
3	vvw	23446	3040		$**0_1$ - 1409 - 1638 + 7
4	vvw	23522	2964		$**0_1$ - 395 - 1164 - 1409 + 4
5	w	23673	2813		$**0_1$ - 2x1409 + 5
6	vvw	23812	2674		$**0_1$ - 1265 - 1409
7	vvw	23915	2571		$**0_1$ - 1164 - 1409 + 2
8	vw	24455	2031		$**0_1$ - 395 - 1638 + 2; $**0_1$ - 627 - 1409 + 5
9	w	24529	1957		$**0_1$ - 395 - 1563 + 1; $**0_1$ - 2x395 - 1164 - 3
10	m	24685	1801	1638	$**0_1$ - 395 - 1409 + 3; 0_2 - 1638
11	vw	24755	1731	1568	0_2 - 1563 - 5
11a	vw	24824	1662		$**0_1$ - 395 - 1265 - 2
12	m	24848	1638		$**0_1$ - 1638
13	s	24923	1563	1400	$**0_1$ - 1563; $**0_1$ - 395 - 1164 - 4; 0_2 - 1409 + 9
14	vs	25077	1409		$**0_1$ - 1409
14a	vvw	25151	1335	1172	0_2 - 1164 - 8
15	w	25221	1265		$**0_1$ - 1265
15a	vvw	25209	1253		$**0_1$ - 2x627 + 1
15b	vw	25300	1186		$**0_1$ - 3x395 - 1
16	m	25322	1164		$**0_1$ - 1164
16a	vvw	25467	1019		$**0_1$ - 395 - 627 + 3

Table III.4 (continued).

No.	Intensity	Energy $\nu(cm^{-1})$	$\Delta\nu(cm^{-1})$		Assignment
			$^{**}0_1$	0_2	
17	vw	25694	792		$^{**}0_1$ - 2x395 - 2
18	vvw	25732	754		$^{**}0_1$ - 754
19	vw	25859	627		$^{**}0_1$ - 627
20	w	25929	557	394	0_2 - 395 + 1
20a	vw	26063	423		$^{**}0_1$ - 395 - latt
21	vs	26091	395		$^{**}0_1$ - 395
21a	vw	26298	188	25	0_2 - latt
22	m	26323	163	0	0_2
23	m	26462	24		$^{**}0_1$ - latt
24	vs	26486	0		$^{**}0_1$

Table III.5 Fluorescence spectrum of anthracene in n-heptane at 4°K.

No.	Intensity	Energy $\nu(cm^{-1})$	$\Delta\nu(cm^{-1})$					Assignment
			0_1	0_2	0_3	0_4	$**0_5$	
1	vvw	22931					3285	?
2	vvw	22938					3278	$**0_5$ - 2x1638 - 2
3	vvw	23177					3039	$**0_5$ - 1406 - 1638 + 5
4	vvw	23249					2967	$**0_5$ - 1406 - 1564 + 3
5	vw	23406		3201			2810	$**0_5$ - 2x1406 + 2; 0_2 - 392 - 2x1406 + 3
6	vvw	23491					2725	$**0_5$ - 1162 - 1564 + 1
7	vvw	23550					2666	$**0_5$ - 1265 - 1406 + 5
8	vw	23554		3053			2662	0_2 - 1406 - 1638 - 9
9	vvw	23585			2813		2631	0_3 - 2x1406 - 1
10	vw	23649					2567	$**0_5$ - 1162 - 1406 + 1
11	vvw	23798		2809			2418	0_2 - 2x1406 + 3 $**0_5$ - 2x392 - 1638 + 4
11a	vvw	24025					2191	$**0_5$ - 2x392 - 1406 - 1
12	vw	24185					2031	$**0_5$ - 392 - 1638 - 1; $**0_5$ - 624 - 1406 - 1
12a	vvw	24210			2188		2006	0_3 - 2x392 - 1406 + 2
13	w	24258					1958	$**0_5$ - 392 - 1564 - 2
14	w	24416		2191			1800	$**0_5$ - 392 - 1406 - 2; 0_2 - 2x392 - 1406 - 1
14a	vw	24441			1957		1775	0_3 - 392 - 1564 - 1
14b	vw	24555					1661	$**0_5$ - 392 - 1265 - 4
15	m	24578		2029			1638	$**0_5$ - 1638; 0_2 - 392 - 1638 + 1
15a	vw	24603			1795		1613	0_3 - 392 - 1406 + 3
16	s	24652		1955			1564	$**0_5$ - 1564; 0_2 - 392 - 1564 + 1
17	m	24659					1557	$**0_5$ - 392 - 1162 - 3

Table III.5 (continued).

No.	Intensity	Energy $\nu(cm^{-1})$	$\Delta\nu(cm^{-1})$					Assignment
			0_1	0_2	0_3	0_4	$**0_5$	
18	vvw	24705					1511	$**0_5$ - 2x757 + 3
19	vw	24765			1633		1451	0_3 - 1638 + 5
19a	vw	24788					1428	$**0_5$ - 1406 - latt
20	vs	24810		1797			1406	$**0_5$ - 1406; 0_2 - 392 - 1406 + 1
21	w	24837			1561	1411	1379	0_3 - 1564 + 3; 0_4 - 1406 - 5
22	m	24951		1656			1265	$**0_5$ - 1265; 0_2 - 392 - 1265 + 1
23	m	24961					1255	?
24	m	24970		1637			1246	0_2 - 1638 + 1
25	w	24980			1418		1236	0_3 - 1406 - latt
26	m	24988			1410		1228	0_3 - 1406 - 4
27	vw	25034					1182	$**0_5$ - 3x392 - 6; $**0_5$ - 1162 - latt
28	m	25054		1553			1162	$**0_5$ - 1162; 0_2 - 392 - 1162 + 1
29	vw	25137			1261		1089	0_3 - 1265 + 4
30	vvw	25172					1044	0_2 - 1406 - latt
31	vvw	25180		1427			1036	0_2 - 1406 - latt
32	m	25201		1406			1015	0_2 - 1406; $**0_5$ - 392 - 624 + 1
33	vvw	25235			1163		981	0_3 - 1162 - 1
33a	vvw	25260	1405				956	0_1 - 1406 + 1
34	vw	25345		1262			871	0_2 - 1265 + 3
35	vw	25428		1179			788	$**0_5$ - 2x392 - 4; 0_2 - 3x392 - 3
36	vw	25442		1163			774	0_2 - 1162 - 1

Table III.5 (continued).

No.	Intensity	Energy $\nu(cm^{-1})$	$\Delta\nu(cm^{-1})$					Assignment
			0_1	0_2	0_3	0_4	$**0_5$	
37	vw	25459					757	$**0_5$ - 757
38	vw	25592					624	$**0_5$ - 624
38a	vvw	25615			783		601	0_3 - 2x392 + 1
39	vvw	25806					410	$**0_5$ - 392 - latt
40	vs	25824		783			392	$**0_5$ - 392; 0_2 - 2x392 + 1
41	vw	25853				395	363	0_4 - 392 - 3
42	vw	25982			416		234	0_3 - 392 - latt
43	w	25994			404		222	0_3 - 392 - latt
44	w	26007			391		209	0_3 - 392 + 1
45	vw	26061					155	0_6
46	m	26198					18	$**0_5$ - latt; 0_2 - 392 - latt
47	m	26216		391			0	$**0_5$; 0_2 - 392 + 1
48	vw	26248				0	-32	0_4
49	m	26372			26		-156	0_3 - latt
50	s	26384			14		-168	0_3 - latt
51	m	26398			0		-182	0_3
52	w	26579		28			-363	0_2 - latt
53	m	26607		0			-391	0_2
54	vw	26665	0				-449	0_1

Table III.6. Fluorescence spectrum of anthracene in n-octane at 4°K.

No.	Intensity	Energy $\nu(cm^{-1})$	$\Delta\nu(cm^{-1})$								Assignment
			0_1	0_2	0_3	0_4	0_5	$^{**}0_6$	0_7	0_8	
1	vw	24033		2567				2129			0_2 - 1165 - 1407 + 5
2	vw	24127						2035			$^{**}0_6$ - 392 - 1642 - 1; $^{**}0_6$ - 625 - 1407 - 3
3	w	24199						1963			$^{**}0_6$ - 392 - 1569 - 2
4	vw	24209						1953			$^{**}0_6$ - 2x392 - 1165 - 4
5	m	24356						1806			$^{**}0_6$ - 392 - 1411 - 3
6	vw	24499						1663			$^{**}0_6$ - 1642 - latt; $^{**}0_6$ - 392 - 1260 - 11
7	m	24520						1642			$^{**}0_6$ - 1642
8	vvw	24532				1803		1630			0_4 - 392 - 1407 - 4
9	vw	24573						1589		1404	$^{**}0_6$ - 1569 - latt; 0_8 - 1407 + 3
10	s	24593						1569			$^{**}0_6$ - 1569
11	m	24602						1560	1411		$^{**}0_6$ - 392 - 1165 - 3; 0_7 - 1407 - 4
12	vvw	24644		1956				1518			$^{**}0_6$ - 2x760 + 2; 0_2 - 392 - 1569 + 5
13	vvw	24654		1946				1508			0_2 - 2x392 - 1165 + 3
14	vvw	24677	1953					1485			0_1 - 2x392 - 1165 - 4
15	vvw	24731						1431			$^{**}0_6$ - 1407 - latt
16	vw	24742						1420			$^{**}0_6$ - 1407 - latt
16a	vs	24751						1411			$^{**}0_6$ - 1411
17	vs	24755						1407			$^{**}0_6$ - 1407
18	vw	24773				1562		1389			0_4 - 1569 + 7; 0_4 - 392 - 1165 - 5
19	vw	24800		1800				1362			0_2 - 392 - 1407 - 1
20	vvw	24872			1560			1290			0_3 - 1569 + 9

Table III.6 (continued).

No.	Intensity	Energy $\nu(cm^{-1})$	$\Delta\nu(cm^{-1})$								Assignment
			0_1	0_2	0_3	0_4	0_5	$**0_6$	0_7	0_8	
21	w	24893				1442		1269			0_4 - 1407 - latt ?
22	m	24902						1260			$**0_6$ - 1260
23	w	24928				1407		1234			0_4 - 1407
24	w	24936		1664				1226			0_2 - 392 - 1260 -12
25	m	24965		1635				1197			0_2 - 1642 + 7
26	w	24977	1653					1185			$**0_6$ - 3x392 - 9; 0_1 - 1642 - 11
27	s	24997						1165			$**0_6$ - 1165
28	m	25039		1561				1123			0_2 - 1569 + 8; 0_2 - 392 - 1165 - 4
29	w	25069	1561					1093			0_1 - 1569 + 8; 0_1 - 392 - 1165 - 4
30	vvw	25095						1067			?
31	vvw	25150						1012			$**0_6$ - 392 - 625 + 5
32	vvw	25179		1421				983			0_2 - 1407 - latt
33	m	25198		1402				964			0_2 - 1407 + 5
34	w	25227	1403					935	786		0_1 - 1407 + 4; 0_7 - 2x392 - 2
35	w	25340		1260				822			0_2 - 1260
36	vw	25352						810			$**0_6$ - 2x392 - latt ?
37	w	25377						785			$**0_6$ - 2x392 - 1
38	vw	25402					787	760			$**0_6$ - 760; 0_5 - 2x392 - 3
39	vvw	25419		1181				743			0_2 - 3x392 - 5
40	w	25438		1162				724			0_2 - 1165 + 3
41	vw	25467	1163					695			0_1 - 1165 + 2
42	vw	25537						625			$**0_6$ - 625

Table III. 6 (continued).

No.	Intensity	Energy $\nu(cm^{-1})$	$\Delta\nu(cm^{-1})$								Assignment
			0_1	0_2	0_3	0_4	0_5	0_6	0_7	0_8	
43	vw	25750						412			$^{**}0_6$ - 392 - latt
44	vs	25770						392			$^{**}0_6$ - 392
45	vw	25819		781				343			0_2 - 2x392 + 3
46	vw	25850	780					312			0_1 - 2x392 + 4
46a	vvw	25940				395		222			0_4 - 392 - 3
47	vvw	25977						185		0	0_8
48	vw	26013						149	0		0_7
49	m	26130						32			$^{**}0_6$ - latt
50	m	26142						20			
51	m	26162						0			$^{**}0_6$
52	vvw	26189		411			0	-27			0_5; 0_2 - 392 - latt
53	m	26209		391				-47			0_2 - 392 + 1
54	vw	26238	392					-76			0_1 - 392
55	vvw	26314				21		-152			0_4 - latt
56	vw	26335				0		-173			0_4
57	vw	26432			0			-270			0_3
58	vvw	26542						-380			0_2 - latt
59	vw	26559						-397			
60	w	26580		20				-418			
61	s	26600		0				-438			0_2
62	m	26630	0					-468			0_1

Table III.7 Absorption spectrum of $[D_{10}]$-anthracene in n-hexane at 4°K.

No.	Intensity	Energy $\nu(cm^{-1})$	$\Delta\nu(cm^{-1})$		Assignment
			0_1	$^{**}0_2$	
0a	--	(26397)	0	-156	0_1
0b	--	(26553)		0	$^{**}0_2$
1	vw	26575		22	$^{**}0_2$ + latt
2	vw	26766	369	213	0_1 + 379 - 10
3	vs	26932		379	$^{**}0_2$ + 379
3a	vw	26952		399	$^{**}0_2$ + 379 + latt
3b	vw	27244		691	$^{**}0_2$ + 691
4	w	27309		756	$^{**}0_2$ + 2x379 - 2
4a	vw	27334		781	$^{**}0_2$ + 781
5	m	27386		833	$^{**}0_2$ + 833
5a	w	27839	1442	1286	0_1 + 1443 - 1
6	vs	27935		1382	$^{**}0_2$ + 1382
7	vs	27945		1392	$^{**}0_2$ + 1392
8	vw	27960		1407	$^{**}0_2$ + 1382 + latt
9	vs	27996		1443	$^{**}0_2$ + 1443
10	vw	28051		1498	?
11	w	28075		1522	$^{**}0_2$ + 1522
11a	vw	28214	1817	1661	0_1 + 379 + 1443 - 5
12	m	28312		1759	$^{**}0_2$ + 379 + 1382 - 2
13	m	28320		1767	$^{**}0_2$ + 379 + 1392 - 4
14	m	28371		1818	$^{**}0_2$ + 379 + 1443 - 4

Table III.8 Absorption spectrum of $[D_{10}]$-anthracene in n-heptane at 4°K.

No.	Intensity	Energy $\nu(cm^{-1})$	$\Delta\nu(cm^{-1})$			Assignment
			$**0_1$	0_2	0_3	
1	vs	26285	0			$**0_1$
2	vs	26310	25			$**0_1$ + latt
2a	--	(26467)	182	0		0_2
3	vs	26661	376			$**0_1$ + 376
3a	--	(26675)	390		0	0_3
4	s	26688	403			$**0_1$ + 376 + latt
5	w	26854	569	387		0_2 + 376 + lt; $**0_1$ + 569
6	w	26973	688			$**0_1$ + 688
7	vw	26989	704			$**0_1$ + 688 + latt
8	s	27037	752			$**0_1$ + 2x376
9	vw	27047	762		372	0_3 + 376 - 4
10	w	27070	785			$**0_1$ + 785
11	s	27114	829			$**0_1$ + 829
11a	vw	27139	854			$**0_1$ + 829 + latt
11b	vw	27354	1069			$**0_1$ + 376 + 688 + 5
12	vw	27419	1134			$**0_1$ + 3x376 + 6
12a	vvw	27449	1164			$**0_1$ + 376 + 785 + 3
13	m	27491	1206			$**0_1$ + 376 + 829 + 1
14	vs	27672	1387			$**0_1$ + 1387
15	s	27686	1401			$**0_1$ + 1401
16	s	27707	1422			$**0_1$ + 1387 + latt?
17	vs	27727	1442			$**0_1$ + 1442
17a	w	27752	1467			$**0_1$ + 1442 + latt

Table III.8 (continued).

No.	Intensity	Energy $\nu(cm^{-1})$	$\Delta\nu(cm^{-1})$			Assignment
			$**0_1$	0_2	0_3	
18	m	17802	1517			$**0_1$ + 1517
19	vw	27848	1563	1381		0_2 + 1387 - 6
20	vw	27946	1661			$**0_1$ + 2x829 + 3
21	s	28049	1764			$**0_1$ + 376 + 1387 + 1
22	m	28063	1778			$**0_1$ + 376 + 1401 + 1
23	m	28087	1802			$**0_1$ + 376 + 1387 + latt?
24	s	28103	1818			$**0_1$ + 376 + 1442
25	vvw	28130	1845			$**0_1$ + 376 + 1442 + latt
26	vw	28188	1903			$**0_1$ + 376 + 1517 + 10
27	vvw	28223	1938	1756		0_2 + 376 + 1387 - 7
27a	vvw	28356	2071			$**0_1$ + 688 + 1387 - 4
28	w	28426	2141			$**0_1$ + 2x376 + 1387 + 2
28a	vw	28456	2171			$**0_1$ + 785 + 1387 - 1
28b	vw	28479	2194			$**0_1$ + 2x376 + 1442; $**0_1$ + 829 + 1401 - 3
29	vw	28499	2214			$**0_1$ + 829 + 1387 - 2
30	vvw	28512	2227			$**0_1$ + 785 + 1442
30a	vw	28554	2269			$**0_1$ + 2x376 + 1517; $**0_1$ + 829 + 1442 - 2
30b	vw	28649	2364			$**0_1$ + 829 + 1517 + 18?
30c	vvw	28804	2519			$**0_1$ + 3x376 + 1387 + 4
30d	vw	28885	2600			$**0_1$ + 376 + 829 + 1387 + 8
30e	vw	28935	2650			$**0_1$ + 376 + 829 + 1442 + 3
30f	vvw	29025	2740			$**0_1$ + 376 + 829 + 1517 + 18?
31	m	29065	2780			$**0_1$ + 2x1387 + 6

Table III.8 (continued)

No.	Intensity	Energy $\nu(cm^{-1})$	$\Delta\nu(cm^{-1})$			Assignment
			$**0_1$	0_2	0_3	
32	m	29114	2829			$**0_1$ + 1387 + 1442
33	vw	29144	2859			$**0_1$ + 1387 + 1442 + latt
34	w	29166	2881			$**0_1$ + 2x1442 - 3
34a	vvw	29206	2921			$**0_1$ + 1401 + 1517 + 3
34b	w	29256	2971			$**0_1$ + 1442 + 1517 + 12?
35	vw	29438	3153			$**0_1$ + 376 + 2x1387 + 3
36	w	29490	3205			$**0_1$ + 376 + 1387 + 1442
37	vw	29521	3236			$**0_1$ + 376 + 1387 + 1442 + latt
38	vw	29541	3256			$**0_1$ + 376 + 2x1442 - 4
38a	vw	29621	3336			$**0_1$ + 376 + 1442 + 1517 + 1

Table III.9 Absorption spectrum of $[D_{10}]$-anthracene in n-octane at 4°K

No.	Intensity	Energy $\nu(cm^{-1})$	$\Delta\nu(cm^{-1})$			Assignment
			**0_1	0_2	0_3	
1	vs	26227	0			**0_1
2	s	26239	12			**0_1 + latt
3	w	26263	36			artifact, see Chapter 4, section (d)
4	w	26300	73			
4a	--	(26500)	273	0		0_2
5	vs	26602	375			**0_1 + 375
5a	vw	26666	439		0	0_3
5b	vvw	26791	564			**0_1 + 564
5c	vw	26873	646	373		0_2 + 375 - 2
5d	vw	26917	690			**0_1 + 690
6	m	26977	750			**0_1 + 2x375
6a	vw	27015	788			**0_1 + 788
7	m	27040	813		374	0_3 + 375 - 1
8	m	27056	829			**0_1 + 829
9	w	27432	1205			**0_1 + 375 + 829 + 1
10	vw	27491	1264		825	0_3 + 829 - 4
11	vs	27613	1386			**0_1 + 1386
12	s	27628	1404			**0_1 + 1404
13	s	27651	1424			**0_1 + 1386 + latt
14	vs	27670	1443			**0_1 + 1443
15	m	27757	1530			**0_1 + 1530
15a	vw	27787	1560			?
16	s	27989	1762			**0_1 + 375 + 1386 + 1
17	vw	28002	1775			?

Table III.9 (continued).

No.	Intensity	Energy $\nu(cm^{-1})$	$\Delta\nu(cm^{-1})$			Assignment
			$**0_1$	0_2	0_3	
18	vw	28031	1804			$**0_1$ + 375 + 1386 + latt
19	s	28042	1815			$**0_1$ + 375 + 1443 - 3
19a	vw	28106	1879		1440	0_3 + 1443 - 3
20	vw	28131	1904			$**0_1$ + 375 + 1530 - 1
20a	vvw	28362	2135			$**0_1$ + 2x375 + 1386 - 1
21	w	28417	2190			$**0_1$ + 2x375 + 1443 - 3
21a	vw	28445	2218			$**0_1$ + 829 + 1386 + 3
21b	vw	28482	2255		1816	0_3 + 375 + 1443 - 2
21c	vw	28498	2271			$**0_1$ + 829 + 1443 - 1
21d	vvw	28815	2588			$**0_1$ + 375 + 829 + 1386 - 2
21e	vvw	28875	2648			$**0_1$ + 375 + 829 + 1443 + 1
21f	w	29003	2776			$**0_1$ + 2x1386 + 4
22	m	29055	2828			$**0_1$ + 1386 + 1443 - 1
23	w	29107	2880			$**0_1$ + 2x1443 - 6
24	vw	29430	3203			$**0_1$ + 375 + 1386 + 1443 - 1
25	vw	29480	3253			$**0_1$ + 375 + 2x1443 - 8

Table III.10 Fluorescence spectrum of $[D_{10}]$-anthracene in n-hexane at 4°K.

No.	Intensity	Energy $\nu(cm^{-1})$	$\Delta\nu(cm^{-1})$		Assignment
			$**0_1$	0_2	
1	vvw	23536	3017		
2	vvw	23551	3002		$**0_1$ - 1389 - 1617 + 4
3	vw	23627	2926		$**0_1$ - 1389 - 1542 + 5
4	vvw	23750	2803		$**0_1$ - 2x1389 - latt
5	vvw	23764	2789		$**0_1$ - 1389 - 1402 + 2
6	vw	23779	2774		$**0_1$ - 2x1389 + 4
7	w	24557	1996		$**0_1$ - 379 - 1617
8	w	24631	1922	1766	$**0_1$ - 379 - 1542 - 1; 0_2 - 379 - 1389 + 2
9	w	24756	1797		$**0_1$ - 379 - 1389 - latt
10	w	24771	1782		$**0_1$ - 379 - 1402 - 1
11	m	24784	1769	1613	$**0_1$ - 379 - 1389 - 1; 0_2 - 1617 + 4
11a	vw	24866	1687	1531	0_2 - 1542 + 11
12	m	24936	1617		$**0_1$ - 1617
13	s	25011	1542	1386	$**0_1$ - 1542; 0_2 - 1389 + 3
14	s	25021	1532		$**0_1$ - 379 - 1155 + 2
15	m	25137	1416		$**0_1$ - 1389 - latt
16	s	25151	1402		$**0_1$ - 1402
17	vs	25164	1389		$**0_1$ - 1389
18	vvw	25338	1215		$**0_1$ - 379 - 835 - 1
19	vw	25398	1155		$**0_1$ - 1155

Table III.10 (continued)

No.	Intensity	Energy $\nu(cm^{-1})$	$\Delta\nu(cm^{-1})$		Assignment
			$^{**}0_1$	0_2	
20	w	25718	835		$^{**}0_{\Pi}$ - 835
21	vw	25795	758		$^{**}0_{\Pi}$ - 2x379
22	vvw	25846	707		$^{**}0_{\Pi}$ - 707
23	vvw	25954	599		$^{**}0_{\Pi}$ - 599
24	vw	26019	534	378	0_2 - 379 + 1
25	vs	26174	379		$^{**}0_{\Pi}$ - 379
26	w	26376	177	21	0_2 - latt
27	m	26397	156	0	0_2
28	m	26505	48		$^{**}0_{\Pi}$ - latt
29	vs	26530	23		$^{**}0_{\Pi}$ - latt
30	vvs	26553	0		$^{**}0_{\Pi}$

Table III.11 Fluorescence spectrum of $[D_{10}]$-anthracene in n-heptane at 4°K

No.	Intensity	Energy $\nu(cm^{-1})$	$\Delta\nu(cm^{-1})$					Assignment
			0_2	0_3	0_4	0_5	$^{**}0_6$	
1	vvw	23125					3159	$^{**}0_6$ - 380 - 2x1391 + 3
2	vvw	23205					3079	$^{**}0_6$ - 2x1545 + 11 ?
3	vvw	23259					3025	$^{**}0_6$ - 1406 - 1619
4	vw	23276					3008	$^{**}0_6$ - 1391 - 1619 + 2
5	w	23350					2934	$^{**}0_6$ - 1391 - 1545 + 2
6	vvw	23457		3010			2827	0_3 - 1391 - 1619
7	vw	23471					2813	$^{**}0_6$ - 2x1406 - 1
8	w	23482					2802	$^{**}0_6$ - 2x1391 - latt
9	w	23487					2797	$^{**}0_6$ - 1391 - 1406
10	m	23504					2780	$^{**}0_6$ - 2x1391 + 2
11	vvw	23720					2564	$^{**}0_6$ - 1158 - 1406
12	vw	23735					2549	$^{**}0_6$ - 1158 - 1391
13	vvw	23904					2380	$^{**}0_6$ - 835 - 1545
14	vvw	23911					2373	$^{**}0_6$ - 2x380 - 1619 + 6
15	vvw	23985					2299	$^{**}0_6$ - 2x380 - 1545 + 6
16	vvw	24047					2237	$^{**}0_6$ - 835 - 1406 + 4
17	vw	24060					2224	$^{**}0_6$ - 835 - 1391 + 2
18	vw	24135					2149	$^{**}0_6$ - 2x380 - 1391 + 2
19	vvw	24183					2101	$^{**}0_6$ - 712 - 1391 + 2
20	vw	24287					1997	$^{**}0_6$ - 380 - 1619 + 2; $^{**}0_6$ - 835 - 1158 - 4
21	w	24359					1925	$^{**}0_6$ - 380 - 1545
22	vw	24480					1804	$^{**}0_6$ - 380 - 1391 - latt
23	w	24497					1787	$^{**}0_6$ - 380 - 1406 - 1
24	m	24514					1770	$^{**}0_6$ - 380 - 1391 + 1

Table III. 11 (continued)

No.	Intensity	Energy $\nu(cm^{-1})$	$\Delta\nu(cm^{-1})$					Assignment
			0_2	0_3	0_4	0_5	$^{**}0_6$	
25	m	24665					1619	$^{**}0_5$ - 1619
26	vvw	24692		1761			1592	0_3 - 380 - 1391 + 10; $^{**}0_6$ - 2x380 - 835 + 3
27	s	24739					1545	$^{**}0_6$ - 1545; $^{**}0_6$ - 380 - 1158 - 7
28	m	24860					1424	$^{**}0_6$ - 1391 - latt
29	s	24878					1406	$^{**}0_6$ - 1406
30	vs	24893					1391	$^{**}0_6$ - 1391
31	vw	24922		1545		1393	1362	0_3 - 1545; 0_5 - 1391 - 2
32	vvw	24937			1395		1347	0_4 - 1391 - 4
33	vw	25057	1618				1227	0_2 - 1619 + 1
34	w	25068					1216	$^{**}0_6$ - 380 - 835 - 1
35	vw	25081		1386			1203	0_3 - 1391 + 5
36	w	25126	1549				1158	$^{**}0_6$ - 1158; 0_2 - 1545 - 4
37	vvw	25142					1142	$^{**}0_6$ - 3x380 - 2
37a	vvw	25188					1096	$^{**}0_6$ - 380 - 712 - 4
38	vw	25258	1417				1026	0_2 - 1391 - latt
39	vw	25273					1011	?
40	w	25287	1388				997	0_2 - 1391 + 3
41	m	25449					835	$^{**}0_6$ - 835
42	vvw	25477				838	807	0_5 - 835 - 3
43	w	25524					760	$^{**}0_6$ - 2x380
44	vw	25572					712	$^{**}0_6$ - 712
45	vw	25682					602	$^{**}0_6$ - 602
46	vvw	25748		719			536	0_3 - 712 - 7

Table III.11 (continued).

No.	Intensity	Energy $\nu(cm^{-1})$	$\Delta\nu(cm^{-1})$					Assignment
			0_2	0_3	0_4	0_5	$^{**}0_6$	
47	vw	25837	838				447	0_2 - 835 - 3
47a	vw	25876					408	$^{**}0_6$ - 380 - latt
48	vs	25904					380	$^{**}0_6$ - 380
49	vw	25933				382	351	0_5 - 380 - 2
50	vvw	25952			380		332	0_4 - 380
51	vw	26076		391			208	0_3 - 380 - latt
52	vw	26090		377			194	0_3 - 380 + 3
53	vvw	26110					174	0_{10}
54	vw	26131					153	0_9
55	vvw	26174					110	0_8
55a	w	26221					63	0_7
56	s	26263					21	$^{**}0_6$ - latt
57	s	26284					0	$^{**}0_6$
58	vw	26296	379				-12	0_2 - 380 + 1
59	vw	26315				0	-31	0_5
60	vvw	26332			0		-48	0_4
61	vw	26442		25			-158	0_3 - latt
62	w	26453		14			-169	0_3 - latt
63	w	26467		0			-183	0_3
64	vw	26647	28				-363	0_2 - latt
65	m	26675	0				-391	0_2
65a	vvw	26730					-446	0_1

Table III.12 Fluorescence spectrum of $[D_{10}]$-anthracene in n-octane at 4°K.

No.	Intensity	Energy $\nu(cm^{-1})$	$\Delta\nu(cm^{-1})$					Assignment
			0_1	0_2	0_3	0_4	0_5	
1	vvw	23220					3006	$^{**}0_5$ - 1391 - 1619 + 4
2	vw	23292					2934	$^{**}0_5$ - 1391 - 1545 + 2
3	vvw	23428					2798	$^{**}0_5$ - 1391 - 1407
4	vw	23447					2779	$^{**}0_5$ - 2x1391 + 3
5	vvw	23679					2547	$^{**}0_5$ - 1159 - 1391 + 3
6	vvw	23745					2481	$^{**}0_5$ - 378 - 713 - 1391 + 1
7	vvw	23999					2227	$^{**}0_5$ - 836 - 1391
8	vvw	24080					2146	$^{**}0_5$ - 2x378 - 1391 + 1
9	vw	24231					1995	$^{**}0_5$ - 378 - 1619 + 2
10	vw	24301					1925	$^{**}0_5$ - 378 - 1545 - 2
11	vw	24311					1915	$^{**}0_5$ - 2x378 - 1159
12	vw	24421					1805	$^{**}0_5$ - 378 - 1391 - latt
13	w	24440					1786	$^{**}0_5$ - 378 - 1407 - 1
14	m	24456					1770	$^{**}0_5$ - 378 - 1391 - 1
15	w	24607					1619	$^{**}0_5$ - 1619
16	m	24681					1545	$^{**}0_5$ - 1545
17	w	24690					1536	$^{**}0_5$ - 378 - 1159 + 1
18	m	24801					1425	$^{**}0_5$ - 1391 - latt
19	s	24819					1407	$^{**}0_5$ - 1407
20	vs	24835					1391	$^{**}0_5$ - 1391
21	vw	24904		1762			1322	0_2 - 378 - 1391 + 7
22	vvw	25011				1392	1215	0_4 - 1391 - 1; $^{**}0_5$ - 378 - 836 - 1
23	vw	25049		1617			1177	0_2 - 1619 + 2
24	vw	25067					1159	$^{**}0_5$ - 1159
25	vvw	25108			1392		1118	0_3 - 1391 - 1
26	vvw	25125		1541			1101	0_2 - 1545 + 4

Table III.12 (continued).

No.	Intensity	Energy $\nu(cm^{-1})$	$\Delta\nu(cm^{-1})$					Assignment
			0_1	0_2	0_3	0_4	0_5	
27	vw	25135					1091	$^{**}0_5$ - 378 - 713
28	vvw	25252		1414			974	0_2 - 1391 - latt
29	vw	25266					960	?
30	w	25280		1386			946	0_2 - 1391 + 5
31	w	25390					836	$^{**}0_5$ - 836
32	vvw	25457					769	$^{**}0_5$ - 2x378 - latt
33	vw	25468					758	$^{**}0_5$ - 2x378 - 2
34	vw	25513		1153			713	$^{**}0_5$ - 713; 0_2 - 1159 + 6
35	vvw	25624					602	$^{**}0_5$ - 602
36	w	25830		836			396	$^{**}0_5$ - 378 - latt; 0_2 - 836
37	vs	25848					378	$^{**}0_5$ - 378
38	vvw	25914		752			312	0_2 - 2x378 + 4
39	vvw	26081					145	0_6
40	vvw	26121			379		105	0_3 - 378 - 1
41	w	26207					19	$^{**}0_5$ - latt
42	vs	26226					0	$^{**}0_5$
43	w	26290		376			-64	0_2 - 378 + 2
43a	vw	26315	382				-89	0_1 - 378 - 4
44	vvw	26380				23	-154	0_4 - latt
45	vw	26403				0	-177	0_4
46	vw	26500			0		-274	0_3
47	vvw	26623		43			-397	0_2 - latt
48	w	26648		18			-422	0_2 - latt
49	m	26666		0			-440	0_2
50	w	26697	0				-471	0_1

b) Vibrational analyses of the spectra

Before the experimental data are discussed, it may be helpful to comment briefly on the nature of the electronic transition which is involved.

For anthracene, the lowest energy transition is the one, starting at ca. 380 nm, studied in the present work. The upper state has $^1B_{1u}^+$ symmetry in the point group D_{2h};[62*] the transition is symmetry allowed, and experimentally has a moderate oscillator strength, ca. 0.1.[63]

The transition dipole lies along the short axis of the molecule. Another transition, symmetry forbidden, is polarized along the long axis. Whereas the latter ($^1L_b \leftarrow {}^1A$ in Platt's notation[63]) lies to lower energy in the case of benzene and naphthalene and is responsible for the weak first band (f ca. 0.002), a further increase in the number of benzenoid rings in the linear system causes a sufficiently large red shift of the short-axis transition ($^1L_a \leftarrow {}^1A$) to reverse this order.

As is expected of a moderately allowed transition, the vibrational structure consists largely of totally symmetrical (A_{1g}) modes. However, as will be seen later, some B_{1g} modes also participate.

Using the methods described in section 3(d), extraction and analysis of data, values of vibrational frequencies for the anthracene and $[D_{10}]$-anthracene molecules were obtained, in absorption and

*Because of a different convention in defining the molecular axes, Pariser actually uses the symbol $^1B_{2u}^+$ in this paper. I have chosen $^1B_{1u}^+$ to conform with the description usually given for benzene.

emission (i.e. for the upper and lower electronic states, respectively) in each of the three matrices, n-hexane, n-heptane, and n-octane.

These values are listed with error estimates in Tables III.13 and III.14; with each vibrational frequency is given the intensity of the line, derived from the main origin, containing one quantum of that vibrational mode.

i) Correspondence of modes in anthracene and $[D_{10}]$-anthracene. A number of criteria have been used in establishing the correspondence:

a) A given mode should be present with the same intensity in the spectra of the two molecules. This was the criterion used by Pesteil and co-workers in similar studies of the naphthalenes and the phenanthrenes;[15,16] where a mode is strongly present in absorption but not in emission, or vice versa, this is a particularly valuable criterion.

b) In comparing the six spectra (absorption and emission in each of three matrices) of each molecule, we might expect to see a similar pattern of frequency changes in corresponding modes.

c) The frequency of a mode in the deuterated molecule will normally be lower than in the undeuterated molecule.

d) The values can be compared with calculated values. To my knowledge there are no experimental studies of the vibrational modes of $[D_{10}]$-anthracene in the literature.

Figures III.14 and III.15 show the frequency changes for the modes of the undeuterated and deuterated molecules, respectively. The symbols used in the abscissa on these figures signify:

Table III.13. Vibrational modes of anthracene in various n-alkane matrices at 4°K. Intensities are given in parentheses

Matrix					
n-hexane		n-heptane		n-octane	
Vibrational frequency (cm^{-1})					
Absorption	Fluorescence	Absorption	Fluorescence	Absorption	Fluorescence
389 ±2 (vs)	395 ±2 (vs)	390 ±2 (vs)	392 ±2 (vs)	390 ±2 (vs)	392 ±2 (vs)
609 ±8 (vw)	627 ±4 (vw)	587 ±4 (w)	624 ±4 (vw)	590 ±8 (vw)	625 ±4 (vw)
---	---	662 ±4 (vw)	---	661 ±8 (vw)	---
731 ±8 (w)	754 ±4 (vvw)	743 ±4 (w)	757 ±4 (vw)	744 ±4 (w)	760 ±4 (vw)
888 ±8 (w)	---	892 ±4 (vw)	---	891 ±4 (vw)	---
1018 ±8 (w)	---	1028 ±2 (m)	---	1029 ±4 (w)	---
1155 ±2 (s)	1164 ±2 (m)	1159 ±4 (s)	1162 ±4 (m)	1160 ±4 (s)	1165 ±2 (s)
---	1265 ±4 (w)	---	1265 ±4 (m)	---	1260 ±4 (m)
1297 ±4 (vw)	1409 ±4 (vs)	1303 ±8 (vw)	1406 ±4 (vs)	1298 ±8(vvw)	1407 ±4 (vs)
1393 ±4 (vs)	---	1397 ±4 (vs)	---	1402 ±4 (vs)	1411 ±4 (vs)
---	---	---	---	---	---
1465 ±4 (vw)	---	1464 ±4 (m)	---	1470 ±4 (w)	---
1497 ±2 (m)	1563 ±4 (s)	1503 ±4 (m)	1564 ±4 (s)	1505 ±4 (w)	1569 ±4 (s)
1563 ±4 (w)	1638 ±2 (m)	1550 ±8 (m)	1638 ±2 (m)	1555 ±8 (w)	1642 ±2 (m)

Table III.14. Vibrational modes of $[D_{10}]$-anthracene in various n-alkane matrices at 4°K. Intensities are given in parentheses.

Matrix					
n-hexane		n-heptane		n-octane	
Vibrational frequency (cm^{-1})					
Absorption	Fluorescence	Absorption	Fluorescence	Absorption	Fluorescence
379 ±4 (vs)	379 ±2 (vs)	376 ±2 (vs)	380 ±2 (vs)	375 ±2 (vs)	378 ±2 (vs)
---	599 ±4(vvw)	---	602 ±4 (vw)	---	602 ±4(vvw)
691 ±8 (vw)	707 ±4(vvw)	688 ±4 (w)	712 ±4 (vw)	690 ±4 (vw)	713 ±4 (vw)
781 ±4 (vw)	---	785 ±2 (w)	---	788 ±4 (vw)	---
833 ±4 (m)	835 ±2 (w)	829 ±2 (s)	835 ±2 (m)	829 ±4 (m)	836 ±2 (w)
---	1155 ±4 (vw)	---	1158 ±4 (w)	---	1159 ±4 (vw)
1382 ±4 (vs)	1389 ±4 (vs)	1387 ±4 (vs)	1391 ±2 (vs)	1386 ±4 (vs)	1391 ±2 (vs)
1392 ±4 (vs)	1402 ±4 (s)	1401 ±4 (s)	1406 ±4 (s)	1404 ±8 (s)	1407 ±4 (s)
1443 ±4 (vs)	---	1442 ±4 (vs)	---	1443 ±4 (vs)	---
1522 ±8 (w)	1542 ±4 (s)	1517 ±8 (m)	1545 ±4 (s)	1530 ±4 (m)	1545 ±4 (m)
---	1617 ±2 (m)	---	1619 ±2 (m)	---	1619 ±2 (w)

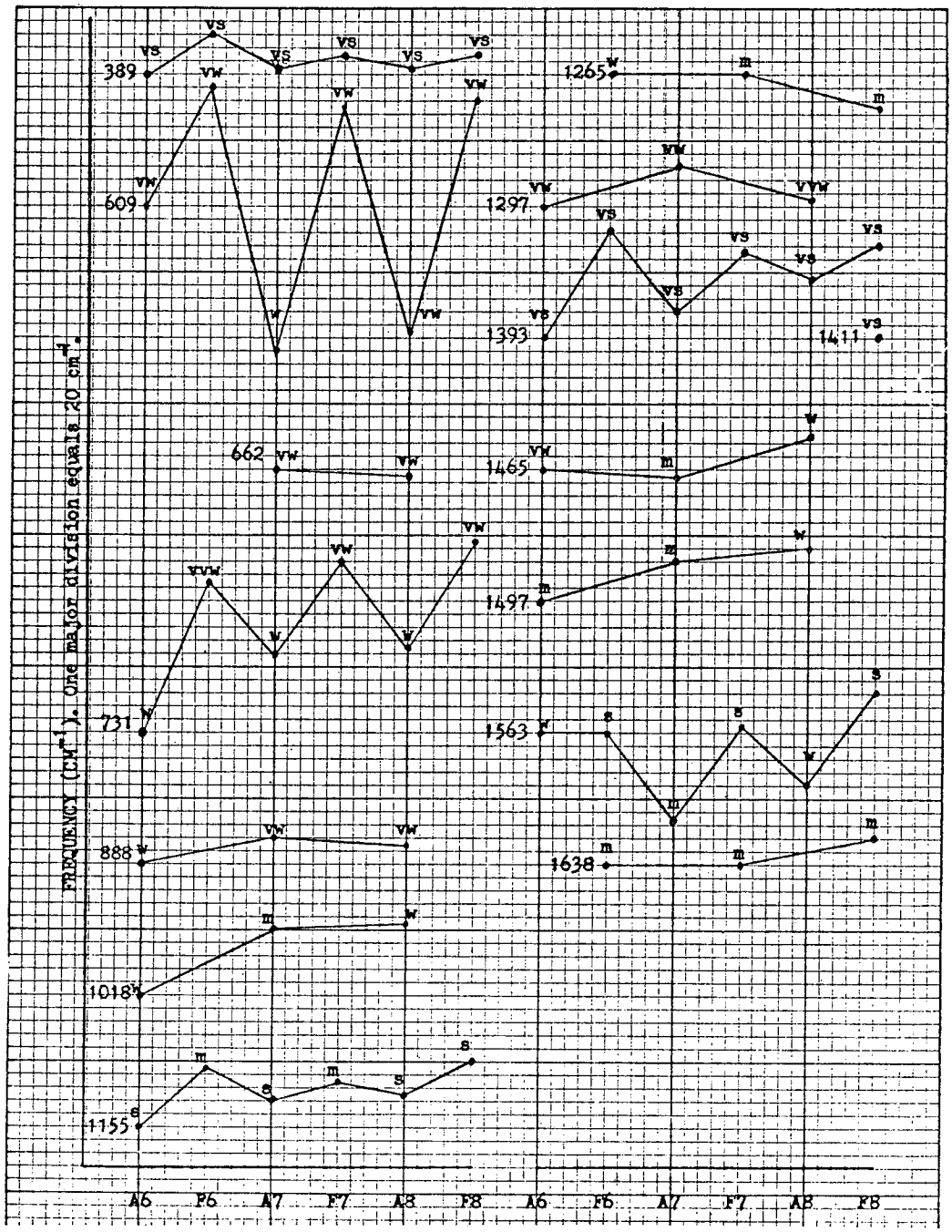

XBL 697-4363

Figure III.14. Vibrational frequencies of anthracene in absorption and emission in n-hexane, n-heptane, and n-octane at 4°K. For description of this figure see text.

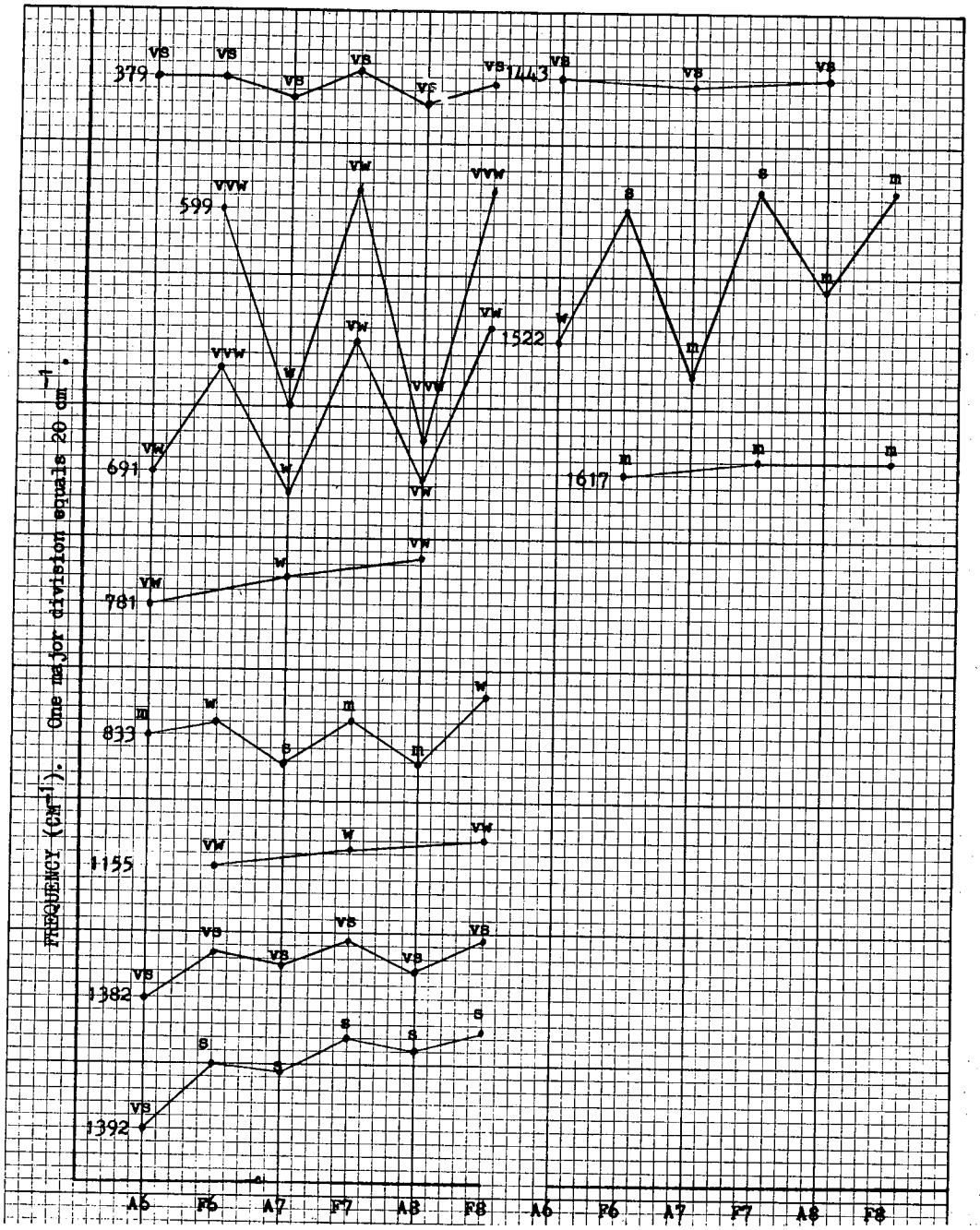

XBL 697-4362

Figure III.15. Vibrational frequencies of [D_{10}]-anthracene in absorption and emission in n-hexane, n-heptane, and n-octane at 4°K. For description of this figure, see text.

A6: Absorption spectrum in n-hexane at 4°K

F6: Fluorescence spectrum in n-hexane at 4°K

A7: Absorption spectrum in n-heptane at 4°K, etc.

The frequency of the first member of each "fingerprint" of a vibrational mode is given in cm^{-1} and other frequencies are related to it. Intensities are also indicated.

From these two figures a number of correspondences were established, using criteria a), b), and c) mentioned above.

The experimental frequencies were then compared with theoretical values calculated by Krainov,[56] as shown in Table III.15. His method of calculation is not clear from the brief account in the published paper; it states that the interaction coefficients for the anthracene molecule were assumed to be the same as the (known) coefficients for naphthalene; interaction between the two outside rings of anthracene was assumed negligible. Inversion of the interaction coefficient matrix gave the force constant matrix, which was then used to solve the secular equations.

In Table III.15, the experimental frequency values are averages for the molecules in the three matrices which were used. As can be seen, the agreement with calculated values is quite good, except for modes 5, 7, and 8. The latter two are very intense modes lying close to one another in the region of 1400 cm^{-1}. Calculation predicts separations for the undeuterated and deuterated molecules of 61 cm^{-1} for mode 7 and 130 cm^{-1} for mode 8, whereas the experimental separations are ca. 14 cm^{-1} and 6 cm^{-1}, respectively. However, on the basis of intensity there can be no doubt that the correspondence

Table III.15. Corresponding vibrational frequencies of anthracene and [D_{10}]-anthracene. (H ≡ anthracene, D ≡ [D_{10}]-anthracene

No.	Experimental (this work)						Calculated (ref. 19)		
	H		D		(H-D)		H	D	(H-D)
	Abs	Fluor	Abs	Fluor	Abs	Fluor			
1	390	393	377	379	13	21	376	363	13
2	595	625	567	601	28	24	623	600	23
3	739	757	567	601	172	156	754	592	162
4	1025	---	785	---	240	---	1029	821	208
5	1158	1164	830	835	328	329	1127	884	243
6	---	1263	---	1157	---	106	1258	1188	70
7	1397	1406	1385	1390	12	16	1396	1335	61
8	---	1411	1399	1405	---	6	1396	1266	130
9	1502	---	1443	---	59	---	1499	1435	64
10	1556	1565	1523	1544	33	21	1569	1535	34
11	---	1639	---	1619	---	20	1633	1619	14

shown in the table is valid, at least to the extent that the pair of frequencies 7,8 correspond. It may be that the order of correspondence of the pair should be reversed.

Those frequencies for which no correspondence could be established are listed in Table III.16. There are 4 for the undeuterated molecule and 1 for the deuterated molecule. All are weak or very weak and so presumably the corresponding frequencies in the other molecule are hidden under stronger bands.

Table III.16. Vibrational frequencies of anthracene and $[D_{10}]$-anthracene for which no correspondence has been established.

No.	Anthracene	
	Abs	Fluor
12	662	---
13	890	---
14	1299	---
15	1466	---
No.	$[D_{10}]$-Anthracene	
	Abs	Fluor
16	690	711

ii) Comparison of vibrational frequencies of anthracene with other values in the literature. The most direct comparison which can be made is with the paper by Bolotnikova,[11] who has investigated the absorption and fluorescence spectra of anthracene in n-heptane at 4°K. As will be seen, care has to be taken in making the comparison, since there are many errors in her Table 2 (absorption spectrum), and some dubious methods of extracting frequencies from the original spectrum; since the original fluorescence spectrum is not tabulated in the paper, no check on the vibrational frequencies extracted from it is possible. The justifications for these criticisms of Bolotnikova's paper will become evident from the ensuing discussion. Table III.17 gives my data for anthracene in n-heptane together with the corresponding data of Bolotnikova (taken from her Table 1). The numbers used to identify modes in the present table do not correspond to those used in Table III.15.

There are clearly many differences between the two sets of data, both with respect to the modes observed and the values of those frequencies which appear in both sets.

Frequencies observed by both authors

These are: #3, 4, 6, 13, 16F, 17A, 18 or 19, 22, 24F.*

The agreement in the values obtained for these modes is sometimes poor (e.g. #4, 6A, 22A) and exceeds the error estimates for the present work.

---

*A numeral such as 17A refers to frequency #17 in absorption,
" " 17F " " " fluorescence, and
" " 17 " " " both.

Table III.17. Vibrational frequencies of anthracene observed in its absorption and fluorescence spectra in n-heptane at 4°K. Comparison of values reported by the present author and by Bolotnikova.[11] (1A, etc. signifies absorption values; 1F, etc. signifies fluorescence values).

No.	Frequency (cm^{-1})				
	Absorption		No.	Fluorescence	
	This work	Bolotnikova		This work	Bolotnikova
(1A)	---	338	(1F)	---	338
(2A)	---	365	(2F)	---	365
(3A)	390	394	(3F)	392	394
(4A)	587	599	(4F)	624	606
(5A)	662	---	(5F)	---	---
(6A)	743	754	(6F)	757	756
(7A)	892	---	(7F)	---	---
(8A)	---	978	(8F)	---	974
(9A)	---	1004	(9F)	---	---
(10A)	1028	---	(10F)	---	---
(11A)	---	---	(11F)	---	1114
(12A)	---	1135	(12F)	---	1135
(13A)	1159	1163	(13F)	1162	1157
(14A)	---	1183	(14F)	---	1181
(15A)	---	1207	(15F)	---	1210
(16A)	---	1251	(16F)	1265	1266
(17A)	1303	1307	(17F)	---	1309
(18A)	1397	1395	(18F)	1406	1402
(19A)		1405	(19F)		1407
(20A)	1464	---	(20F)	---	---
(21A)	1503	---	(21F)	---	---
(22A)	1550	1565	(22F)	1564	1565
(23A)	---	1608	(23F)	---	1603
(24A)	---	1647	(24F)	1638	1647

Examination of Table 2 in ref. 11 (absorption spectrum) reveals that it contains numerous errors in the subtractions of lines from their origins; in a few cases the line positions themselves appear to be incorrect since they do not fall within the monotonically increasing energy sequence. There also seems to be little sense or system to the method of specifying the values of the vibrational frequencies. They appear to be "averages" of the values from various multiplet origins, weighted in some arbitrary manner to some of the less intense origins.

After errors have been corrected, and the frequencies from the most intense origin (which agrees with the main origin in my spectra) are used, agreement (Table III.18) between the two sets of absorption data is extremely good. It was not possible to check Bolotnikova's fluorescence data since the original spectrum was not given.

Of the two frequencies 18 and 19 observed by Bolotnikova at 1395 and 1387 cm^{-1}, only one was observed by me, at 1397 cm^{-1}. However, her value of 1387 cm^{-1} cannot usefully be discussed since the position of the line giving rise to it is in doubt (see table). That there may be two frequencies lying very close together in my spectrum is indicated by the width of the line, and in fact two frequencies (1407 and 1411 cm^{-1}) were observed in the fluorescence spectrum in n-octane, and in all the spectra of $[D_{10}]$-anthracene.

Frequencies observed in the present work only

These are: #5A, 7A, 10A, 20A, and 21A.

The lines from which these frequencies were extracted were all observed by Bolotnikova also. It therefore becomes a matter of

Table III.18. Vibrational frequencies of anthracene in n-heptane at 4°K; values for modes observed in the absorption spectrum both by the present author and by Bolotnikova.[11] Bolotnikova's data altered as discussed in text, with values before alteration in parentheses.

No.	Frequency (cm^{-1})		
	This work	Bolotnikova	
(3A)	390	390	(394)
(4A)	587	589	(599)
(6A)	743	743	(754)
(13A)	1159	1160	(1163)
(17A)	1303	1304	(1307)
(18A)	1397	1395	(1395)
(19A)		1387*	(1405)
(22A)	1550	1549	(1565)

*Uncertain, since the line giving rise to this frequency may be in error (see text).

comparing the assignments of the two authors. The line giving rise to frequency 7A, although described as 'intense', is given no assignment by Bolotnikova. The lines giving rise to frequencies 5A, 10A, 20A, and 21A, described as 'medium', 'intense', 'intense', and 'intense', respectively, are all assigned to modes derived from origins other than the main one, even though these same frequencies only appear with

an equal or lower intensity when derived from the main origin.* Because of this the assignments made by Bolotnikova are, I believe, incorrect or at best secondary. The assignments made in the present work are justified as follows:

(a) The frequencies were observed in all three solvents (except for #5A, which was very weak and was not observed in n-hexane). This indicates that the lines are not derived from secondary origins, since these vary from solvent to solvent. It also shows the advantage in measuring the spectrum in several solvents.

(b) The frequencies 10A, 20A, and 21A were observed in combination with other anthracene frequencies, showing that the lines were not associated with an impurity. Frequencies 5A and 7A were too weak to be observed in combination.

Re-assignments made by me are compared with values from the present work, in Table III.19. Agreement is extremely good.

---

*A specific example may make this clearer. The line which I assign to $^{**}0_1$ + 1028 is assigned by Bolotnikova to 0_2 + 978 and is described as 'intense'. Yet $^{**}0_1$ + 978, the corresponding line derived from the main origin, is 'medium'. This conflicts with other lines derived from these origins; e.g. 0_2 + 390 is 'medium', while $^{**}0_1$ + 390 is 'very intense'.

Table III.19. Comparison of anthracene vibrational frequencies 5A, 7A, 10A, 20A, and 21A, extracted by the author from his own data and those of Bolotnikova.

No.	Frequency (cm^{-1})	
	This work	Bolotnikova
(5A)	662	661
(7A)	892	893
(10A)	1028	1026
(20A)	1464	1463
(21A)	1503	1504

Frequencies observed by Bolotnikova only

These are: #1, 2, 8, 9A, 11F, 12, 14, 15, 16A, 17F, 23, and 24A.

Lines giving rise to frequencies 2F, 8F, 14F, and 23F were observed in the present work but were not given the same assignments as by Bolotnikova. A closer search of the present spectra for lines which could have given rise to the remaining frequencies did reveal several, close to the threshold of observation. These frequencies are #8A, 9A, 12A, 12F, 14A, 23A, and 24A. However, again the assignment made does not always agree with Bolotnikova's.

Table III.20 compares the two sets of data, gives the alternative assignments, and indicates whether or not, in my opinion, the mode has been observed. Where a frequency is derived from a secondary origin, and does not appear from the main origin, the assignment is

Table III.20. Examination of vibrational frequencies of anthracene reported by Bolotnikova only. Frequencies in cm^{-1}.

No.	This work		Bolotnikova		Status
	Freq.	Assignment	Freq.	Comments by present author	
(1A)	--	--	338	Not derived from main origin	No
(2A)	--	--	365	Not derived from main origin	No
(8A)	(978)	390 + 587 + 1; 978(?)	978	--	Uncertain
(9A)	(1002)	1002	1004	--	Yes
(12A)	(1136)	390 + 743 + 3; 1136(?)	1135	--	Uncertain
(14A)	(1188)	1159 + latt; 1188(?)	1183	--	Uncertain
(15A)	--	--	1207	--	Uncertain
(16A)	--	--	1251	Not derived from main origin	No
(23A)	(1618)	secondary origin + 1394	1608	Not derived from main origin	No
(24A)	(1638)	1638	1647	Not derived from main origin	Uncertain
(1F)	--	--	338	--	Unlikely
(2F)	363	secondary origin + 392	365	--	Unlikely
(8F)	981	secondary origin + 1162	974	--	Uncertain
(11F)	--	--	1114	This frequency was placed next to the frequency 1004 in abs, & is probably in error	No
(12F)	(1137)	1137	1135	--	Yes
(14F)	1182	3x392 + 6; 1182(?)	1181	--	Uncertain
(15F)	--	--	1210	--	Uncertain
(17F)	--	--	1309	--	Uncertain
(23F)	1613	secondary origin +392 +1406	1603	--	Unlikely

rejected, with the exception of frequency 24A, which is observed from the main origin in the present work.

Notes on Table III.20:

(1) All frequencies derived from present work relate to the main origin. This is not true of Bolotnikova's data.

(2) Values in parentheses are derived from lines on the threshold of observation; the lines are not included in the main data tables (III.1 - III.12).

(3) The status column indicates whether I consider that mode has been observed by the Shpolskii technique. It is not intended to reflect on the validity of observations made by other techniques such as Raman.

(4) Examination of Bolotnikova's assignments in fluorescence was not possible since the original spectrum was not given.

A cursory examination of this table shows that only two additional frequencies are accepted by me, #9A at 1002 cm^{-1}, and #12F at 1137 cm^{-1}. The remainder are either rejected or considered unproved.

Comparison with Raman data

Anthracene has been studied by Raman spectroscopy, in solution by Manzoni[52] and by Abasbegovic et al.,[51] and as the pure crystal by Colombo and Mathieu.[55] Abasbegovic's paper lists 31 frequencies, most of which were observed in all of the three solvents he used. He also made symmetry assignments on the basis of polarization measurements. Since his data are the most recent and the most comprehensive, they will be used here for comparison with the present work.

Table III.21 gives this comparison, and where possible a comparison with the theoretical values of Krainov.[56] Agreement between the values obtained from fluorescence and Raman spectra is quite close; with the exception of the second frequency listed, the differences are <10 cm^{-1}. Agreement between Raman and absorption data is of course much less close, since the vibrations now belong to a different electronic state. Vibrational frequencies of the excited electronic state are typically 5 - 25 cm^{-1} lower than in the ground state, indicating a reduction in the degree of bonding.

Abasbegovic's symmetry assignments are based on polarization measurements, made at right angles to the incident unpolarized light. Theory predicts (e.g. ref. 57, p. 52) that for non-totally symmetric vibrations the depolarization ratio should be 6/7; for totally symmetric vibrations the ratio should be lower, and in the limit of an isotropically polarizable molecule it should be zero. In Abasbegovic's nomenclature, vibrations with A_{1g} symmetry should give polarized lines while those with B type symmetry should give depolarized lines. However, there is no quantitative data on depolarization ratios in his paper and this makes it hard to assess the validity of his results.

In the case of Krainov's theoretical data, the symmetries are initial parameters of the calculation, and it is the uncertainty in the vibrational frequency values, and hence the matching of modes to those obtained experimentally, which introduces ambiguity. For a number of the modes, however, the correspondence seems clear--in particular the correspondence of the predicted A_{1g} mode at 376 cm^{-1} to the observed mode at 396 cm^{-1} (assigned as B_{1g} symmetry), and the

Table III.21. Comparison between vibrational frequencies of anthracene obtained in the present work, and those obtained by Raman spectroscopy. The calculated data of Krainov are also included. Frequencies are given in cm^{-1}.

This work		Raman (ref. 14)		Calculated (ref. 20)	
Abs.	Fluor.				
390	393	396	B_{1g}	376	A_{1g}
595	625	601	A_{1g}	623	A_{1g}
662	---	698?			
739	757	755	A_{1g}	754	B_{2g}
890	---	---		894	B_{1g}
1002	---	1007	A_{1g}		
1025	---	---		1029	A_{1g}
---	1137	(1130)*			
1158	1164	1165	A_{1g}	1127	A_{1g}
---	1263	1261	A_{1g}	1258	A_{1g}
1299	---	1304		1279	B_{1g}
1397	1406	1403	A_{1g}	1396	A_{1g}
---	1411	1414	A_{1g}	1396	B_{1g}
1466	---	1480	B_{1g}	1499	A_{1g}?
1502	---	(1520)*		1499	A_{1g}?
1556	1565	1561	A_{1g}	1569	A_{1g}
---	1639	1634	B_{1g}	1633	B_{1g}

*Observed by Manzoni,[52] but not by Abasbegovic.

correspondence of the two predicted modes, of A_{1g} and B_{1g} symmetry respectively, at 1396 cm^{-1}, to the observed modes at 1403 and 1414 cm^{-1} (both assigned A_{1g} symmetry).

It seems likely, therefore, that some of the symmetry assignments made by Abasbegovic are in error.

c) Hypothesis of fluorescence before vibrational relaxation is complete

This was described in the introduction to this part of the thesis. Briefly, Bolotnikova observed[11] in the fluorescence spectrum of anthracene in n-heptane at 4°K, that there was a line displaced to high energy of the main origin by exactly the amount of one of the most intense vibrational frequencies of anthracene. I made the hypothesis that the line represents emission from molecules which still possess one quantum of vibrational energy, i.e. molecules which have failed to relax.

i) Attempt to confirm Bolotnikova's observation. The absorption and fluorescence spectra of anthracene in n-heptane at 4°K were taken. Figure III.16 shows the strip-chart recording of the fluorescence spectrum in the region of the main origin. The numbers used to index lines are the same as those in the main data tables, section (a) of this chapter.

The main origin, line 47, is easily identified by its relation to the spectrum as a whole, and by comparison with the absorption spectrum. Line 46, at about 20 cm^{-1} lower energy, and of comparable intensity, is believed to involve lattice vibrations, as are lines

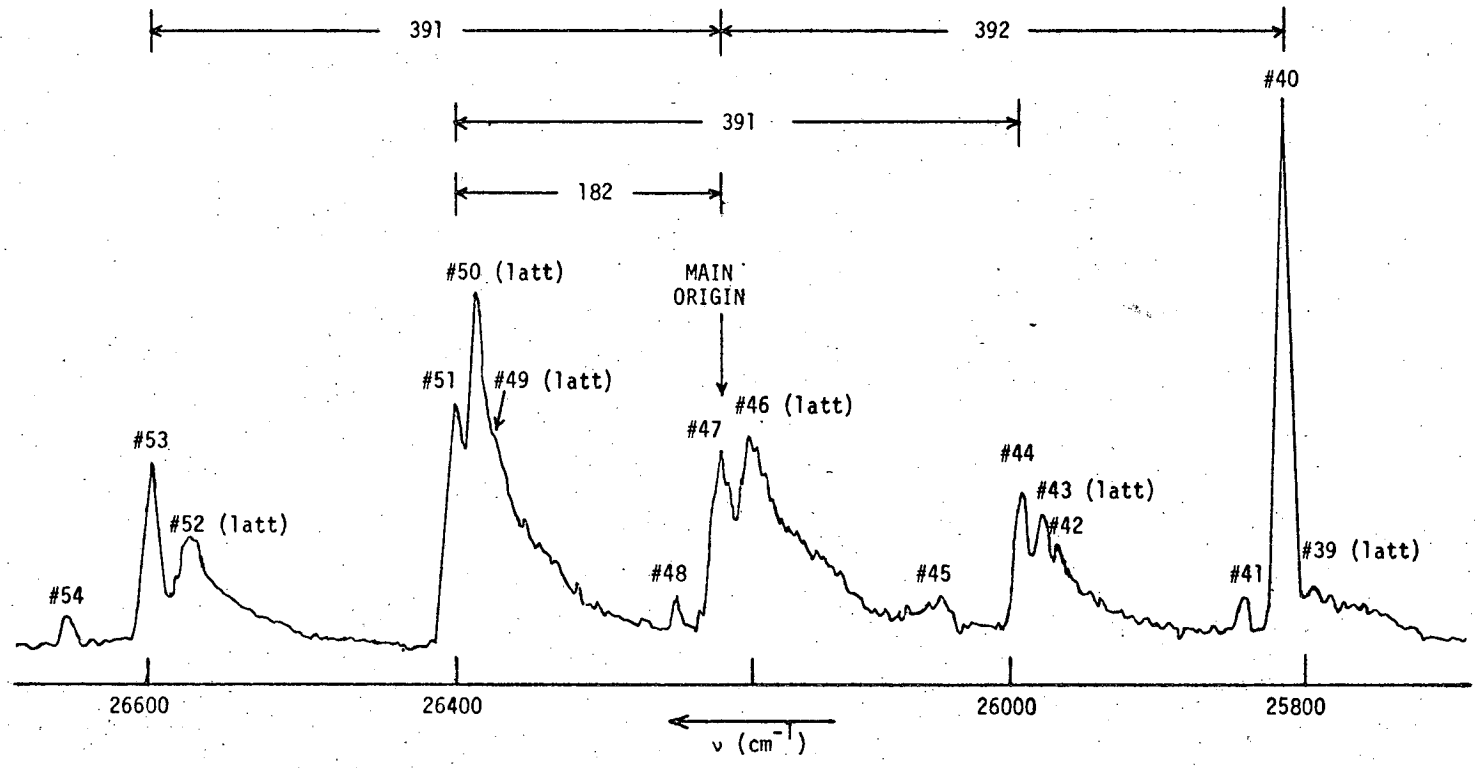

XBL 696-4292

Figure III.16. Fluorescence spectrum of anthracene in n-heptane at 4°K, in the region of the main origin. Line 53 was the basis for the hypothesis of fluorescence from vibrationally excited molecules.

52, 50, 49, 43, 42, and 39. For a discussion of these lines see section (d) of this chapter, on the nature of the multiplet structure.

Line 53 confirms Bolotnikova's observation; it is 391 cm^{-1} to the high energy side of the main origin, in close agreement with the first intense vibrational line of the spectrum (#40) which is at 392 cm^{-1} to the low energy side. Strictly, the comparison should be made with the vibrational quantum in absorption (390 cm^{-1}) since we are considering vibrational energy in the upper electronic state.

There are other features which were not evident from Bolotnikova's paper, since details were not given of the fluorescence spectrum. The most notable of these is line 51 (with its satellite lattice lines), 182 cm^{-1} to the high energy side of the main origin, and more intense than either the main origin or line 53.* 391 cm^{-1} to lower energy from line 51 is line 44. If line 44 is a secondary origin (i.e. is for molecules in a secondary site) line 51 would correspond to emission from vibrationally excited molecules in this secondary site; if, on the other hand, line 51 is a secondary origin, line 44 would be a normal vibrational line of its spectrum, corresponding to emission from a pure upper electronic state to a vibrationally excited lower state. The absence in the absorption spectrum of an origin at the position of line 44 suggests that the latter explanation may be the correct one.** If so, this demonstrates that secondary origins to

*For a discussion of intensities in the region of overlap between absorption and fluorescence spectra see section (d) of this chapter.

**Note that no information can be gained by using this argument in the case of line 53. It is just the existence of a line at 391 cm^{-1} from the main origin that has posed the question in the first place. No observation of a vibrational line of line 53, if it were a secondary origin, is possible, since this would be obscured by the main origin.

considerably higher energy than the main origin are possible, and reduces one of the arguments against line 53 being a secondary origin. This remark about line 51 applies *a fortiori* to the weak line 54.

Obviously, every line in the spectrum assigned to the main origin can also be given an explanation in terms of line 53, as these differ by one 392 cm^{-1} quantum. In addition, there are a number of lines related to line 53 by other vibrational modes only (*e.g.* lines 36, 33, 32; see Table III.5 in section (a) of this chapter). This is to be expected whether or not line 53 represents emission from vibrationally excited molecules.

ii) *Selective excitation experiments.* Svishchev[25] showed that when he selectively excited one component of the multiplet (in this case a doublet) of coronene (Figure III.17), only the portion of the spectrum derived from that component appeared in emission. This is considered a major piece of evidence in support of the hypothesis of separate sites (see part I, and also section (d) of this chapter).

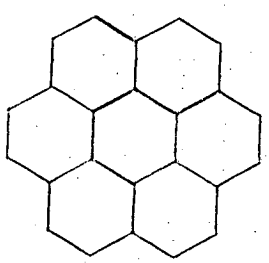

Figure III.17. Coronene.

I carried out this experiment on anthracene in n-heptane, using a narrow slit on the excitation monochromator to give a bandwidth of ca. 200 cm^{-1}. When the excitation band was centered around the main origin, lines attributable to line 53, including line 53 itself, disappeared. (The latter, of course, is a necessary consequence of energy conservation.)

When the excitation was centered around line 53, lines derived from line 53 and from the main origin were observed, although those derived from line 53 were more intense than they had been in broad band excitation experiments. For example, the lines representing one quantum of the 1406 cm^{-1} mode had intensities in the ratio 0.38 when broad band excitation was used, and 0.47 when line 53 was selectively excited.

Partial relaxation of vibrationally excited molecules would allow both systems of lines to be observed, but so would the existence of two molecular environments in this particular system, because re-absorption at the other site and subsequent emission is made possible by coincidence (Figure III.18).

iii) Search for higher excited vibrational levels. Broad band excitation at a suitably high energy was used, and with the amplifier sensitivity 10 times that normally used for recording fluorescence spectra, a search was made for emission to the high energy side of the main origin, particularly in the region of the spectrum around 1400 cm^{-1} (an intense vibrational frequency) from the main origin. No emission was found beyond line 54 (449 cm^{-1} from the main origin).

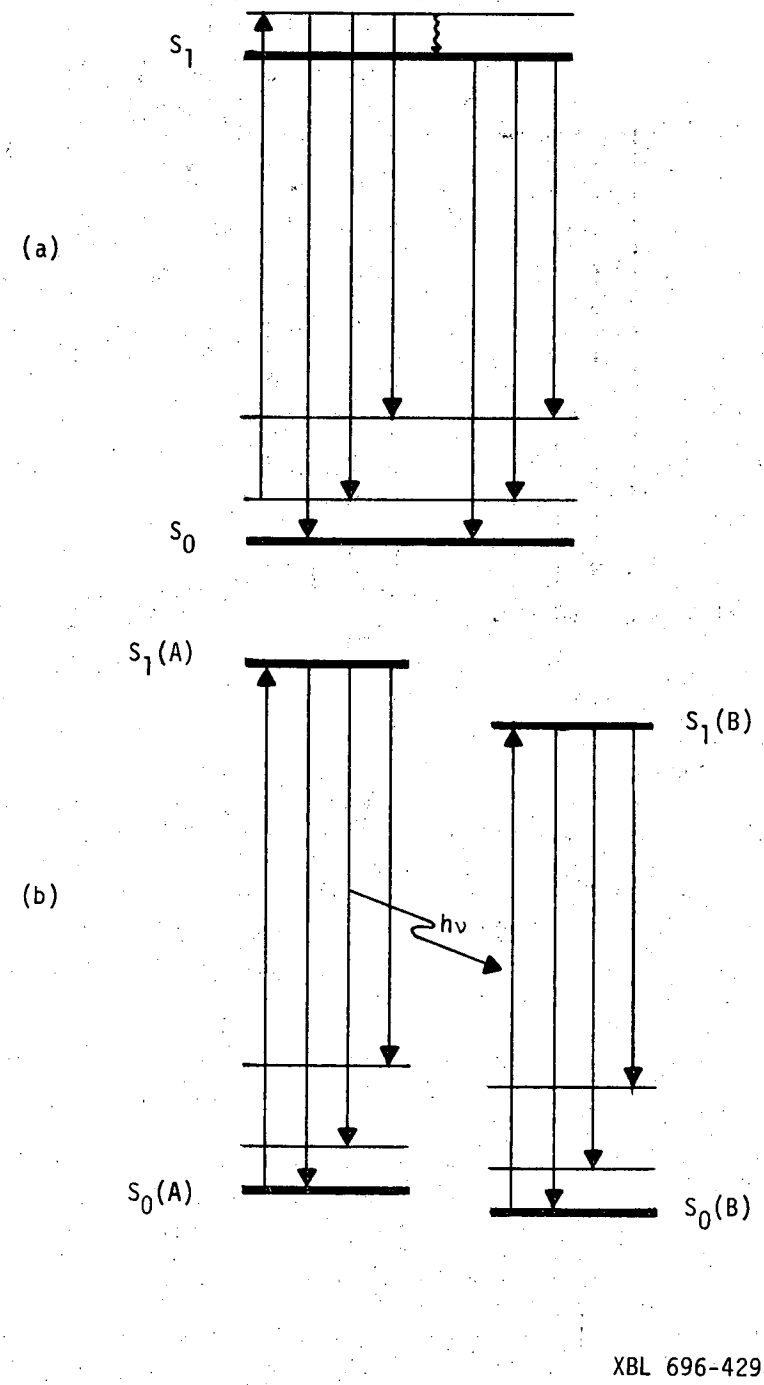

Figure III.18. Two schemes to explain the results of selective excitation experiments. (a) Vibrational relaxation before emission; (b) Reabsorption at another site followed by emission.

iv) Spectra of anthracene in n-hexane and n-octane at 4°K. In n-hexane, anthracene displayed no fluorescence on the high energy side of the main origin.

In n-octane, the picture was more complex. Figure III.19 shows schematically the fluorescence spectra, to the high energy side of the main origin, of anthracene in n-heptane and in n-octane. Lines which are believed to involve lattice vibrations are not shown.

As can be seen, in n-octane there is no obvious line at 391 cm^{-1} above the main origin. However, such a line would, unless very intense, be difficult to observe because of the lattice vibrational bands associated with line 61. These bands have maxima at 380, 397, and 418 cm^{-1} above the main origin.

On the other hand, in the pairs of lines (62, 54) and (61, 53) we have the 391 cm^{-1} spacing (see Figure III.19b) and are faced with the same choice as we had with the pair of lines (51, 44) of the spectrum in the n-heptane matrix. Lines 62 and 61 could be secondary origins and lines 54 and 53 the first vibrational bands of their respective fluorescence spectra; alternatively, lines 54 and 53 could be secondary origins and lines 62 and 61 fluorescence from vibrationally excited levels related to them. A search of the absorption spectrum of anthracene in n-octane revealed that there are lines resonant with lines 62 and 61 of the fluorescence spectrum, but none resonant with lines 54 and 53. This reduces the likelihood that the latter two are secondary origins but it does not completely remove it, since lines in the region of overlap of the absorption

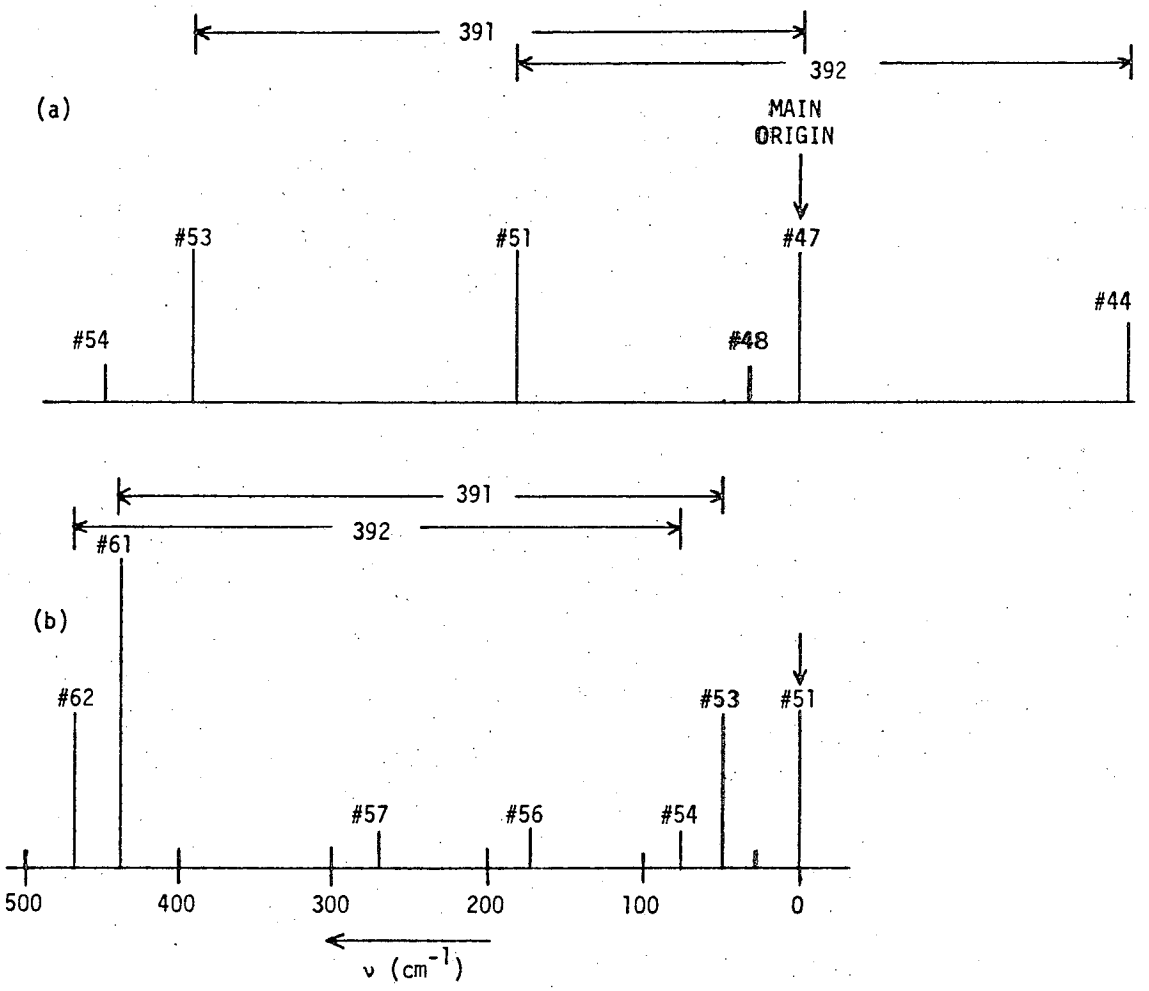

XBL 696-4295

Figure III.19. Anthracene in (a) n-heptane and (b) n-octane. Diagram of the fluorescence spectra at 4°K, in the region of the main origin. Frequencies are referred to it.

and fluorescence spectra are sometimes very difficult to observe because of re-absorption.

To sum up the results of this sub-section, vibrationally excited fluorescence of anthracene does not occur in a n-hexane matrix, and it is doubtful whether it occurs in a n-octane matrix: if it does, it is more intense with respect to secondary origins than with respect to the main origin.

v) The spectrum of $[D_{10}]$-anthracene in n-heptane at 4°K. Of the various matrices which were studied, n-heptane is the one of greatest interest in the context of the hypothesis of vibrationally excited fluorescence, since it was the spectrum of undeuterated anthracene in this matrix which gave rise to the hypothesis in the first place. The spectra of deuterated and undeuterated anthracene in n-heptane at 4°K are shown schematically in Figure III.20, which shows the region to the high energy side of the main origin.

There is an immediate and striking resemblance between the two spectra. When the main origins are brought into coincidence (as they have been in this figure) lines 54, 53, 51, 48, and 47 of the undeuterated molecule spectrum coincide with lines 65a, 65, 63, 59, and 57 respectively of the deuterated molecule spectrum, as is shown in Table III.22.

The postulate made previously that lines, 54, 53, and 51 of the undeuterated molecule's spectrum might represent fluorescence from vibrationally excited molecules in various sites, is now unambiguously shown to be wrong, since lines in the same positions

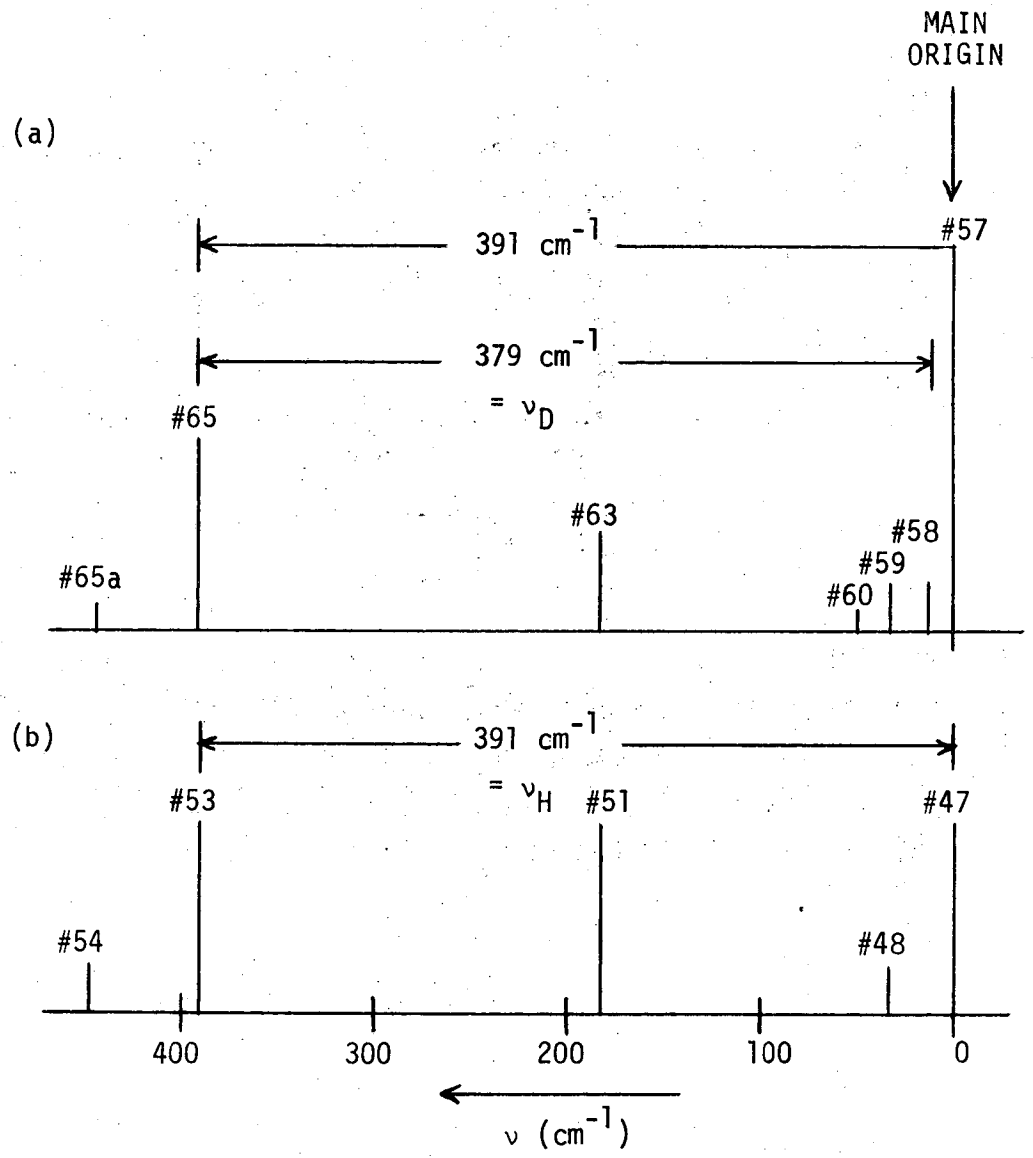

XBL 696-4296

Figure III.20. (a) [D_{10}]-anthracene, and (b) anthracene, both in n-heptane at 4°K. Diagram of the fluorescence spectra to the high energy side of the main origin. Frequency scale is referred to the main origin.

Table III.22. Comparison of lines observed above the origin in the fluorescence spectra of anthracene and $[D_{10}]$-anthracene in an n-heptane matrix at 4°K. Energies are in cm^{-1} and are given with respect to the main origin.

Anthracene		$[D_{10}]$-Anthracene	
No.	Δν	No.	Δν
54	449	65a	446
53	391	65	391
51	182	63	183
48	32	59	31
47	0	57	0

occur in the spectrum of the deuterated molecule, in spite of the fact that the size of the vibrational quantum has been reduced from 392 to 380 cm^{-1}, as shown by the vibrational structure of the spectrum in this and also in other matrices. More specifically, the position of line 53 in the spectrum of the undeuterated molecule, 391 cm^{-1} to the high energy side of the main origin, is shown to be quite unrelated to a vibrational quantum, since line 65 of the spectrum of the deuterated molecule also appears in just this position.

So these high energy lines appear to be secondary origins of the usual type encountered in Shpolskii spectra, in spite of their

large displacements from the main origin, and in spite of the remarkable coincidence with the vibrational quantum in the case of line 53. The close agreement between the positions of secondary origins of the two molecules is also found in n-hexane and n-octane matrices (see next section).

Figure III.20a shows two lines not seen in the spectrum of the undeuterated molecule. Line 60, of very low intensity, is thought to be a secondary origin, presumably too weak to be observed in the anthracene spectrum. Line 58, on the other hand, is the first vibrational band of the secondary origin (line 65). The corresponding line in the case of the undeuterated molecule is of course line 47, which by coincidence is also the main origin.

d) The multiplet structure

Before going on to discuss the multiplet structure, a general comment is necessary on the appearance of spectra in the region of overlap between absorption and fluorescence. Because of the highly scattering nature of the matrix, it was difficult to avoid the measurement of some emission during intended absorption measurements, and vice versa. In the experiments described here, no particular effort was made to minimize this difficulty, since their prinicpal purpose did not require accurate intensity measurements. The effect is particularly marked where lines are exactly resonant in absorption and emission; secondary origins were generally observed with reduced intensity or in some cases not at all, even when vibrational lines derived from them could be detected.

i) Lattice vibrations. One of the most obvious features of the spectra is that intense lines have a satellite structure which lies to high energy in absorption and to low energy in emission. A typical example is shown in Figure III.21, for anthracene in n-heptane at 4°K, (a) being the group of lines around the main origin in absorption, and (b) being in emission.

That these satellite lines are not secondary origins for molecules in different sites is clear from the fact that they are not resonant in absorption and emission, but in fact have an approximately mirror relationship, suggesting that they represent some kind of additional excitation, associated with the upper state in the case of absorption, and the ground state in the case of emission.

In spite of this, these lines are repeatedly classified in Russian publications (e.g., refs. 10, 11, 17) as secondary origins.

If the non-resonant satellite lines do represent some excitation of non-electronic quantum states, these can not be vibrational states of the guest molecule since they are of much too low energy. For anthracene, the lowest energy vibrational modes are of the order of hundreds of wavenumbers, whereas the lines under discussion start at about 25 cm^{-1} from the parent line.

There remains the possibility of either librational movement of the molecule within its solvent cage or of localized lattice vibrations.

This explanation has also been put forward by Spangler and Kilmer[39] for similar lines observed in the spectrum of benzene in a low temperature cyclohexane matrix.

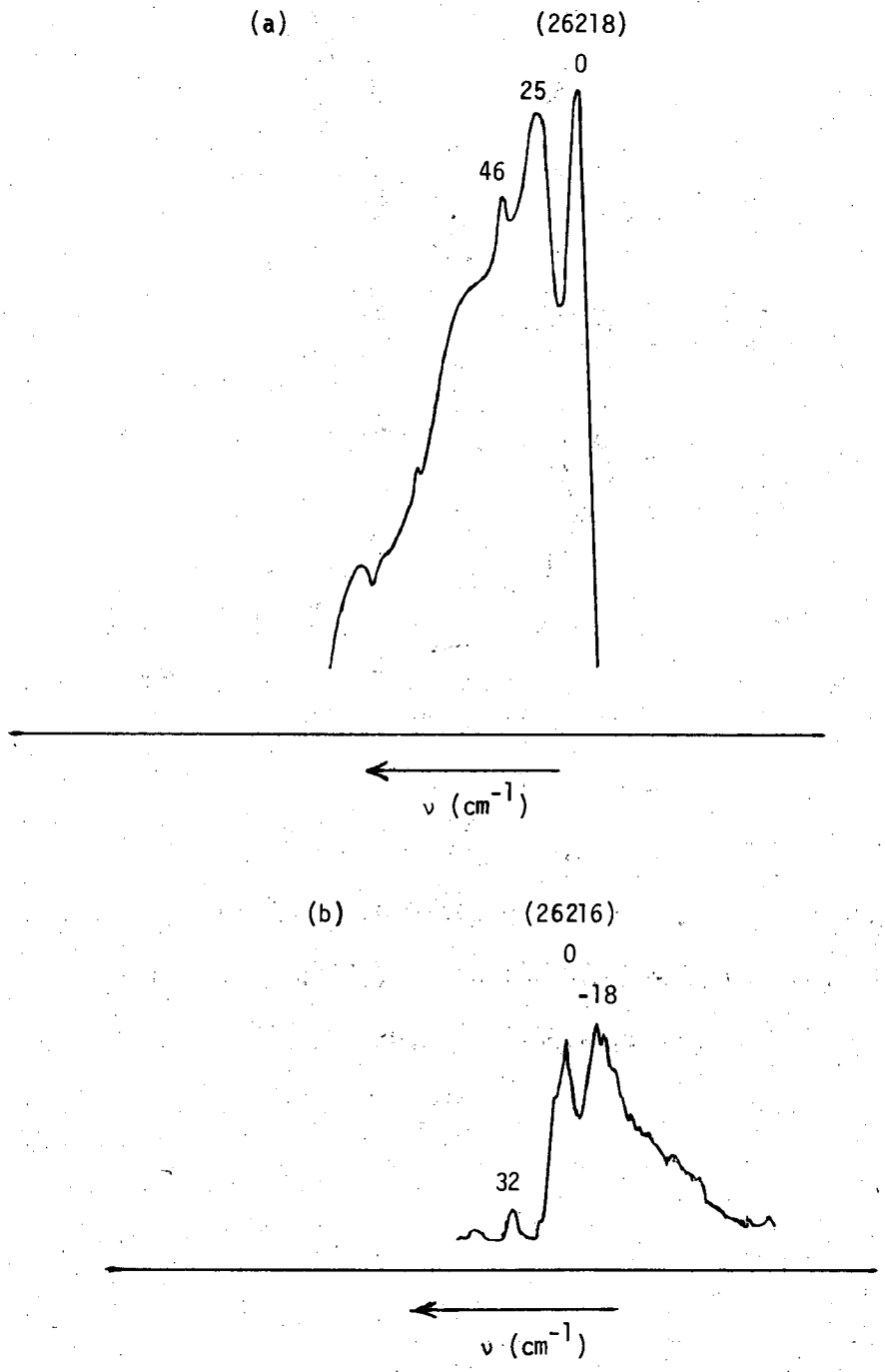

XBL 696-4293

Figure III.21. Anthracene in n-heptane at 4°K. Lattice vibrational bands associated with the main origin. (a) in absorption, and (b) in fluorescence.

The appearance of distinct peaks in this satellite structure is of interest; the theory of Shpolskii spectra predicts[27] that where there is a high probability of phononless transitions, there is also an appreciable probability of transitions involving small changes in the quantum numbers of localized lattice modes, and that this probability increases with the average Stokes energy losses associated with the transition. Localized modes, being of relatively high energy, would tend to give a discrete structure.

The satellite structure does not remain constant throughout the spectrum, indicating that different vibronic transitions couple differently to the phonon modes of the lattice. Typically, the first lattice band is ca. 25 cm^{-1} from the parent line. It is interesting that the appearance of lattice modes is much less prevalent in emission, particularly as satellites of vibronic lines rather than of pure electronic lines. Figure III.22, for example, shows for anthracene in n-heptane at 4°K the structure around the 390 cm^{-1} fundamental of the mode in absorption and emission.

This difference can be explained if we assume that the solvent cage surrounding a guest molecule cannot, because it is a solid matrix, accommodate itself to changes in the state of the guest. The cage formed itself originally around a molecule which was in its ground electronic state. An absorption transition is therefore one to a non-equilibrium environment and the consequent "Stokes energy pressure" encourages the creation of localized phonons.[26] Emission, on the other hand, is to an electronic

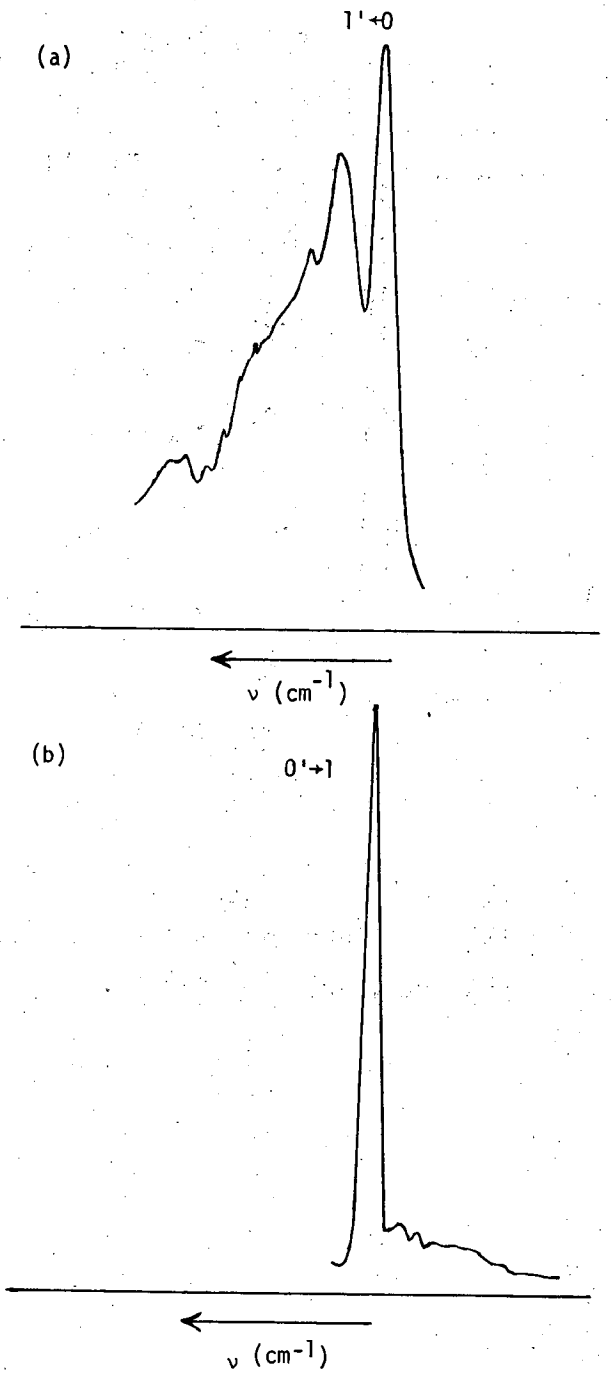

XBL 696-4294

Figure III.22. Anthracene in n-heptane at 4°K. Lattice vibrational bands associated with the first molecular vibrational band (a) in absorption, and (b) in fluorescence.

state in equilibrium with its environment and is less likely to create phonons. This argument would not, of course, apply to liquid solvents, as their structure can relax during the lifetime of the excited state.

As to why vibronic transitions have lower intensity satellites than do pure electronic transitions, it may be that the change in the vibrational state of the guest molecule is able to compensate to some degree for the "Stokes energy pressure" caused by the electronic transition, although it is hard to see in detail how it would do so.

ii) Resonance between absorption and fluorescence. As has been observed for the Shpolskii spectra of many other systems, a number of lines, in the region of the main origin, are found to be resonant (coincide) in absorption and emission. These have been described as multiple origins for molecules in different sites in the host crystal, and this description has been confirmed by the selective excitation experiments of Svishchev.[25]

Table III.23 lists the origins observed in absorption and fluorescence for anthracene and $[D_{10}]$-anthracene in the various matrices. Values in parentheses were not observed directly, but their existence was inferred from the observation of vibronic lines derived from them. As can be seen from this table the observation of weak secondary origins is much harder in absorption; many could not be detected. It was particularly difficult to detect origins which were imbedded in the lattice structure of another intense origin.

Table III.23. Multiple origins observed in the absorption and fluorescence spectra of anthracene and [D_{10}]-anthracene in various matrices at 4°K. Energies are in cm^{-1}.

n-hexane		n-heptane		n-octane	
Abs.	Fluor.	Abs.	Fluor.	Abs.	Fluor.
		Anthracene			
(26323)	26323	---	26061	---	25977
26447	---	26218	26216	---	26013
26487	26486	---	26248	26161	26162
		26264	---	---	26189
		26402	26398	---	26335
		---	26607	(26432)	26432
		---	26665	26600	26600
				26630	26628
		[D_{10}]-Anthracene			
(26397)	26397	---	26110	---	26081
(26553)	26553	---	26131	26227	26226
		---	26174	---	26403
		---	26221	(26500)	26500
		26285	26284	26666	26666
		---	26315	---	26697
		---	26332		
		(26467)	26467		
		(26675)	26675		
		---	26730		

N.B. This table is intended for comparison of absorption and fluorescence within a given solvent only. There is no significance to origins, from different solvents, placed on the same horizontal line of the table.

iii) Multiplet structure of anthracene and $[D_{10}]$-anthracene in different environments. The degree of similarity between the multiplet structures of anthracene and $[D_{10}]$-anthracene is remarkable. In this context different matrices and multiple sites within a given matrix can be thought of in the same way, namely as different hydrocarbon environments. The main origin of $[D_{10}]$-anthracene in n-heptane at 4°K lies 68 cm^{-1} to higher energy than that for anthracene. By referring each origin for the molecule to the main origin in n-heptane, we obtain a "multiplet structure" covering all three matrices. This is shown for both molecules in Figure III.23. With minor exceptions, the structure is identical.

The shift in the origin upon deuteration is a result of changes in the zero-point energy of the upper and lower electronic states. Figures III.14 and III.15, used to find the correspondence between the vibrational modes of the two molecules, showed that for the modes observed (admittedly only a small fraction of the total contributing to the zero-point energy, which includes all modes regardless of symmetry) changes in the values of the vibrational quanta of a given state as a function of environment were not large (generally 5 - 10 cm^{-1}), and the changes undergone by anthracene and $[D_{10}]$-anthracene were similar. Nevertheless, the virtual identity of the multiplet structures of the two molecules is surprising.

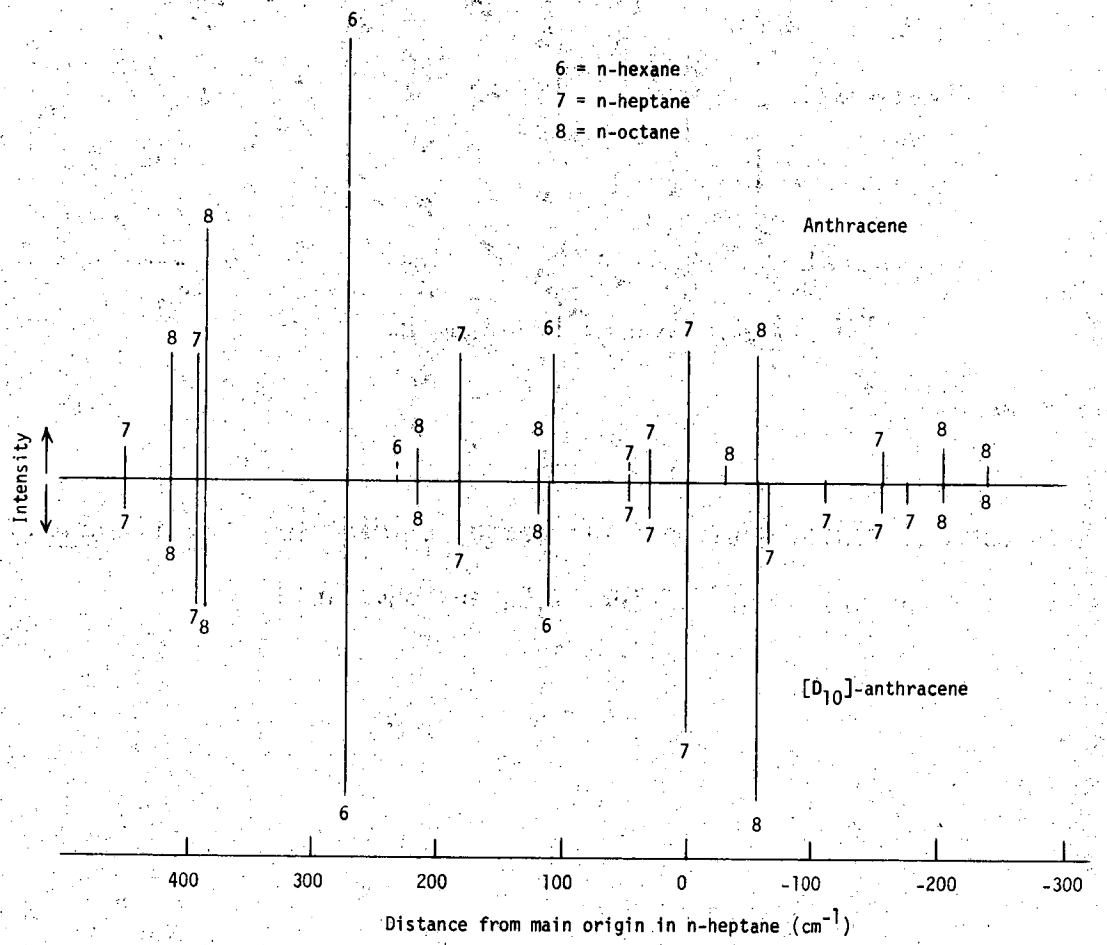

XBL 697-4361

Figure III.23. Multiplet structure in the fluorescence spectra of anthracene and $[D_{10}]$-anthracene in various matrices.

The shift of 68 cm^{-1} to higher energy for anthracene upon deuteration agrees with the trend shown by benzene (ca. 200 cm^{-1})[58] and naphthalene (ca. 100 cm^{-1}).[59]

iv) Multiplet structure in the various matrices. Since the multiplet structures of anthracene and [D_{10}]-anthracene are so similar (see section iii), only that of anthracene will be discussed here.

Figure III.24 shows the multiplet structures of anthracene in n-hexane, n-heptane, and n-octane at 4°K, with positions referred to the main origin in each case. There is an increase in the multiplicity as the chain length of the solvent molecule increases. This may lend support to the theory[17] that rotational isomers of the solvent molecules in the crystal create different environments for the solute.

There is some similarity in the multiplet structures of the three solvents. Intense origins tend to be at about 400, 200, and -150 cm^{-1} from the main origin. Weaker origins are often found close (<50 cm^{-1}) to the intense ones. This suggests that two types of environmental variation may be present.

However, it must be said that neither this study nor any other that I have encountered has indicated with any certainty the precise nature of the environmental variation which is responsible for the multiplet structure of the guest. A detailed study of n-alkane crystals would seem to offer the best prospect of clarifying this matter.

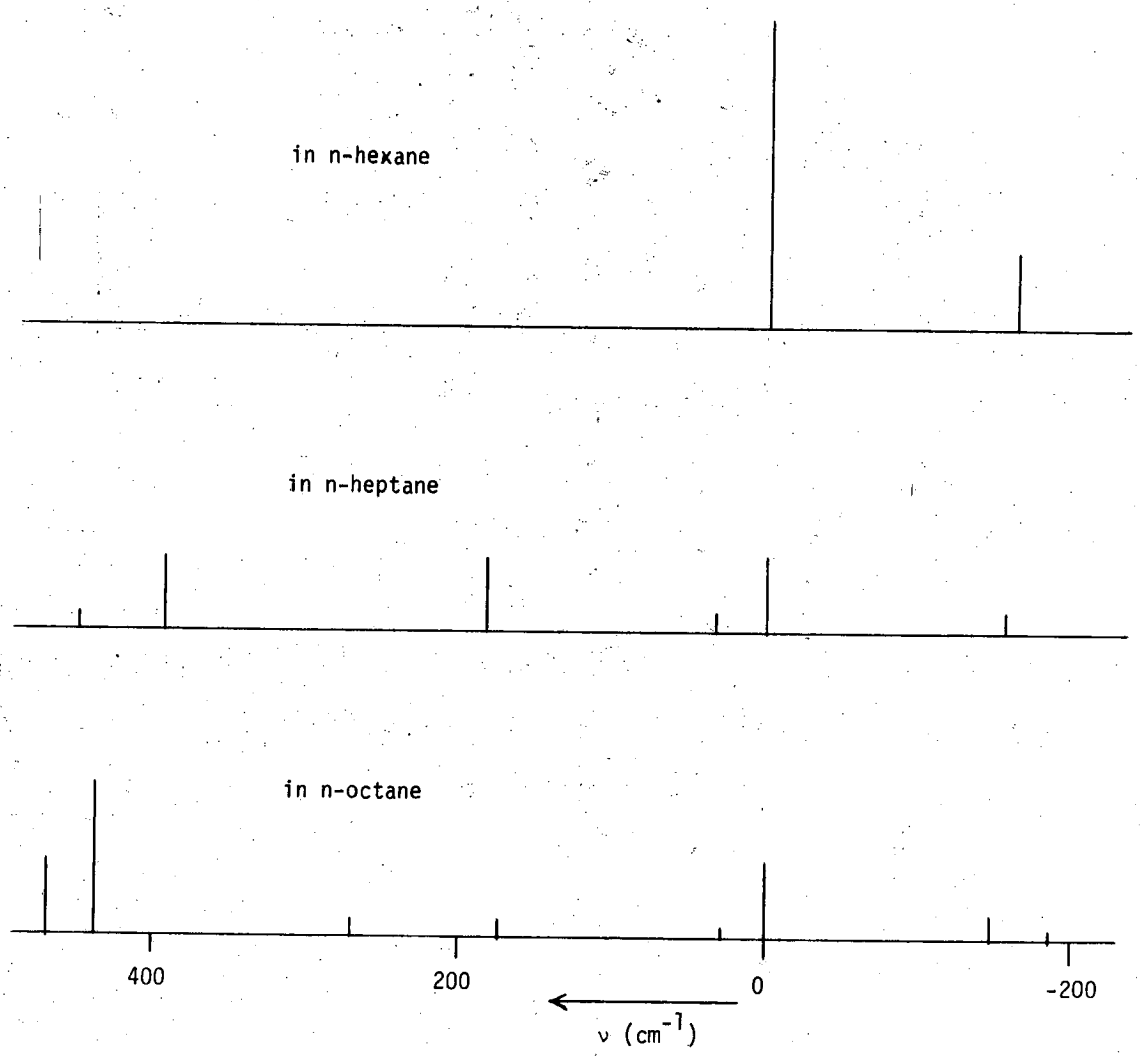

XBL 697-4351

Figure III.24. Multiplet structure of anthracene in various n-alkane matrices. Frequencies are referred to the main origin in each case.

5. Conclusions

(i) The apparatus and procedure for the taking and analysis of low temperature absorption and fluorescence spectra was satisfactory. Some attempt to reduce re-absorption would be desirable if intensity measurements were critical.

(ii) Absorption and fluorescence spectra of anthracene and $[D_{10}]$-anthracene at 4°K were taken in n-hexane, n-heptane, and n-octane. A vibrational analysis of all these spectra was made. Several new modes were assigned for anthracene, and all the data for $[D_{10}]$-anthracene are new. The vibrational analysis of anthracene published by Bolotnikova was found to contain a number of omissions and errors. Agreement of the present work with data obtained from Raman spectra was good.

(iii) Correspondence between the vibrational modes of the undeuterated and deuterated molecules was established in most cases. The changes in the value of a mode in absorption and fluorescence in the various matrices was used as a guide in establishing the correspondence; assistance was also obtained from the calculated values of Krainov. Many of these values agreed well with experiment, but there were some substantial discrepancies.

(iv) Vibrational symmetry assignments made by Abasbegovic from polarized Raman data are thought in some cases to be wrong, for some modes where Krainov's calculated energies agree well with experiment.

(v) The observation by Bolotnikova of a line 391 cm^{-1} to the high energy side of the main origin was confirmed. The hypothesis was put that the line might represent fluorescence from molecules which had retained a quantum of vibrational energy, since one of the most intense modes of anthracene has just this energy. After several experiments (different matrices, selective excitation) which gave somewhat ambiguous support to the hypothesis, it was clearly shown to be incorrect when a line was found in exactly the same position (with respect to the main origin) in the spectrum of the deuterated molecule, in spite of the fact that the vibrational quantum in question had a value of 380 cm^{-1}.

(vi) As is usual in Shpolskii spectra, a number of lines were observed which could not be assigned as vibronic bands derived from the main origin. A distinction was made between those lines which had an approximately mirror relationship in absorption and fluorescence, and those which had a resonance (coincidence) relationship. The former were ascribed to localized lattice vibrational

modes of the lattice, or perhaps to librational modes of the guest; the latter were ascribed to emission from guest molecules in different sites in the crystal host. The distinction between the two types of lines has not been made in the Russian literature, which contains most of the work in this field.

(vii) The existence of discrete peaks in the lattice bands confirms the theoretical prediction that excitation of localized modes is preferred.

(viii) The highest degree of lattice excitation is observed for pure electronic transitions in absorption; the least for vibrational bands in fluorescence. These variations are explained in terms of the frozen-in ground state environment of the lattice.

(ix) Many origins were found resonant in absorption and fluorescence, although weak ones were hard to detect, particularly in absorption, or when masked by lattice vibrational bands.

(x) The multiplet structure of $[D_{10}]$-anthracene in all three matrices is shifted 68 cm^{-1} to higher energies from that of anthracene. This shift agrees with the trend shown by benzene (ca. 200 cm^{-1}) and naphthalene (ca. 100 cm^{-1}).

(xi) Apart from the shift, the multiplet structures of the two molecules are virtually identical. Even though large differences were not anticipated, the degree of matching is remarkable.

(xii) The main purpose of this work was to substantiate the hypothesis of fluorescence from vibrationally excited anthracene. Had this been successful, the importance of the work to those interested in radiationless energy transfer would have been considerable. The hypothesis was shown to be false, but there is at least the satisfaction of a question being settled conclusively; another outcome of the work is the useful warning that unlikely coincidences do sometimes occur. The work also represents a more systematic study of Shpolskii spectra than is usually found in the literature, and has provided new data, including a vibrational analysis of deuterated anthracene.

ACKNOWLEDGEMENTS

Many people have assisted me at various points in my graduate career. Professor Ken Sauer, my research supervisor, Drs. Mel Klein, Lelia Coyne, Charles Weiss, Mr. David Downie and others have given their time for discussions and advice.

The helpful cooperation of the typing and drawing staff, particularly Mrs. Evie Litton, and the excellent workmanship of Messrs. Dick O'Brien (carpenter), Bill Hart (glassblower), Bob Creedy and John Despotakis (electronics), and Pete Dowling, Del Coleman, and Frank Upham (Donner shops) were essential to the work described in this thesis.

I consider the two years I spent teaching as important to me as the time I spent on research, and I am grateful for the enthusiasm imparted by such fellow-teachers as Professor Fred Reif, Messrs. George Brackett, Jay Shelton, and others. I wish that more people had their concept of the importance of undergraduate, and particularly lower division, teaching.

Finally, my thanks to Barbara, my wife-to-be, for her encouragement during the long process of writing the thesis.

APPENDIX A

List of Equipment Model Numbers and Manufacturers or Suppliers

Light source: 450 watt high-pressure xenon arc lamp, XBO-450, Osram, ex Geo. W. Gates and Co.

Lamp housing: model C-60-50, ex Oriel Optics Corp.

Lamp power supply and igniter: model C-72-50, ex Oriel Optics Corp.

Optical Dewar: model 8DT with two interchangeable tail assemblies: (i) rectangular two-window design, Janis Research drawing 6-20-6A, and (ii) cylindrical three-window design, Janis Research drawing 10-19-7A. All ex Janis Research Co.

Epoxy: Bakelite #2774 Epoxy, ex Union Carbide, and Versamid #140 Hardener, ex General Mills. Ratio to be used, 11:15.

Rapid couplings: Tri-Clamp series, ex Ladish Co., Kenosha, Wisc.

Liquid helium transfer tube: model FHT, ex Janis Research Co.

Temperature controller: model TC-101, ex Cryogenic Research Co.

Cryogenic liquid level indicator: model LP-6, ex Cryogenic Research Co.

Thermocouple vacuum gage: model DV-3M, with 6Z3842 power supply, ex Hastings Co.

Micro-thermocouple: model CO-CO-003, ex Omega Engineering Inc. Output measured by model 2733 potentiometer, ex Honeywell (Rubicon Instruments).

Vacuum pumps: Duo-Seal, models 1400 (pump A) and 1402 (pump B), ex Welch Scientific Co.

Analyzing monochromator: 25-050 One-meter Czerny-Turener scanning spectrometer-spectrograph with 12 speed electrical drive, cosecant scanning, having a screw accuracy of plus or minus 1 micron, with direct linear wave-number readout, 115v. 60 Hz.

78-472 Dual unilateral entrance and exit slit assembly with curved jaws opening from 5 to 400 microns, height adjustable from 1 to 20 mm.

78-474 Mirror system for deflecting exit beam to side-mounted camera.

78-477 Camera mounting plate.

15-200 Camera adapter.

15-209 Spacer.

980-43-20-18 Grating 1180 grooves/mm blazed for 3000 A.

980-43-20-22 ditto, blazed for 5000 A.

11-033 Grating holder.

MgF_2 coating of optical surfaces.

15-201 Graflex 4 in x 5 in plate-holder.

15-210 Polaroid 4 in x 5 in cut film back.

78-468 Shutter, manually released, 1/400 sec to "time".

Photographic materials:

Polaroid 4 in x 5 in film, type 57, speed ASA 3000.

Kodak 4 in x 5 in Spectroscopic plates, type 103-0.

Kodak D-19 Developer.

Kodak Rapid-Fix.

Kodak Photo-Flo Solution.

Calibration sources: Spectral Calibration Set, model C-13-02, consisting of argon, helium, krypton, neon, xenon, and mercury arc lamps with two appropriate power supplies, all in case, ex Oriel Optics Corp.

Photomultiplier tube: EMI model 6256S, ex Gencom Whittaker Corp.

Photo-tube power supply: model 1544, 1-3 kv, ex Power Designs Pacific Inc., Palo Alto, California.

Cooled tube housing: model 78, ex Pacific Photometric Instruments, Berkeley.

Amplification system:

Model 131 Lock-in Voltmeter.

Model 261 Pre-amplifier.

Model 312 Chopper, with appropriate blades for the chosen frequency boards. All ex Brower Laboratories.

Recorder: Moseley Autograf model 680, ex Hewlett, Packard.

Excitation monochromator: Beckmann DK.

Lenses: ex Oriel Optics Corp.

APPENDIX B

Typical Operating Conditions Used in Measuring the Spectra in Part II of this Thesis

Solute: Acridine.

Solvent: n-heptane.

Concentration: 4.9×10^{-5} M.

Temperature: 77°K.

Spectrometer: Cary 14MR

Sample path length: 1.5 mm.

Light source: High intensity tungsten lamp, operating at line voltage.

Wavelength range scanned: 420 - 320 nm.

Photomultiplier gain setting: 2.

Time constant: 1 sec.

Slit control: 15.

Slit height: full.

Slit width: 0.01 mm.

Scan speed: 0.5 A/sec.

Filter: 1.0 O.D. neutral density.

APPENDIX C

Typical Operating Conditions Used in Measuring the Spectra in Part III of this Thesis

Table 1. Absorption spectrum, photo-electric detection.

Light source

Blower on, flap 1/2 open, range select midway between positions F and G.

Sample

Solute	Anthracene
Solvent	n-Octane
Concentration	2.5×10^{-5} M
Pathlength	4 mm
Temperature	4°K

Dewar

Vacuum jacket pressure	<<1 micron
Sample chamber pressure	200 mm

Analyzing monochromator

Slit height	20 mm
Slit width	50 microns
Scan start	30.0 kK
Scan finish	25.5 kK
Scan rate	100 cm^{-1}/min

Photomultiplier tube	
Temperature	Dry ice (-78.5°C)
Dynode potential	-2 kv
Amplifier	
Chopper frequency	95 Hz
Trigger mode	EXT +
Phase	0°
Risetime	1 sec, double filter
Center zero	Off
Zero offset	Off
Sensitivity	2.5×10^{-6} and 5.0×10^{-6} amp
Chart recorder	
Range	0 - 100 mv
Chart speed	1 div/min
Scale of spectrum	100 cm^{-1}/chart div

Table 2. Absorption spectrum, photographic detection.

(Conditions of light source, sample and dewar as in Table 1.)

Analyzing monochromator	
Slit height	4 mm (Hartmann diaphragm)
Slit width	50 microns
Scan drive position	30.0 kK

Photographic

(i) Polaroid, type 57, ASA 3000

Exposure	1 sec

(ii) Conventional plates

Exposure	1/2, 1, 2, and 4 sec
Calibration sources	Neon, exposure 2 sec
	Helium, exposure 5 sec

Table 3. Fluorescence spectru, photo-electric detection

(Conditions of light source, sample, dewar, photomultiplier tube, and chart recorder as in Table 1.)

Excitation monochromator

Slit width	2.0 mm
Wavelength	350 nm (28.6 kK)

Analyzing monochromator

Slit height	20 mm
Slit width	100 microns
Scan start	26.8 kK
Scan finish	23.0 kK
Scan rate	100 cm^{-1}/min

Amplifier (As in Table 1, except:)

Sensitivity	5×10^{-7} amp

Table 4. Fluorescence spectrum, photographic detection

(Conditions of light source, sample and dewar as in Table 1.)

(Conditions of excitation monochromator as in Table 3.)

Analyzing monochromator

Slit height	4 mm (Hartmann diaphragm)
Slit width	50 microns
Scan drive position	26.8 kK

Photographic

(i) Polaroid, type 57, ASA 3000

Exposure	1 min

(ii) Conventional plates

Exposure	1/2, 1, 2, and 4 min
Calibration sources	Argon, 3 sec
	Helium, 5 sec
	Krypton, 30 sec

Table 5. Processing of photographic plates

Type of plate	Kodak Spectroscopic 103-0
Safelight	Wratten #2 (dark red)
Processing temperature	21°C
Developer	D-19, 4 min
Stop bath	2% acetic acid, 1/2 min
Fixer	Rapid Fixer, 4 min
Wash	30 min
Rinse	Photo-flo solution, 30 sec

APPENDIX D

Computer Programs

For each program, the data deck set-up will be given, followed by the source listing and some sample output.

---

1. Program RREDUK

(i) Data deck set-up

A. Title card

Columns 1-80, field 16A5: WORDS, anything.

Example:

bRMMb382bFLUORbANTHRACENE/N-C6b4bDEGbKbMACNABb28bOCTOBERb1968bbb, etc.*

B. Corrections card

Columns 1-35: Same as last card of standards deck.

Columns 36-42, field F7.5: MOLCOR, the correction to be made to a 3-punched molecular line screw reading (see molecular deck). XL = XL - MOLCOR.

Columns 43-49, field F7.5: COR, the correction to be made to a 8-punched standard (calibration) line screw reading (see standards deck). SCREW = SCREW - COR.

---

*'b' indicates blank.

Columns 50-55, field F6.4: DISCR, the discriminant in angstroms; all LAMBDA RESIDS larger than DISCR will be deleted when the second least squares routine is called, and N.G. will be printed in the remarks column.

Columns 56-59, field 4X: Blank.

Column 60, field I1: N, the degree of the polynomial in the least squares routine; if no N is given, an eighth degree polynomial will be used.

Example:

bbbbb9bbbbbJb44468bbb466bbb3665.3bb-bbbb13b.1bbbbbbb, etc.

C. Standards deck

Columns 1-24 are punched by the AMP comparator (see Professor Phillips, Astronomy Department), as follows:

Columns 1-5, field 5X: Blank.

Column 6, field I1: NETAG, 9 if no correction needed, 8, if COR needed.

Columns 7-11, field 5X: Blank.

Column 12, field A1: SYMB, see program.

Columns 13-18, field F6.5: SCREW, screw reading on comparator.

Columns 19-24, field F6.0: XIN, density of line.

Columns 25-35, field F11.3: LAMTRU, the true wavelength in angstroms. If the program is being run only to identify standards, only the first and last standards will contain LAMTRU.

Example:

bbbbb9bbbbb-b55634bbb134bbb4376.1bbbbb, etc.

D. Blank card

Sentinel card to indicate end of standards deck.

E. Transfer card

(a) If program is being run to identify standards only, bbbbbbSTANIDbbb, etc.

(b) Otherwise, blank card.

F. Molecular deck, if E is option (b).

Punched by AMP comparator, as for standards deck, except

Column 6, field I1: 4-punch if no correction needed,
3-punch if MOLCOR needed.

G. Blank card, if E is option (b).

Sentinel to indicate end of molecular lines.

H. Transfer card

(a) If more sets of data to be processed, bbbbbbNEXDATbbb, etc.

(b) Otherwise, blank card.

I. If H is option (a), return to A.

(ii) Source listing and sample output

See overleaf.

```
      PROGRAM RREDUK (INPUT, OUTPUT,TAPE5)
C
C     THIS IS A SIMPLIFIED VERSION OF REDUKT
C
000052      DIMENSION A(10,10)
000052      DIMENSION WORDS (16)
000052      DIMENSION NETAG(100), XIN(100),  INT(100), LAMTRU(100), SGMA(100),
     1LAMLIN(100), NOTE(100)
000052      DIMENSION SCREW(150), DELTAL(150), T(150), Z(150), WT(150)
000052      DIMENSION HADES(500), BIN(500), SINK(500), VACUM(500),INTMOL(500)
C
000052      COMMON SCREW, DELTAL, WT, T, Z
000052      COMMON A
C
000052      REAL LAMLIN, LAMTRU, LAMTRR, NOTE, COR, MOLCOR, DISCR, SCREWW,
     1SCREW, XL, XINN, XIN, HADES, WT, DISP, SGM, SGMA, V, VACUM,
     2RFRCTN, T, Z, SYMBB, SYMB, ZAM, DELTAL, F, SUM, SICK, SMEAN1,
     3SMEAN2, BIN, SINK
C
000052      INTEGER I, J, K, KJ, KJL, KM, NETAGG, NETAG, NETA, N, NPLUS, NTH,
     1IGOR, INT, INTMOL,MORE, YES
C
000052      DOUBLE PRECISION A
C
000052      DATA REMARK, STANID, YES, BLANK/4HN.G., 6HSTANID, 6HNEXDAT,
     1 4H    /
C
C
000052    1 CONTINUE                                                    /READ
000052  800 FORMAT (16A5)                                               AND
000052      READ 800, (WORDS(I), I = 1,16)                              PRINT
000063  801 FORMAT (1H1)                                                TITLE
000063      PRINT 801                                                   CARD
000066      PRINT 800, (WORDS(I), I = 1,16)
000077  802 FORMAT (1H //)
000077      PRINT 802
C
C     CORRECTIONS CARD IS ALSO LAST STANDARD                          /READ
000102  805 FORMAT (5X, I1, 5X, A1, F6.5, F6.0, F11.3, 2F7.5, F6.4, 4X, I1) CORREC
000102      READ805,NETAGG,SYMBB,SCREWW,XINN,LAMTRR,MOLCOR,COR,DISCR,N  TIONS
000127      IF (NETAGG - 9) 2,3,2                                       CARD/
000131    2 SCREWW = (SCREWW - COR)                                     /COR IF
C                                                                       8 PCH,/
C     FIXUP READS SYMBB (OUTPUT OF MICROSWITCH ON COMPARATOR) AND
C     DETERMINES WHETHER, E.G, J 49692 SHOULD MEAN SCREW=049692 OR 149692
000133    3 CALL FIXUP (SYMBB, SCREWW)                                  /FIXUP/
C                                                                       /READ
000135  806 FORMAT (5X, I1, 5X, A1, F6.5, F6.0, F11.3)                  FIRST
000135      READ 806, NETAG(1), SYMB, SCREW(1), XIN(1), LAMTRU(1)       STAND,/
000152      IF (NETAG(1) - 9) 4,5,4                                     /COR IF
000154    4 SCREW(1) = SCREW(1) - COR                                   8-PCH,/
C
000156    5 CALL FIXUP (SYMB, SCREW(1))                                 /FIXUP/
C
C     OBTAIN LINEAR DISPERSION                                        /DISP/
000160      DISP = (LAMTRR - LAMTRU(1))/(SCREWW - SCREW(1))
C
000164      DO 12 J = 1,100                                             /READ
000166      WT(J) = 1.                                                  COR,
000170      K = J + 1                                                   FIXUP
C     INDEXING SECOND CARD CORRECTLY                                    REST OF
000172      READ 806, NETAG(K), SYMB, SCREW(K), XIN(K), LAMTRU(K)       STANDS,/
C     SENTINEL FOR END OF STANDARDS DECK
```

```
000207          IF (XIN(K)) 701,702,701
000211      701 IF (NETAG(K) - 9) 6,7,6
000214        6 SCREW(K) = SCREW(K) - COR
              C
000217        7 CALL FIXUP (SYMB, SCREW(K))                                  /FIXUP/
              C
000222       12 CONTINUE
              C
              C     OBTAIN INTENSITY (INT), LINEAR WAVELENGTH (LAMLIN), CORRESPONDING
              C     WAVENUMBER (SGMA), AND DEVIATION FROM LAMLIN (DELTAL)
000224      702 CONTINUE
000224          DO 704 I = 1,J
000226      703 INT(I) = IFIX((1000. - XIN(I))/100. + 0.5)
000235          LAMLIN(I) = LAMTRU(I) + (SCREW(I) - SCREW (1))*DISP
              C     CORRECTION TO IN VACUO VALUES
000242          SGM  = 1.0E4/LAMLIN(I)
000244          RFRCTN=643.28+294981./(146.-SGM **2)+2554./(41.-SGM **2)
000254          SGMA(I) = 1.E8/(LAMLIN(I) + LAMLIN(I)*RFRCTN/1.E7)
000261      704 DELTAL(I) = LAMTRU(I) - LAMLIN(I)
              C                                                              /WANT
              C     IF PURPOSE OF RUN IS TO IDENTIFY CALIBRATION LINES -- STANID   STANDS.
000266      706 FORMAT (6X, A6)                                              ONLY/
000266          READ 706, PASWD
000273          IF (PASWD.EQ.STANID) GO TO 707
              C
000275       13 IF (N.EQ.0) N = 8
000277          N = N + 1
000301          NTH = N
000302          NPLUS = N + 1
              C                                                              /LEAST
000303          CALL SQARE (N, J, SCREW, DELTAL, WT, T, Z, A)                  SQUARES
              C                                                              ROUTINE/
000311          F = 0.
000312          SUM = 0.
000313          IGOR = 2
              C
000314          DO 15 I = 1,J                                                  /FIND
000315          SICK = ABS(T(I))                                               BAD
000320          F = F + 1.                                                     STAND
000322          SUM = SUM + SICK                                               ARDS/
000324          NOTE(I) = BLANK
000326          IF (SICK - DISCR) 15,15,14
000330       14 NOTE(I) = REMARK
000332          WT(I) = 0.
000333          IGOR = 1
000334       15 CONTINUE
              C                                                              /FIRST
000337          SMEAN1 = SUM/F                                                 AVERAGE/
000341          IF (IGOR.EQ.2) GO TO 35
              C                                                              /LEAST
              C     ONLY CALLED IF BAD STANDARDS PRESENT                     SQUARES
000343          CALL SQARE (N, J, SCREW, DELTAL, WT, T, Z, A)                  MINUS
              C                                                              REJECTS/
000351       36 FORMAT (120H  SCREW     WEIGHT        SIGMA          LAMBDA      /PRINT
                1  LAMBDA        DELTA        LEAST        LAMBDA      LINE    REMARKSTAND
                2)                                                             ARDS
000351       37 FORMAT (120H MEASURE      TAG       LINEAR          LINEAR        NORMAL/
                1    TRUE         LAMBDA       SQUARES      RESIDS      INTY    COLUMN
                2/)
000351       35 PRINT 36
000354          PRINT 37
000357       38 FORMAT (2PF8.4,6X,I1,6X,0PF10.1,7X,F 9.2,7X,F10.4,5X,F7.4,5X,F7.4,
                16X,F7.4,4X,I4,6X,A4)
000357       16 PRINT 38,(SCREW(I),NETAG(I),SGMA(I),LAMLIN(I),LAMTRU(I),DELTAL(I),
```

```
          1Z(I), T(I), INT(I), NOTE(I), I = 1,J)
000413          GO TO 709
C
000414    707 CONTINUE                                                          /PRINT
000414    715 FORMAT (38H  FOR IDENTIFICATION OF STANDARDS ONLY)                STAND
000414          PRINT 715                                                       ARDS
000417          PRINT 802                                                       WHEN FOR
000422          PRINT 36                                                        STAND.
000425          PRINT 37                                                        IDENT.
000430    708 FORMAT (2PF8.4, 6X, I1, 6X,0PF10.1, 7X, F 9.2, 58X, I4)           ONLY
000430          PRINT 708,(SCREW(I), NETAG(I), SGMA(I), LAMLIN(I), INT(I), I=1,J)
000452          GO TO 143
C
000453    709 CONTINUE
000453     18 PRINT 802
000456          F = 0.
000457          SUM = 0.
C
000460          DO 20 I = 1,J
000461          IF (WT(I)) 19,20,19
000463     19 F = F + 1.
000465          SUM = SUM + ABS (T(I))
000471     20 CONTINUE
C                                                                             /SECOND
000474          SMEAN2 = SUM/F                                                AVERAGE/
000476    810 FORMAT (16H FIRST AVERAGE =F9.6, 18H  SECOND AVERAGE =F9.6,       /PRINT
          1 16H  DISCRIMINANT =F7.4, 21H  LINEAR DISPERSION =-2PF9.6)         POLY-
000476          PRINT 810, SMEAN1, SMEAN2, DISCR, DISP                        NOMIAL
000511    811 FORMAT (30H COEFFICIENTS OF POLYNOMIAL = 5(D16.8,2X)/28X,5(D16.8, DATA/
          1 2X))
000511          PRINT 811, (A(I,NPLUS), I = 1,NTH)
C                                                                             /READ
000526    104 DO 108 K = 1,500                                                MOLE-
000530    814 FORMAT (5X, I1, 5X, A1, F6.5, F6.0)                             CULAR
000530          READ 814, NETA, ZAM, XL, HADES(K)                             LINES/
C         SENTINEL FOR LAST MOLECULAR CARD
000543          IF (HADES(K))116,117,116
C
000545    116 CALL FIXUP (ZAM, XL)                                            /FIXUP/
C
000547    113 BIN(K)=A(1,NPLUS)                                               /MOLCOR
000555          IF (NETA - 4)  710,711,710                                    IF 3 PCH
000557    710 XL = XL - MOLCOR                                                /INTENS-
000561    711 SINK(K)=XL                                                      ITY/
000563          INTMOL(K) = IFIX((1000. - HADES(K))/100. + 0.5)
C
000571          DO 152 KJ=2,NTH                                               /OBTAIN
000573          KJL=KJ-1                                                      LAMTRU
000575    152 BIN(K)=BIN(K)+A(KJ,NPLUS)*XL**KJL                               FROM
C                                                                             POLY-
000615          BIN(K) = BIN(K) + LAMTRU(1) + DISP*(XL - SCREW(1))            NOMIAL/
000623          V=1.E4/BIN(K)                                                 /OBTAIN
000625          RFRCTN=643.28+294981./(146.-V**2)+2554.0/(41.-V**2)           MOL.
000635          VACUM(K)=RFRCTN*BIN(K)/1.E7                                   DATA/
000640          VACUM( K )=1.E8/(BIN( K )+VACUM( K ))
000643          IF (NETA - 4) 118,108,118                                     /SHOW IF
000645    118 BIN(K)=-BIN(K)                                                  3-PCH./
000647    108 CONTINUE
C
C         IGNORE SENTINEL AS MOLECULAR CARD                                   /PRINT,
000651    117 KM=K-1                                                          PUNCH
000653          PRINT 801                                                     MOL.
000656    712 FORMAT   (48H   MMS         LAMBDA          SIGMA         INTY )  DATA/
000656          PRINT 712
000661          PRINT 802
000664    713 FORMAT (2PF8.4,4X,0PF9.2, 6X, F9.1, 6X, I4)
000664          PRINT 713, ( SINK(I), BIN(I), VACUM(I), INTMOL(I), I = 1,KM)
000704          WRITE (5,713) (SINK(I),BIN(I),VACUM(I),INTMOL(I), I=1,KM)
000724    716 FORMAT (80H**********************************************************
          1**********************)
000724          WRITE (5,716)
C
000727    143 CONTINUE
000727    714 FORMAT (6X, A6)                                                 /REPEAT
000727          READ 714, MORE                                                PROGRAM
000734          IF (MORE.EQ.YES) GO TO 1                                      IF MORE
C                                                                             DATA/
000736          CALL EXIT
000737          RETURN
000741          END
```

```
                SUBROUTINE SQARE(N, IT, X, DELTAL, W, T, Z, A)
          C     LEAST SQUARES FOR POLYNOMIAL OF DEGREE N-1
007515          DIMENSION A(10,10),ZAX(20)
007515          DIMENSION X(150), DELTAL(150), W(150), Z(150), T(150)
007515          COMMON X, DELTAL, W, T, Z
007515          COMMON A
007515          DOUBLE PRECISION A, ZAX
007515          DO 15 J=1,IT
007517       15 Z(J) = DELTAL(J)
007525          NM=N+1
007527          DO 16 M=1,N
007530          DO 17 K=1,NM
007531       17 A(M,K)=0.
007543       16 CONTINUE
007545          MPL=N+N-1
007547          DO 18 M=1,MPL
007550       18 ZAX(M)=0.
007556          DO 19 KM=1,IT
007560          DO 20 M=2,MPL
007561          MDEC=M-1
007563          STORE=W(KM)
007565          CARRY=X(KM)
007567          SHOVE=Z(KM)
007572       20 ZAX(M)=ZAX(M)+STORE*CARRY**MDEC
007611          ZAX(1)=ZAX(1)+STORE
007617          DO 21 LO=2,N
007621          LOW=LO-1
007623       21 A(LO,NM    )=A(LO,NM    )+STORE*SHOVE*CARRY**LOW
007647          A(1,NM    )=A(1,NM    )+STORE*SHOVE
007663       19 CONTINUE
007665          NLES=N-1
007667          DO 22 ND=1,NLES
007670          DO 23 KID=1,ND
007671          LUG=ND+ 1-KID
007673          A(KID,LUG)=ZAX(ND)
007703          KIX=NM-KID
007705          LUX=NM-LUG
007707          JAN=MPL+1-ND
007711       23 A(KIX,LUX)=ZAX(JAN)
007724       22 CONTINUE
007726          DO 24 KID=1,N
007730          LUG=N+ 1-KID
007732       24 A(KID,LUG)=ZAX(N)
007744          DO 401 IN=1,N
007745          IK=IN+1
007747          DO 402 IM=IN,N
007750          DO 403 IL=IK,NM
007752          IF (A(IM,IN)) 403,1000,403
007760      403 A(IM,IL)=A(IM,IL)/A(IM,IN)
010004      402 CONTINUE
010006          IF (IN-N) 407,488,407
010007      407 DO 404 IJ=IK,N
010011          DO 405 IL=IK,NM
010013      405 A(IJ,IL)=A(IJ,IL)-A(IN,IL)
010035      404 CONTINUE
010040      401 CONTINUE
010042      488 DO 408 IN=2,N
010044          IK=N+1-IN
010046          IM=IK+1
010047          DO 409 IL=IM,N
010050      409 A(IK,NM)=A(IK,NM)-A(IK,IL)*A(IL,NM)
```

```
010102      408 CONTINUE
010104       41 DO 42 J=1,IT
010106       42 Z(J)=A(1,NM    )
010123          DO 43 J=1,IT
010125          DO 44 KJ=2,N
010126          KJL=KJ-1
010130       44 Z(J)=Z(J)+A(KJ,NM    )*X(J)**KJL
010155       43 CONTINUE
010157          DO 46 J=1,IT
010160       46 T(J) = DELTAL(J) - Z(J)
010170          GO TO 199
010170     1000 PRINT 209
010177          PRINT 207,IM,IN
010212      199 CONTINUE
010212      207 FORMAT (3H A(,I2,2H ,,I2,5H )=0.)
010212      209 FORMAT (16H SINGULAR MATRIX//)
010212          RETURN
010213          END
```

```
                SUBROUTINE FIXUP (SYMBOL, SCR)
010347          REAL JAY
010347          DATA JAY, ONE /1HJ, 1H1 /
010347          Q = 0.
010350          IF (SYMBOL.EQ.JAY.AND.SCR.LE..98) Q = 1.
010361          IF (SYMBOL.EQ.ONE.AND.SCR.GE..90) Q = 1.
010372          IF (SYMBOL.EQ.ONE.AND.SCR.LT..90) Q = 2.
010403          SCR = SCR + Q
010405          RETURN
010405          END
```

RMM 446 ANTHRACENE(D10)/N-C8 ABS 4 DEG K DEC 17 1968 MACNAB 1

SCREW MEASURE	WEIGHT TAG	SIGMA LINEAR	LAMBDA LINEAR	LAMBDA TRUE	DELTA LAMBDA	LEAST SQUARES	LAMBDA RESIDS	LINE INTY	REMARK COLUMN
7.0692	9	25215.3	3964.73	3964.7300	0.	.0000	-.0000	8	
8.8853	9	26181.1	3818.46	3819.6100	1.1454	1.1437	.0017	8	
9.6991	9	26638.3	3752.92	3754.2100	1.2873	1.2949	-.0076	6	
10.3135	9	26994.2	3703.44	3705.0000	1.5600	1.3683	.1916	6	N.G.
10.3579	9	27020.3	3699.86	3701.2300	1.3659	1.3714	-.0055	7	
10.5506	9	27134.1	3684.34	3685.7400	1.3956	1.3800	.0156	7	
10.5941	9	27160.0	3680.84	3682.2400	1.3990	1.3808	.0181	7	
11.1957	9	27522.2	3632.39	3633.6600	1.2708	1.3419	-.0712	8	
11.4454	8	27675.5	3612.28	3613.6400	1.3611	1.2949	.0662	3	
11.6111	9	27778.1	3598.93	3600.1700	1.2363	1.2530	-.0167	8	
12.5955	9	28403.8	3519.65	3520.4700	.8181	.8420	-.0239	9	
12.6608	9	28446.3	3514.39	3515.1900	.7972	.8065	-.0092	8	
12.7164	9	28482.6	3509.91	3510.7200	.8051	.7756	.0296	7	
12.8334	9	28559.2	3500.49	3501.2200	.7281	.7088	.0194	8	
12.8722	9	28584.8	3497.37	3498.0600	.6930	.6861	.0069	8	
13.1857	9	28792.6	3472.12	3472.5800	.4617	.4949	-.0332	9	
13.2599	9	28842.3	3466.14	3466.5800	.4376	.4477	-.0101	9	
13.2877	9	28860.9	3463.90	3464.3400	.4366	.4299	.0067	8	
13.3347	9	28892.5	3460.12	3460.5200	.4019	.3995	.0024	8	
13.4127	9	28945.0	3453.84	3454.1900	.3539	.3484	.0055	9	
13.4552	9	28973.7	3450.41	3450.7600	.3467	.3202	.0265	8	
13.4921	9	28998.7	3447.44	3447.7000	.2586	.2956	-.0370	9	
13.7861	9	29199.3	3423.76	3423.9100	.1468	.0919	.0550	6	
13.8589	9	29249.3	3417.90	3417.9000	0.	.0390	-.0390	9	

FIRST AVERAGE = .031181 SECOND AVERAGE = .022047 DISCRIMINANT = .1000 LINEAR DISPERSION = -.805382
COEFFICIENTS OF POLYNOMIAL = -3.31518425D+02 1.36497952D+03 -1.53481343D+03 -1.19458110D+03 4.47608531D+03
-4.43493767D+03 2.05646943D+03 -4.23921770D+02 2.35753314D+01

MMS	LAMBDA	SIGMA	INTY
8.9831	3811.75	26227.2	4
9.0038	3810.09	26238.7	4
9.0474	3806.59	26262.8	5
9.1145	3801.20	26300.0	5
9.6509	3758.09	26601.7	2
10.3014	3705.78	26977.2	5
10.4081	3697.20	27039.8	5
10.4361	3694.94	27056.3	4
11.0639	3644.36	27431.8	6
11.1618	3636.47	27491.4	6
11.3604	3620.44	27613.1	2
11.3844	3618.50	27627.9	3
11.4220	3615.46	27651.1	3
11.4530	3612.96	27670.2	2
11.5928	3601.67	27757.0	3
11.9613	3571.87	27988.6	4
11.9825	3570.15	28002.0	4
12.0276	3566.50	28030.7	4
12.0451	3565.08	28041.8	3
12.1843	3553.81	28130.7	4
12.6265	3517.98	28417.3	4
13.5778	3440.78	29054.9	3
13.6531	3434.66	29106.6	4
14.1177	3396.90	29430.2	4
14.1877	3391.20	29479.6	4

2. Program VIBRAN

(i) Data deck set-up

A. Title card

Columns 1-80, field 16A5: WORDS, anything.

Example:

bRMMbFLUORbANTHRACENE/N-C6b4bDEGbKbMACNABb28bOCTOBERb1968bbbb, etc.

B. Molecular lines

These cards are the punched output from program RREDUK.

Columns 1-27, field 27X: Contain data, but are ignored by VIBRAN.

Columns 28-36, field F9.1: NUU, frequency of line in cm^{-1}.

Columns 37-42, field 6X: Blank.

Columns 43-46, field I4: INT, intensity of line.

Example:

bb6.6126bbbbbb4293.32bbbbbbbb23285.4bbbbbbbbb3bbbb, etc.

C. Blank card

Sentinel to indicate end of molecular lines.

D. Transfer card

(a) If more sets of data to be processed, bbbbbbNEXDATbbbb, etc.

(b) Otherwise, blank card.

E. If D is option (a), return to A.

(ii) Source listing and sample output

See overleaf.

```
                PROGRAM VIBRAN (INPUT, OUTPUT, TAPE 5)

      C PROGRAM USING RREDUK OUTPUT TO OBTAIN AND SORT FREQUENCY DIFFERENCES
      C BETWEEN SPECTRAL LINES.

000052        DIMENSION WORDS(16)
000052        DIMENSION NUU( 70), NU( 70), INT( 70), S( 70)
000052        DIMENSION  DELNU(2500), NUHI(2500), NULO(2500), INTHI(2500),
     1  INTLO(2500), EN(2500), JAY(2500)

000052        REAL NUU, WORDS
000052        INTEGER  F,I,J,K,L,M,N,S,JK,INT,NU,DELNU,DDELNU,NUHI,NULO,INTHI,
     1  INTLO, EN,JAY,TEMP, MORE, YES
000052        DATA YES/6HNEXDAT/

000052      7 CONTINUE
      C READ AND PRINT TITLE CARD.
000052    801 FORMAT (1H1)
000052        PRINT 801
000055    800 FORMAT (16A5)
000055        READ 800,(WORDS(I),I = 1,16)
000066        PRINT 800, (WORDS(I),I = 1,16)
000077    802 FORMAT (1H //)
000077        PRINT 802

      C READ IN FREQUENCY AND INTENSITY OF LINES.
000102        DO 1 I = 1, 70
000104      6 CONTINUE
000104    803 FORMAT (27X, F 9.1, 6X, I4)
000104        READ 803    , NUU(I), INT(I)
000113        S(I) = I
000115        NU(I) = IFIX(NUU(I) + 0.5)
      C SENTINEL.
000120        IF (NUU(I))1,702,1
000122      1 CONTINUE
000124    702 K = I -1

      C PRINT LINE INDEX, FREQUENCY, AND INTENSITY.
000126    804 FORMAT ( 51H  LINE       LINE          LINE       INTERPRETATION)
000126    805 FORMAT (33H NUMBER     FREQUENCY     INTENSITY)
000126    806 FORMAT (2X, 1H(, I3, 1H), 6X, I5, 9X, I2)
000126        PRINT 804
000131        PRINT 805
000134        PRINT 802
000137        PRINT 806, (S(I),  NU(I), INT(I), I = 1,K )

      C SUBTRACT EACH FREQUENCY FROM SUBSEQUENT FREQUENCIES, KEEPING ALL DATA IN STEP.
000155        M = K -1
000157        F = 0
000160        DO 2 J=1,M
000161        JK = K - J
000163        DO 3 L = 1,JK
000164        N = J + L
000166        F = F + 1
000167        DELNU(F) = NU(N) - NU(J)
000173        NUHI(F) = NU(N)
000175        NULO(F) = NU(J)
000177        INTHI(F) = INT(N)
000202        INTLO(F) = INT(J)
000204        EN(F) = N
000206        JAY(F) = J
```

```
000207          3 CONTINUE
000212          2 CONTINUE

          C COMPARE FREQUENCY DIFFERENCES AND ORDER THEM, KEEPING ALL OTHER
          C DATA IN STEP.
000214            K = F
000215            M = K - 1
000216            DO 4 J = 1,M
000220            JK = K - J
000222            DO 5 L = 1,JK
000223            N = J + L
000225            IF ( DELNU(N) -  DELNU(J))  703,5,5
000230       703  TEMP =  DELNU(N)
000232             DELNU(N) =  DELNU(J)
000235             DELNU(J) = TEMP
000236            TEMP = NUHI(N)
000240            NUHI(N) = NUHI(J)
000242            NUHI(J) = TEMP
000243            TEMP = NULO(N)
000244            NULO(N) = NULO(J)
000246            NULO(J) = TEMP
000250            TEMP = INTHI(N)
000251            INTHI(N) = INTHI(J)
000253            INTHI(J) = TEMP
000254            TEMP = INTLO(N)
000255            INTLO(N) = INTLO(J)
000257            INTLO(J) = TEMP
000261            TEMP = EN(N)
000262            EN(N) = EN(J)
000264            EN(J) = TEMP
000265            TEMP = JAY(N)
000266            JAY(N) = JAY(J)
000270            JAY(J) = TEMP
000272          5 CONTINUE
000275          4 CONTINUE

          C PRINT FREQUENCY DIFFERENCES TOGETHER WITH FREQUENCIES AND INTENSITIES
          C OF COMPONENT LINES.
000277            PRINT 801
000302            PRINT 802, (WORDS(I),I = 1,16)
000313            PRINT 802
000316       807  FORMAT (15X, 94HUPPER LINE     UPPER LINE    LOWER LINE    LOWER LI
                 1NE     FREQUENCY DIFFERENCE    INTERPRETATION)
000316       808  FORMAT (15X, 74HFREQUENCY       INTENSITY     FREQUENCY     INTENSIT
                 1Y       BETWEEN UPPER AND)
000316       809  FORMAT (75X, 10HLOWER LINE)
000316       810  FORMAT (1H(, I3, 3H)-(, I3, 1H), 6X, I5, 10X, I2, 11X, I5, 10X,
                 1 I2, 12X, I5)
000316            PRINT 807
000321            PRINT 808
000324            PRINT 809
000327            PRINT 802
000332            PRINT 810, (EN(I),JAY(I),NUHI(I),INTHI(I),NULO(I),INTLO(I),
                 1  DELNU(I), I=1,K)

          C CHECK IF MORE SPECTRA HAVE TO BE PROCESSED.
000360       714  FORMAT (6X, A6)
000360            READ 714, MORE
000365            IF (MORE.EQ.YES) GO TO 7
000367            CALL EXIT
000370            RETURN
000372            END
```

RMM 446 ANTHRACENE(D10)/N-C8 ABS 4 DEG K DEC 17 1963 MACNAB

LINE NUMBER	LINE FREQUENCY	LINE INTENSITY	INTERPRETATION
(1)	26227	4	
(2)	26239	4	
(3)	26263	5	
(4)	26300	5	
(5)	26602	2	
(6)	26977	5	
(7)	27040	5	
(8)	27056	4	
(9)	27432	6	
(10)	27491	6	
(11)	27613	2	
(12)	27628	3	
(13)	27651	3	
(14)	27670	2	
(15)	27757	3	
(16)	27989	4	
(17)	28002	4	
(18)	28031	4	
(19)	28042	3	
(20)	28131	4	
(21)	28417	4	
(22)	29055	3	
(23)	29107	4	
(24)	29430	4	
(25)	29480	4	

	UPPER LINE FREQUENCY	UPPER LINE INTENSITY	LOWER LINE FREQUENCY	LOWER LINE INTENSITY	FREQUENCY DIFFERENCE BETWEEN UPPER AND LOWER LINE	INTERPRETATION
(19)-(18)	28042	3	28031	4	11	
(2)-(1)	26239	4	26227	4	12	
(17)-(16)	28002	4	27989	4	13	
(12)-(11)	27628	3	27613	2	15	
(8)-(7)	27056	4	27040	5	16	
(14)-(13)	27670	2	27651	3	19	
(13)-(12)	27651	3	27628	3	23	
(3)-(2)	26263	5	26239	4	24	
(18)-(17)	28031	4	28002	4	29	
(3)-(1)	26263	5	26227	4	36	
(4)-(3)	26300	5	26263	5	37	
(13)-(11)	27651	3	27613	2	38	
(19)-(17)	28042	3	28002	4	40	
(18)-(16)	28031	4	27989	4	42	
(14)-(12)	27670	2	27628	3	42	
(25)-(24)	29480	4	29430	4	50	
(23)-(22)	29107	4	29055	3	52	
(19)-(16)	28042	3	27989	4	53	
(14)-(11)	27670	2	27613	2	57	
(10)-(9)	27491	6	27432	6	59	
(4)-(2)	26300	5	26239	4	61	
(7)-(6)	27040	5	26977	5	63	
(4)-(1)	26300	5	26227	4	73	
(8)-(6)	27056	4	26977	5	79	
(15)-(14)	27757	3	27670	2	87	
(20)-(19)	28131	4	28042	3	89	
(20)-(18)	28131	4	28031	4	100	
(15)-(13)	27757	3	27651	3	106	
(11)-(10)	27613	2	27491	6	122	
(20)-(17)	28131	4	28002	4	129	
(15)-(12)	27757	3	27628	3	129	
(12)-(10)	27628	3	27491	6	137	
(20)-(16)	28131	4	27989	4	142	
(15)-(11)	27757	3	27613	2	144	
(13)-(10)	27651	3	27491	6	160	
(14)-(10)	27670	2	27491	6	179	
(11)-(9)	27613	2	27432	6	181	
(12)-(9)	27628	3	27432	6	196	
(13)-(9)	27651	3	27432	6	219	
(16)-(15)	27989	4	27757	3	232	
(14)-(9)	27670	2	27432	6	238	
(17)-(15)	28002	4	27757	3	245	
(15)-(10)	27757	3	27491	6	266	
(18)-(15)	28031	4	27757	3	274	
(19)-(15)	28042	3	27757	3	285	
(21)-(20)	28417	4	28131	4	286	
(5)-(4)	26602	2	26300	5	302	
(16)-(14)	27989	4	27670	2	319	
(24)-(23)	29430	4	29107	4	323	
(15)-(9)	27757	3	27432	6	325	
(17)-(14)	28002	4	27670	2	332	
(16)-(13)	27989	4	27651	3	338	
(5)-(3)	26602	2	26263	5	339	

3. Program WISHFUL

(i) Data deck set-up

A. Title card

Columns 1-75, field 15A5: WORDS(1) to WORDS(15), anything.

Columns 76-80, field I5: WORDS(16), +1 if absorption spectrum being synthesized, -1 if fluorescence spectrum being synthesized.

Example:

bRMMb446bANTHRACENE(D10)/N-C8bABSbb4bDEGbKbDECb17bb1968bMACNABbbbbbbb1

B. Origins deck

Columns 1-6, field A6: ORNAME, name of origin.

Columns 7-8, field 2X: Blank.

Columns 9-13, field I5: ORIGIN, position of origin in cm^{-1}.

Columns 14-18, field 5X: Blank.

Column 19, field I1: ORINT, intensity of origin; value between 0 and 5.

Examples:

**b01bbb26227bbbbb5bbbb, etc., asterisks indicating that this is the main origin. bbb02bbb26500bbbbb1bbbb, etc.

C. Blank card

Sentinel to indicate end of origins deck.

D. Vibrational modes deck

Columns 1-4, field A4: MODE, name of mode.

Columns 5-6, field 2X: Blank.

Columns 7-10, field I4: SET(1,I), frequency of mode in cm^{-1}.

Columns 11-15, field 5X: Blank.

Column 16, field I1: INT(1,I), intensity of mode: value between 0 and 5.

Example:

NU4bbb1386bbbbb5bbbb, etc.

E. Blank card

Sentinel to indicate end of vibrational modes deck.

F. Transfer card

(a) If more sets of data to be processed, bbbbbbNEXDATbbbb,etc.

(b) Otherwise, bland card.

G. If F is option (a), return to A.

(ii) Source listing and sample output

See overleaf.

```
      PROGRAM WISHFUL(INPUT,OUTPUT)

C THIS PROGRAM SYNTHESISES A SPECTRUM FROM ASSUMED VALUES OF ORIGINS AND
C VIBRATIONAL MODES. COMBINATION LINES HAVE NO MORE THAN THREE VIBRATIONAL
C QUANTA, AND ONLY APPEAR IF THE INTENSITY (CALCULATED BY EMPIRICAL COMBINATION
C RULES) IS GREATER THAN OR EQUAL TO ZERO.

000037        COMMON  MULT, HIINDEX
000037        COMMON  /BLK1/NO,YES
000037        EQUIVALENCE (MULTI,WORDMUL)

000037        DIMENSION WORDS(16),ORNAME(15),ORIGIN(15),ORINT(15),MODE(12),
             1 SET(6,100),INT(6,100),NUMSET(6),MULT(6,100,12),TOTSET(200),
             2 TOTINT(200),MULTI(350,12),SUPSET(350),SUPINT(350),SUPMULT(350,12)
             3,ORIG(350),WORD1(350,12),WORD2(350,12),FORM(18) ,WORDMUL(350,12),
             4 ASTRISK(6), HIINDEX(100), NUMBER(15)

000037        INTEGER WORDS,ORNAME,ORIGIN,ORINT,NUMORS,I,MODE,SET,INT,NUMSET,N,
             1 NNUMSET,NUMSET1 ,MULT,K,N1,N2,M,B,PASWD,NO,YES,L,TOT,TOTSET,J,
             2 TOTINT,MULTI,SUPSET,SUPINT,ORIG,SUPMULT,TEST,SUPTOT,NLESS,JPLUS,
             3 TEMP,ASTRISK,WORD1,WORD2,PLUSSP,WORDMUL,VOID,ZILCH,FORM,HIINDEX,
             4NUMBER,  MORE,NEXDAT

000037        DATA NEXDAT/6HNEXDAT/,(ASTRISK(I) ,I = 1,6) /1OH          ,
             1 1OH         ==,1OH       ====,1OH     ====== ,1OH  ========= ,
             2 1OH========== /,(FORM(I),I=1,10)/2H(2,2HX,,
             3 2HA1,2HO,,2H4X,2H,I,2H5,,2H5X,2H,A,2H6,/,(FORM(I), I = 12,17)/
             4 2H(A,2H2,,2HA1,2H,A,2H4),2H) /,PLUSSP,VOID,ZILCH/2H+ ,1H ,
             5 2H  /,(NUMBER(I),I=1,15)/1H1,1H2,1H3,1H4,1H5,1H6,1H7,
             6 2H 8,2H 9,2H10,2H11,2H12,2H13,2H14,2H15/,FORM(18)/0000055/

C READ AND PRINT TITLE CARD.
000037     36 CONTINUE
000037    801 FORMAT (1H1)
000037        PRINT 801
000042    800 FORMAT(1545,I5)
000042        READ 800, (WORDS(I), I = 1,16)
000053        PRINT800, (WORDS(I), I = 1,16)
000064    802 FORMAT(1H //)
000064        PRINT 802

C READ ORIGIN NAME, POSITION , AND INTENSITY.
000067    803 FORMAT (A6, 2X, I5, 5X, I1)
000067        DO 1  I = 1,20
000071        READ 803,    ORNAME(I), ORIGIN(I), ORINT(I)
C SENTINEL.
000102        IF (ORIGIN(I)) 1,2,1
000104      1 CONTINUE
000106        I = I + 1
000110      2 NUMORS = I - 1

C PRINT ORIGIN NAME, POSITION, AND INTENSITY.
000112    804 FORMAT (24HORIGIN  POSN.  INTENSITY)
000112        PRINT 804
000115        PRINT 802
000120        PRINT 803,    (ORNAME(I), ORIGIN(I), ORINT(I), I = 1,NUMORS)
000136        PRINT 802
000141        PRINT 802

C READ VIBRATIONAL MODE NAME, FREQUENCY, AND INTENSITY.
000144    805 FORMAT (A4, 2X, I4, 5X, I1)
```

```
000144          DO 3  I = 1,20
000146          READ 805,     MODE(I), SET(1,I), INT(1,I)
        C SENTINEL.
000163          IF  (SET(1,I)) 3,4,3
000165        3 CONTINUE
000167          I = I + 1
000171        4 NUMSET(1) = I - 1
000173          NUMSET1 = NUMSET(1)

        C PRINT MODE NAME, FREQUENCY, AND INTENSITY.
000174      806 FORMAT (21HMODE   FREQ  INTENSITY)
000174          PRINT 806
000177          PRINT 805,     (MODE(I), SET(1,I), INT(1,I), I = 1, NUMSET1)
000221          PRINT 801

        C MEMBERS OF FIRST SET HAVE SIMPLY ONE QUANTUM OF ONE MODE. MULTIPLICITY OF
        C THAT MODE SET TO ONE, OTHERS SET TO ZERO.
000224          DO 5 I = 1,NUMSET1
000226          DO 6  J = 1,NUMSET1
000227          IF (I.EQ.J) GO TO 7
000230          MULT (1,I,J) = 0
000235          GO TO 6
000236        7 MULT(1,I,J) = 1
000244        6 CONTINUE
000247        5 CONTINUE

        C FORM REMAINING SETS. EACH IS MADE FROM SET(1) AND ONE OTHER PREVIOUSLY
        C CONSTRUCTED SET DETERMINED BY #CRITRN#.
000251          DO 9  K = 2,6
000252          CALL  CRITRN(K,N1)
000254          M = 0
000255          NNUMSET = NUMSET(N1)
000257          DO 10 I = 1, NUMSET1
000261          DO 11 J = 1, NNUMSET
        C EMPIRICAL INTENSITY COMBINATION RULE.
000262          B = INT(1,I) + INT(N1,J) - 6
        C IF INTENSITY IS NEGATIVE, OR IF #PASWD# SAYS THESE PARTICULAR MEMBERS SHOULD
        C NOT BE COMBINED (TO PREVENT DUPLICATION) COMBINATION IS REJECTED.
000271          IF (B.LT.0.OR.PASWD(K,I,J,MULT,HIINDEX).EQ.NO)  GO TO 11
000303          M = M + 1
000304          IF (K.EQ.4)  GO TO 31
000305          GO TO 32
000307       31 HIINDEX (M) = J
000311       32 SET(K,M) =  SET(1,I) + SET(N1,J)
000322          INT(K,M) = B
000326          DO 12  L = 1,NUMSET1
000327       12 MULT(K,M,L) = MULT(1,I,L) + MULT(N1,J,L)
000347       11 CONTINUE
000352       10 CONTINUE
000354          NUMSET(K) = M
        C EXIT IF SET IS TOO LARGE.
000356          IF (NUMSET(K).LE.100)  GO TO  9
000361      810 FORMAT (7HNUMSET(,I1,4H) = ,I3)
000361          PRINT 810, K, NUMSET(K)
000370          GO TO  33
000371        9  CONTINUE

        C LIST SETS 1 THROUGH 6 AS ONE TOTSET.
000373          TOT = 0
000374          DO 13  K = 1,6
000376          NNUMSET = NUMSET(K)
000400          DO 14  I = 1,NNUMSET
```

```
000401          N = I + TOT
000403          TOTSET(N) = SET(K,I)
000407          TOTINT(N) = INT(K,I)
000411          DO 15  J = 1,NUMSET1
000413          MULTI(N,J) = MULT(K,I,J)
000425       15 CONTINUE
000430       14 CONTINUE
000433          TOT = TOT + NUMSET(K)
000435       13 CONTINUE
             C EXIT IF TOTSET IS TOO LARGE.
000437          IF (TOT.LE.200)  GO TO 34
000441      811 FORMAT (6HTOT = ,I3)
000441          PRINT 811, TOT
000446          GO TO 33
000447       34 CONTINUE

             C START MAKING SUPSET (VIBRATIONAL COMBINATIONS WITH ORIGINS). FIRST MEMBERS
             C ARE PURE ORIGINS. VIBRATIONAL MULTIPLICITIES MUST BE SET TO ZERO.
000447          DO 28  I = 1,NUMORS
000451          SUPSET(I) = ORIGIN(I)
000453          TEST = ORINT(I) + 1
             C CONVERT INTENSITY TO GRAPHICAL FORM.
000456          SUPINT(I) = ASTRISK(TEST)
000460          ORIG(I) = ORNAME(I)
000462          DO 29  L = 1,NUMSET1
000463       29 SUPMULT(I,L) = 0
000471       28 CONTINUE

             C BY COMBINING TOTSET WITH ORIGINS , COMPLETE SUPSET.
000473          N = NUMORS
000474          DO 16  I = 1,NUMORS
000475          DO 17  J = 1,TOT
000476          TEST = ORINT(I) + TOTINT(J) - 5
000502          IF (TEST.LT.0)  GO TO 17
000503          N = N + 1
             C WORDS(16) DETERMINES WHETHER WE ADD OR SUBTRACT TOTSET FROM ORIGINS
             C I.E. ABSORPTION OR FLUORESCENCE.
000504          SUPSET(N) = ORIGIN(I) + WORDS(16)*TOTSET(J)
000512          TEST = TEST + 1
000514          SUPINT(N) = ASTRISK(TEST)
000517          ORIG(N) = ORNAME(I)
000521          DO 18  L = 1,NUMSET1
000523       18 SUPMULT(N,L) = MULTI(J,L)
000535       17 CONTINUE
000540       16 CONTINUE
000542          SUPTOT = N
             C EXIT IF SUPSET IS TOO LARGE.
000544          IF (SUPTOT.LE.350)  GO TO 35
000546      812 FORMAT (9HSUPTOT = ,I3)
000546          PRINT 812, SUPTOT
000553          GO TO 33

             C ARRANGE SUPSET IN ORDER OF INCREASING ENERGY.
000554       35 NLESS = N - 1
000556          DO 19  J = 1,NLESS
000560          JPLUS = J + 1
000562          DO 20  K = JPLUS,N
000563          IF (SUPSET(J) -SUPSET(K))  20,20,21
000567       21 TEMP = SUPSET(J)
000571          SUPSET(J) = SUPSET(K)
000574          SUPSET(K) = TEMP
000575          TEMP = SUPINT(J)
```

```
000577          SUPINT(J) = SUPINT(K)
000601          SUPINT(K) = TEMP
000602          TEMP = ORIG(J)
000603          ORIG(J) = ORIG(K)
000605          ORIG(K) = TEMP
000607          DO 22  L = 1,NUMSET1
000610          TEMP = SUPMULT(J,L)
000614          SUPMULT(J,L) = SUPMULT(K,L)
000617       22 SUPMULT(K,L) = TEMP
000624       20 CONTINUE
000627       19 CONTINUE

            C THIS SECTION PREPARES DATA IN FORMAT DESIRED FOR PRINTOUT
000631          DO 23  K = 1,SUPTOT
000633          DO 24  L = 1,NUMSET1
000634          IF (1 - SUPMULT(K,L))  25,26,27
000641       25 WORD1(K,L) = PLUSSP
000646          WORD2(K,L) = MODE(L)
000650          TEMP = SUPMULT(K,L)
000651          WORDMUL(K,L) = NUMBER(TEMP)
000654          GO TO 24
000654       26 WORD1(K,L) = PLUSSP
000661          WORD2(K,L)= MODE(L)
000663          WORDMUL(K,L) = VOID
000664          GO TO 24
000665       27 WORD1(K,L) = ZILCH
000672          WORD2(K,L) = ZILCH
000673          WORDMUL(K,L) = VOID
000675       24 CONTINUE
000700       23 CONTINUE

            C PRINT SYNTHESISED SPECTRUM.
000702         807 FORMAT(39HINTENSITY  ENERGY           COMPOSITION)
000702         808 FORMAT(50H           (CM-1)  (ORIGIN)   (VIBRATIONAL QUANTA))
000702          PRINT 807
000705          PRINT 808
000710          PRINT 802
000713          FORM(11) = NUMBER(NUMSET1)
000715          DO 30  K = 1,SUPTOT
            C OBJECT TIME FORMAT STATEMENT DTERMINING HOW MANY VIBRATIONAL MODE COLUMNS ARE
            C REQUIRED.
000717          PRINT FORM, SUPINT(K),SUPSET(K),ORIG(K),(WORD1(K,L),WORDMUL(K,L),
               1WORD2(K,L), L = 1,NUMSET1)
000747         809 FORMAT (1H /)
000747          30 PRINT 809
000755          33 CONTINUE

            C CHECK IF PROGRAM HAS TO BE REPEATED ON FRESH DATA.
000755         813 FORMAT (6X,A6)
000755          READ 813, MORE
000762          IF (MORE.EQ.NEXDAT)  GO TO 36
000764          CALL EXIT
000765          RETURN
000767          END
```

```
                      SUBROUTINE  CRITRN (K,N1)
047327                IF (K.NE.2)  GO TO 701
047331                N1 = 1
047332                GO TO 711
047332           701  IF (K.NE.3)  GO TO 703
047334                N1 = 2
047335                GO TO 711
047335           703  IF (K.NE.4)  GO TO 705
047337                N1 = 1
047340                GO TO 711
047340           705  IF (K.NE.5)  GO TO 707
047342                N1 = 4
047343                GO TO 711
047343           707  N1 = 2
047344           711  RETURN
047345                END
```

```
                INTEGER FUNCTION  PASWD(K,I,J,MULT,HIINDEX)

047366          COMMON  MULT, HIINDEX
047366          COMMON  /BLK1/NO,YES
047366          DIMENSION  MULT(6,100,12), HIINDEX(100)
047366          INTEGER K,I,J,MULT,HIINDEX

              C SET(2), OBTAINED FROM SET(1) AND SET(1), OF TYPE NU1 + NU1.
047366          IF (K.NE.2)  GO TO 701
047370          IF (I.EQ.J)  GO TO 702
047371          PASWD = NO
047373          GO TO 711
047373        702 PASWD = YES
047375          GO TO 711

              C SET(3), OBTAINED FROM SET(1) AND SET(2), OF TYPE NU1 + 2NU1.
047375        701 IF (K.NE.3)  GO TO 703
047377          IF (MULT(2,J,I).EQ.2)  GO TO 704
047405          PASWD = NO
047406          GO TO 711
047407        704 PASWD = YES
047411          GO TO 711

              C SET(4), OBTAINED FROM SET(1) AND SET(1), OF TYPE NU1 + NU2.
047411        703 IF (K.NE.4)  GO TO 705
047413          IF (I.LT.J)  GO TO 706
047414          PASWD = NO
047416          GO TO 711
047416        706 PASWD = YES
047420          GO TO 711

              C SET(5), OBTAINED FROM SET(1) AND SET(4), OF TYPE (NU4) + (NU1 + NU2).
047420        705 IF (K.NE.5)  GO TO 707
047422          IF (I.GT.HIINDEX(J))  GO TO 708
047426          PASWD = NO
047427          GO TO 711
047427        708 PASWD = YES
047431          GO TO 711

              C SET(6), OBTAINED FROM SET(1) AND SET(2), OF TYPE NU1 + 2NU2.
047431        707 IF (MULT(2,J,I).EQ.0)  GO TO 710
047436          PASWD = NO
047440          GO TO 711
047440        710 PASWD = YES
047442        711 RETURN
047444          END


                BLOCK DATA
047456          COMMON/BLK1/NO,YES
047456          INTEGER  NO,YES
047456          DATA  NO,YES/2HNO,3HYES/
047456          END
```

RMM 446 ANTHRACENE(D10)/N-C8 ABS 4 DEG K DEC 17 1968 MACNAB

ORIGIN	POSN.	INTENSITY
** 01	26227	5
02	26500	1
03	26666	3

MODE	FREQ	INTENSITY
NU1	375	5
NU2	690	2
NU3	829	4
NU4	1386	5
NU5	1530	3
NU10	1443	4
NU11	813	3

INTENSITY	ENERGY (CM-1)	(ORIGIN)	COMPOSITION (VIBRATIONAL QUANTA)
==========	26227	** 01	
==	26500	02	
==========	26602	** 01 + NU1	
======	26666	03	
==	26875	02 + NU1	
====	26917	** 01 + NU2	
========	26977	** 01 + 2NU1	
======	27040	** 01	+ NU11
======	27041	03 + NU1	
========	27056	** 01 + NU3	
	27250	02 + 2NU1	
==	27292	** 01 + NU1 + NU2	
	27329	02 + NU3	
======	27352	** 01 + 3NU1	
	27356	03 + NU2	
====	27415	** 01 + NU1	+ NU11
====	27416	03 + 2NU1	
======	27431	** 01 + NU1 + NU3	
==	27479	03	+ NU11
====	27495	03 + NU3	
==========	27613	** 01 + NU4	
	27667	** 01 + 2NU1 + NU2	
========	27670	** 01	+ NU10
	27746	** 01 + NU2 + NU3	
======	27757	** 01 + NU5	
==	27790	** 01 + 2NU1	+ NU11
==	27791	03 + 3NU1	
====	27806	** 01 + 2NU1 + NU3	
	27853	** 01	+ 2NU11

REFERENCES

1. E. V. Shpolskii, A. A. Ilina, and L. A. Klimova, Doklady Akad. Nauk. SSSR, 87, 935 (1952).
2. E. V. Shpolskii and L. A. Klimova, Soviet Phys. Dokl. 1, 782 (1956).
3. E. V. Shpolskii and L. A. Klimova, Opt. and Spectr. 13, 97 (1962).
4. E. V. Shpolskii, L. A. Klimova, and R. I. Personov, Opt. and Spectr. 13, 188 (1962).
5. G. V. Gobov and T. N. Bolotnikova, Opt. and Spectr. 15, 18 (1963).
6. R. I. Personov, Opt. and Spectr. 15, 30 (1963).
7. L. A. Klimova, Opt. and Stectr. 15, 185 (1963).
8. S. F. Shkirman and K. N. Solov'ev, Isv. Akad. Nauk SSSR, Phys. Ser. 29, 1385 (1965).
9. M. M. Valdman and R. I. Personov, Opt. and Spectr. 18, 296 (1965).
10. N. A. Fenina, Opt. and Spectr. 20, 428 (1966).
11. T. N. Bolotnikova, L. A. Klimova, G. N. Nersesova, and L. F. Utkina, Opt. and Spectr. 21, 237 (1966).
12. A. N. Sevchenko, K. N. Solov'ev, A. T. Gradyushko, and S. F. Shkirman, Soviet Phys. Dokl. 11, 587 (1967).
13. E. J. Bowen and B. Brocklehurst, J. Chem. Soc., 3875 (1954).

14. E. J. Bowen and B. Brocklehurst, J. Chem. Soc., 4320 (1955).

15. Louise Pesteil, Compt. Rend. 250, 497 (1960).

16. Louise Pesteil and Madeleine Rabaud, J. Chim. Phys. 59, 167 (1962).

17. E. V. Shpolskii, Soviet Phys. Uspekhi, 6, 411 (1963).

18. Jaffe and Orchin, Theory and Applications of Ultra-violet Spectroscopy (John Wiley & Sons), p. 245.

19. H. Sponer and E. Teller, Rev. Mod. Phys. 13, 75 (1941).

20. P. Pringsheim and A. Kronenberger, Zeits. f. Physik, 40, 75 (1926).

21. A. Kronenberger, Zeits. f. Physik, 63, 494 (1930).

22. D. S. McClure and O. Schnepp, J. Chem. Phys. 23, 1575 (1955).

23. A. Prikhotyko, JETP (USSR), 19, 383 (1949).

24. D. S. McClure, J. Chem. Phys. 25, 481 (1956).

25. G. V. Svishchev, Opt. and Spectr. 18, 350 (1965).

26. E. D. Trifonov, Soviet Phys. Dokl. 7, 1105 (1963).

27. K. K. Rebane and V. V. Khizhnyakov, Opt. and Spectr. 14, 193 (1963).

28. K. K. Rebane and V. V. Khizhnyakov, Opt. and Spectr. 14, 262 (1963).

29. R. L. Mössbauer, Zeits. f. Physik, 151, 124 (1958).

30. The Mössbauer Effect, ed. Hans Frauenfelder (W. A. Benjamin Press, 1963).

31. H. J. Lipkin, Ann. Phys. 9, 332 (1960).

32. H. J. Lipkin, Ann. Phys. 18, 182 (1962).

33. Handbook of Fluorescent Spectra of Aromatic Molecules, ed. I. B. Berlman (Academic Press, 1965), p. 123.

34. E. Whittle, D. A. Dows, and G. C. Pimentel, J. Chem. Phys. 22, 1943 (1954).

35. G. W. Robinson, J. Mol. Spectr. 6, 58 (1961).

36. O. Schnepp, J. Mol. Spectr. 18, 158 (1965).

37. W. C. Johnson, Jr., and I. Tinoco, Jr., Biopolymers (in press).

38. B. T. Tomlinson, Ph.D. Thesis, University of California, Berkeley, 1969.

39. J. D. Spangler and N. G. Kilmer, J. Chem. Phys. 48, 698 (1968).

40. D. S. McClure, J. Chem. Phys. 22, 1668 (1954).

41. F. Halversen and R. C. Hirt, J. Chem. Phys. 17, 1165 (1949).

42. J. Drobnik and L. Augenstein, Photochem. and Photobiol. 5, 13 (1966).

43. V. Sanker, Z. physik. Chem. 2, 52 (1954).

44. E. A. Chandross, J. Ferguson, and E. G. McRae, J. Chem. Phys. 45, 3456 (1966).

45. G. Wald, Nature, 184, 620 (1959).

46. Th. Förster, Chapter III.B.1. of Modern Quantum Chemistry (Istanbul Lectures), ed. O. Sinanoglu (Academic Press, 1965).

47. G. W. Robinson and R. P. Frosch, J. Chem. Phys. 37, 1962 (1962).

48. G. R. Hunt, E. F. McCoy, and I. G. Ross, Austr. J. Chem. 15, 591 (1962).

49. G. W. Robinson and R. P. Frosch, J. Chem. Phys. 38, 1187 (1963).

50. G. W. Robinson, J. Chem. Phys. 47, 1967 (1967).

51. N. Abasbegovic and N. Vukotic, J. Chem. Phys. 41, 2575 (1964).

52. R. Manzoni, Rend. Accad. Lincei, 26, 166 (1937).

53. S. Califano, J. Chem. Phys. 36, 903 (1962).

54. V. P. Klochkov and T. S. Smironova, Opt. and Spectr. 22, 464 (1967).

55. L. Colombo and J. P. Mathieu, Bull. Soc. France Mineral. Crist. 83, 250 (1960).

56. E. P. Krainov, Opt. and Spectr. 16, 532 (1964).

57. Wilson, Decius, and Cross, Molecular Vibrations (McGraw-Hill).

58. G. C. Nieman and D. S. Tinti, J. Chem. Phys. 46, 1432 (1967).

59. M. A. ElSayed, M. T. Wauk, and G. W. Robinson, Mol. Phys. 5, 205 (1962).

60. S. Leach and R. Lopez-Delgado, J. Chim. phys. 64, 1247 (1967).

61. S. Leach and R. Lopez-Delgado, J. Chim. phys. 61, 1636 (1964).

62. R. Pariser, J. Chem. Phys. 24, 250 (1956).

63. H. B. Klevens and J. R. Platt, J. Chem. Phys. 17, 470 (1949).

TECHNICAL INFORMATION DIVISION
LAWRENCE RADIATION LABORATORY
UNIVERSITY OF CALIFORNIA
BERKELEY, CALIFORNIA 94720